Differential Localization of Hic-5 and Paxillin in the Brain of Alzheimer's Disease Subjects

by

John Michael Caltagarone

Associate of Science, Pennsylvania State University, 1992

Bachelor of Science in Neuroscience, University of Pittsburgh, 1997

Submitted to the Graduate Faculty of

University of Pittsburgh School of Medicine Department of Pharmacology in partial fulfillment

of the requirements for the degree of

Doctor of Philosophy in Molecular Pharmacology

University of Pittsburgh

2008

UNIVERSITY OF PITTSBURGH

School of Medicine Department of Pharmacology

This thesis was presented

by

John Michael Caltagarone

It was defended on

June 11th, 2008

and approved by

Mentor: Dr. Donald DeFranco, Professor, Department of Pharmacology & Chemical Biology

Mentor: Dr. Robert Bowser, Associate Professor, Department of Pathology,

Division of Neuropathology

Thesis Chairman: Dr. Jack C. Yalowich, Associate Professor, Department of Pharmacology &

Chemical Biology

Dr. Mark D. Nichols, Assistant Professor, Department of Pharmacology & Chemical Biology

Dr. Michael J. Palladino, Assistant Professor, Department of Pharmacology & Chemical

Biology

Differential Localization of Hic-5 and Paxillin in Brain of Alzheimer's Disease Subjects

John Michael Caltagarone, AS/BS/PhD

University of Pittsburgh, 2008

ABSTRACT

Alzheimer's disease (AD) is a neurodegenerative disorder that results from a loss of synaptic transmission and ultimately results in cell death. However, the mechanisms that induce neuronal cell death remain elusive. Amyloid plaques composed of amyloid fibrils (Aβ) and neurofibrillary tangles (NFTs) composed of hyperphosphorylated tau (pTau) are the main pathogenic hallmarks of AD. Aβ and NFT generation is influenced by reactive oxygen species and altered signaling pathways. Focal adhesion proteins assemble into intracellular complexes involved in integrin-mediated communication between the extracellular matrix (ECM) and the actin cytoskeleton, regulating many cell physiological processes. Interestingly, recent studies report that integrins bind to Aβ fibrils, mediating Aβ signal transmission from extracellular sites of Aβ deposits into the cell and ultimately to the nucleus. Hydrogen peroxide-inducible-clone 5 (Hic-5) and paxillin are members of the group III LIM domain protein family that localize to both the nucleus and focal adhesions. Hic-5 and paxillin are expressed in numerous regions of the rat brain including cerebellum, striatum, prefrontal cortex, hippocampus, hypothalamus, thalamus, and spinal cord. While little is known about the specific roles of paxillin and Hic-5 in

regulating focal adhesion signaling and gene expression within brain, non-genomic roles for both paxillin and Hic-5 in brain have been described. For example, in cultured neurons, paxillin is rapidly phosphorylated in the presence of fibrillar β-amyloid and colocalized with pTau, leading to altered focal adhesion turnover and loss of synaptic integrity. A functional role for Hic-5 in the brain was revealed by its ability to (1) decrease surface levels of dopamine transporter (DAT) in rat midbrain neuronal cultures and to (2) negatively affect dopamine uptake. A direct interaction between Hic-5 and DAT may be responsible for this effect. While these reports suggest biologic functions of Hic-5 and paxillin in brain, a detailed analysis of paxillin and Hic-5 expression and distribution in normal or AD brain has not been performed. Given the *in vitro* association between paxillin and β-amyloid-induced toxicity and Hic-5 response to oxidative stress, a blinded retrospective cross-sectional study of the human hippocampus for Hic-5 and paxillin was performed. The expression and subcellular distribution of Hic-5 and paxillin in AD and control hippocampus were determined by immunohistochemistry (IHC) from early and late-stage AD and age-matched control subjects. IHC was also used to examine the subcellular distribution of specific phosphorylated isoforms of paxillin. Laser scanning confocal microscopy (LSCM) was used to visualize or demonstrate colocalization of Hic-5, paxillin and phosphorylated isoforms of paxillin. Observations demonstrate changes in the subcellular distribution of Hic-5, paxillin and specific phosphorylated isoforms of paxillin within particular regions of the hippocampus in AD brain. Hic-5 and phosphorylated isoforms of paxillin colocalize with NFTs, while paxillin is predominantly found in reactive astrocytes (stellate-shaped) in the hippocampus of AD brains. Thus, important scaffolding proteins that link various intracellular signaling pathways to the ECM are modified and exhibit altered subcellular distribution in hippocampus during AD.

TABLE OF CONTENTS

LIST OF TABLES

LIST OF FIGURES

PREFACE

I would like to dedicate this work to my children, Duncan and Ariana.

1.0 INTRODUCTION: ALZHEIMER'S DISEASE

1.1 HISTORY

Dementia is a brain disorder that adversely affects one's ability to perform daily activities due to cognitive impairment and memory loss. The cause of dementia is believed to be due to synaptic and neuronal losses in specific brain regions that regulate congnition, memory, and executive functions. Alzheimer's disease (AD) is the most common dementia and is considered a disease of the aging population that was first described by Dr. Alois Alzheimer in 1907 as a progressive brain disorder (1). His patient in 1901, Frau Auguste Deter, progressively developed memory and behavioral abnormalities within a few years until her death in 1906 (1). Upon autopsy of post-mortem brain, Dr. Alzheimer used Bodian's silver stain and observed "cerebral atrophy" (shrinkage of the cortex), "abnormal deposits" now known to be beta-amyloid (Aβ) peptide and "tangled bundles of fibre" that are now known as neurofibrillary tangles (NTFs) (1). In 1910 Dr. Perusini published similar findings from four more cases and the disorder was named after Dr. Alzheimer (2). Dr. Alzheimer's techniques and observations are still currently used to identify the major pathological hallmarks of AD. To date, no known effective cure is available to hault the progression of AD. The cause of AD is unclear but genetic, behavioral and environmental risk factors are believed to contribute to the pathogenesis of this neurodegenerative disease. Increasing age is still the greatest risk factor for AD and the national average life expectancy

continues to rise. Continued research in AD pathology is needed to identify new targets, establish early diagnosis, and obtain better therapies to enhance the quality of life of an ever-increasing aging population (3).

1.2 EPIDEMIOLOGY OF ALZHEIMER'S DISEASE

Increasing age and a family history of dementia are considered the major risk factors for developing late-onset AD, the most common form of AD (4). In the United States, AD is the seventh leading cause of death in the overall population and the fifth leading cause of death in people age 65 and older (3). At this time, most cases of AD are sporadic and do not follow single familial inheritance patterns. Approximately 5.2 million Americans currently live with AD. In general, 5% of adults aged 65 to 74 years have AD and this number doubles every 5 years at which time 50% of adults aged at least 85 years have the disease. The Alzheimer's Association reports that 10 million of the 78 million baby boomers (born between the years 1946 and 1964) currently living (aged 44 to 62 years) will develop AD in their lifetime. It was once thought that women were at higher risk to develop AD but this is now believed not to be the case. More women do have AD but it is because they typically live longer (5). Gender is no longer considered a risk factor as men and woman are equally at risk to develop AD. Interestingly, researchers once believed that a higher education (more than 15 years vs. less than 12 years of education) reduced one's risk of AD (6-9). However, researchers now believe that higher education provides an individual with more synapses and creates a "cognitive reserve" that only delays the time before symptoms of AD are observable (8, 9).

A recent study focusing on the heritability of AD published data comparing 11,884 twins by evaluating genetic vs. environmental risk factors associated with AD including 392 pairs of monozygotic twins or dizygotic twins having AD (10). The concordance of twins with AD is between 58% and 78% with both sets of twins having a similar age of onset (78.1 years) (10). The intrapair standard deviation in the age of onset between the sets of twins showed that monozygotic twins (3.66 $\pm$ 3.63 years) vs. dizygotic twin (8.12 $\pm$ 7.04 years) corresponded to an increased risk of AD in monozygotic twins (10). These authors also published results suggesting that environment factors including the complexity of work based on the rankings from the *Dictionary of Occupational Titles* (United States Department of Labor, 1977) influences whether an individual is at risk of developing AD (11). Thus, studies using data from twins confirms that genetics, behavior, and environmental factors are associated risk factors of AD. Modifying behavior may therefore reduce one's risk of AD.

Four key genes have been linked to the less common autosomal dominant familial early-onset AD (FAD) that manifests before the age of 65 years (12). Strikingly, mutations or presence of specific alleles in each of these four genes lead to increased levels of Aβ (13-16). Three of these genes encode transmembrane proteins that, when combined, account for only 3% of all AD cases including amyloid precursor protein (APP) on chromosome 21 (21q22.3), presenilin 1 (PS1) on chromosome 14, and presenilin 2 (PS2) on chromosome 1 (13-16). The frequency of a mutant apolipoprotein E4 (ApoE4) allele on chromosome 19 (19q13.2) is the only gene linked to both FAD and sporadic late-onset AD (LOAD) (17). Though different genes may be responsible for the development of AD, the same symptoms and pathogenic lesions are observed in both FAD and LOAD. A more detailed description of the mutations in these genes and possible mechanisms of sporadic AD are provided in Section 1.3.2.

Non-genetic risk factors for AD include those related to heart disease and stroke including blood pressure/hypertension, cholesterol levels, diabetes/insulin levels, and obesity as well as other factors including inflammation, homocysteine levels, hormonal levels, head injury, vitamin levels, and smoking (18). Though some of these risk factors have stong correlation with developing AD, heart disease and stroke related risk factors have gained from recent publications. Type II diabetes leads to increased insulin levels due to insulin resistance in liver and muscle cells. Increased insulin levels have been associated with increased levels of Aβ in the cerebrospinal fluid (19). Numerous studies have determined that type II diabetes subjects had at least twice the risk of developing AD (20). In 1996, Selkoe and colleagues published the first report linking insulin and AD (21). They showed that insulin competes with Aβ for insulin-degrading enzyme and in type II diabetes insulin-degrading enzyme does not effectively remove Aβ (22). Mice lacking insulin-degrading enzyme developed both AD (50% increase in Aβ) and type II diabetes pathologies (23, 24). These studies support that diabetes may be associated with the relative risk (RR) of AD (25). Researchers have also shown a correlation between obesity and the increased risk of AD (26, 27). Metabolic syndrome is now described as a disease that encompasses multiple conditions including heart disease, abnormal cholesterol levels, obesity, and diabetes (28). Researchers have found that metabolic syndrome patients become resistant to insulin and lose their ability to utilize glucose efficiently that leads to increased levels of blood sugar levels. Not surprisingly, metabolic syndrome has recently been associated with increased risk of AD (29).

These risk factors point to potential causes or markers of AD that in some cases may be treated either with behavioral changes or drug therapies. However, some of these observations have led to inconsistencies in the findings. For example, cholesterol levels have been implicated

in the risk of AD. However, contradictory results have been reported. In the Kuppio cohort (RR: 2.2) higher cholesterol levels were associated with AD (30). While another study, the Famingham cohort (RR: 0.95), observed no association of cholesterol with AD. Finally, a third study (RR: 0.55) showed higher cholesterol levels to be protective. Thus, this risk factor may not be a viable candidate to monitor AD susceptibility and inconsistent findings may be due to extrinsic or intrinsic factors that will impede the success of determining a viable candidate for monitoring AD. Noteworthy, cholesterol levels have been shown to greatly decrease with age and fluctuate in the presence of other pathologic conditions, such as cancer and cardiovascular disease (31).

Other inconsistencies have been observed in attempts to link particular factors with the risk of AD. For example, the risk of high blood pressure was also thought to be associated with increased RR of AD (32, 33). While other studies found that very high blood pressure to be protective while very low blood pressure was associated with a high risk of AD (34). However, these inconsistencies may be attributable to the test itself. For example, studies with a cohort of Japanese Americans born in Hawaii determined that systolic and diastolic blood pressure peaked at different ages, 59 years and 60 years of age (35). Thus, the age when one specific risk factor (systolic or diastolics blood pressure) is monitored may alter the outcome of a test used to determine the RR of AD. Some variables from the Japanese cohort, including smoking, suggested both behavioral and genetic linkage for the RR of AD (36). Smoking increased the RR of AD (nonsmokers (RR: 1), light smoker (RR: 2), and heavy smoker (RR: 2.5). However, compared to light smokers a decreased RR (though still increased compared to nonsmokers) was found in very heavy smokers (RR: 1.5). These results seem inconsistent and point toward other factors that may be affecting the relevance of associating this risk factor with AD susceptibility.

In fact, genetic analysis of alleles of members of the ApoE family of proteins determined survival rates in these smoking patients correlated to either the presence of either the ApoE2, ApoE3, or ApoE4 alleles (36). ApoE proteins are the major components of the very low-density lipoproteins and known for their role as the principle cholesterol carrier in the brain (37). Smoking patients with both ApoE4 alleles showed the lowest survival rate. ApoE4 is a 299 amino acid glycoprotein that is translated and secreted by astrocytes (38). Mutations in the ApoE4 gene are linked to both FAD and LOAD. Approximately 15% of the total population express the ApoE4 isoform that has been implicated in 50% of all AD cases (39).

Thus, many variables can affect the outcome of a test used to determine the RR of AD including the presence of other conditions or diseases when monitoring cholesterol levels, the age when blood pressure is monitored, and smoking with a susceptible genetic linkage. Combined with genetic links, those related to metabolic syndrome, and other factors including inflammation, homocysteine levels, hormonal levels, head injury, vitamin levels, and smoking, the risk of AD is now beginning to identify not only individual risk factors but those that share common pathologies (18). Therapies are now targeting the etiologies of AD and focused on combinations of risk factors in attempts to slow disease progression or eliminate the contributions of specific risk factors associated with AD.

1.3 CLINICAL FEATURES AND PATHOLOGY OF ALZHEIMER'S DISEASE

1.3.1 Diagnosis

Typically, a family member or those close to the affected individual initially recognizes signs of memory loss or inability to perform daily activities. The Alzheimer's Association has created ten warning signs to distinguish AD associated changes in memory affecting daily activities, each of which justify seeking professional help from a physician. These include memory loss, difficulty performing familiar tasks, problems with language, disorientation in time or place, poor or decreased judgment, problems with abstract thinking, misplaced things, changes in mood or behavior, changes in personality, and loss of initiative (Table 1). Other forms of dementia that are clinically distinct include: vascular or multi-infarct dementia, mixed dementia, Parkinson's disease (PD), dementia with Lewy bodies, physical injury to brain, Huntington's disease, Creutzfeldt-Jacob disease (CJD), frontotemporal dementia/Pick's disease (FTD), and normal pressure hydrocephalus (Table 2) (40). To diagnose AD in living subjects, physicians must utilize family history, patient history, neurological characteristics, neuropsychological evaluations, psychological testing, blood tests, and neuroimaging. The overall observation that confirms a diagnosis of AD is loss of memory over time. The Functional Assessment Staging scale has been developed to chart the progressive decline in AD patients (Table 3) (41).

Patients that have symptoms but do not necessarily meet the criteria to be diagnosed with a dementia are considered to have mild cognitive impairment (42-44). Mild cognitive impairment is considered a stage between normal aging and dementia. Over time, mild cognitive impairment patients may develop dementia, fail to progress to dementia or even revert to normal cognitive status. Not surprisingly, researchers have found that mild cognitive impairment

Table 1. 10 warning signs of AD

	Signs	Examples	What's Normal
1	Memory Loss	Forgetting recently learned information is one of the most common early signs of dementia.	Forgetting names or appointments occasionally.
2	Difficulty performing familiar tasks	People with dementia often find it hard to plan or complete everyday tasks.	Occasionally forgetting why you came into a room or what you planned to say.
3	Problems with language	People with AD often forget simple words or substitute unusual works, making their speech or writing hard to understand.	Sometimes having trouble finding the right word.
4	Disorientation to time and place	People with AD can become lost in their own neighborhoods, forget where they are and how they got there, and not know how to get back home.	Forgetting the day of the week or where you were going.
5	Poor or decreased judgment	Those with AD may dress inappropriately, wearing several layers on a warm day or little clothing in the cold.	Making a questionable or debatable decision from time to time.
6	Problems with abstract thinking	Someone with AD may have unusual difficulty performing complex mental tasks, like forgetting what numbers are and how they should be used.	Finding it challenging to balance a checkbook.
7	Misplacing things	A person with AD disease may put things in unusual places.	Misplacing keys or a wallet temporarily.
8	Changes in mood or behavior	Someone with AD may show rapid mood swings.	Occasionally feeling sad or moody.
9	Changes in personality	The personalities of people with dementia can change dramatically. They become extremely confused, suspicious, fearful or dependent on a family member.	People's personalities do change somewhat with age.
10	Loss of initiative	A person with AD may become very passive, sitting in front of the TV for hours, sleeping more than usual or not wanting to do usual activities.	Sometime feeling weary of work or social obligations.
Derived from the Alzheimer's Association.			

patients have an increased risk of AD when the symptom involves memory loss (45). Thus, proper diagnosis of mild cognitive impairment in patients provides a window of treatment opportunity to slow or stop the progression of dementias including AD.Psychological tests for subjects that take between 5 to 15 minutes including the Abbreviated Mental Test Score, the Mini Mental State Examination, Modified Mini-Mental State Examination, the Cognitive

Table 2. 10 Forms of Dementia

Dementia	Observations
Alzheimer's Disease	Accounts for 60-70% of dementia cases.
Vascular or multi-infarct dementia	Second most common form, refers to impairment caused by reduced blood flow to parts of the brain. A series of very small strokes block small arteries, overtime noticeable.
Mixed dementia	Condition of AD and vascular dementia occur together.
Parkinson's disease	Affects loss of movement, resulting in tremors, stiffness and impaired speech.
Dementia with Lewy bodies	Often starts with wide variations in attention and a lertness. Individuals have visual hallucinations and Parkinson's disease symptoms.
Physical injury to brain	Trauma can damage or destroy brain cells, and cause symptoms of dementia including memory loss and behavioral changes.
Huntington's disease	An i nherited, progressive disorder that causes irregular movements, personality changes, and ability to think clearly.
Creutzfeldt-Jacob disease	A rare rapidly fatal disorder that impairs memory and coordination, and causes behavioral changes.
Frontotemporal dementia or Pick's disease	A rare disorder that may be hard to distinguish from AD. Personality changers often occur before memory loss.
Normal pressure hydrocephalus	Caused by a buildup of fluid in brain for mostly unknown causes and l eads to difficulty walking, memory loss, and inability to control urine.
Derived from the Alzheimer's Association.	

Abilities Screening Instrument, and the clock drawing test have been developed to provide a quick screen for cognitive deficits with varying success rates (46-50). The Mini Mental State Examination has been the most studied, though the other tests listed above are gaining popularity. However, these tests determine rate of change in memory loss during the course of dementia and only help make a "probable" or "possible" diagnosis of AD. In 2000, Gelb published four areas that could be used in the diagnosis of living AD including cognitive testing, global assessment, functional assessment, and behavioral rating scales that can be scaled to determine rate of progress in the disease and provide individuals the capability to manage the disease (51).

Table 3. A Functional Assessment for 7 Stages of AD Progression

Stages of AD Progression	Diagnosis
No impairment	Normal function
Very mild decline	May be normal age-related changes or earliest signs of AD
Mild cognitive decline	Early-stage AD may be diagnosed in some, but not all, individuals at this point
Moderate cognitive decline	Mild or early-stage AD
Moderately severe cognitive decline	Moderate or mid-stage AD
Severe cognitive decline	Moderately severe or mid-stage AD
Very severe cognitive decline	Severe or late-stage AD

Derived from the Alzheimer's Association

New medical tests are attempting to provide a cost-effective diagnostic tool to improve the accuracy in the identification of AD subjects early enough to provide corrective therapeutic opportunities. The presence of Aβ in the retina has been reported and could lead to early and non invasive diagnosis of AD (52). Neuroimaging, including magnetic resonance imaging (MRI) and computed tomography (CT scan), can reveal structural changes in brain. Positron emission tomography (PET scan) and functional MRI can determine functional alterations in sugar or oxygen consumption at the cellular level (53-56). The Pittsburgh Compound B has been shown to noninvasively detect plaques in living subjects with a PET scan and recent studies suggest this compound may be useful in distinguishing the difference between mild cognitive impairment and AD (53, 56). Studies are ongoing that utilize novel imaging tools to follow the progression of brain pathological changes and identify individuals at risk for AD.

Voorheis and colleagues have developed a blood test, tPST, that detects tau-peptide fragments that are released into the blood by degenerating neurons (57). Normal blood does not contain this marker and this test is believed to be sensitive to the early-stages of AD. Another blood test, NuroPro, measures levels of 59 biomarkers in blood by 2D-PAGE and reports the ablility to distinguish between AD, PD, and amytrophic lateral sclerosis (ALS) (58, 59).

Cerebrospinal fluid levels of Aβ, tau, pTau, and ubiquitin have been studied and may help in the diagnosis of AD. Lower levels of Aβ (1-42), increased levels of tau, pTau, and ubiquitin have been shown to correlate significantly with AD (60-62). In 2005, researchers classified 353 AD patients into 5 subgroups based on cerebrospinal fluid levels of Aβ, tau, and ubiquitin suggesting these 5 groups may benefit from different therapies (63). Though all of these diagnostic measures provide potential resources to better identify the likelihood of developing AD, further studies are needed to enhance and more completely examine their predictive outcomes. The diagnosis of AD is further complicated by the presence of similar pathological lesions in more than one type of dementia. For example, Lewy bodies are now considered to be present in up to 50% of AD cases (64). According to the Alzheimer's Association, experts in Neuropathology can diagnose an AD subject with 90% accuracy. However, post-mortem pathologic analysis is still required to positively identify the underlying brain lesions.

Efforts have been made to standardize the protocols for the classification of AD or determine the underlying cause of the disability. In 1985, the National Institute of Aging established the first consensus of age-related criteria for the neuropathologic diagnosis for AD (65). The Bielschowsky stain, similar to the stain used by Dr. Alzheimer, has been used to count the three types of labeled senile plaques (diffuse, neuritic, and central/dense core) in specific brain regions. Neuritic plaques are considered the best indicator in the diagnosis of AD. In 1991, the Consortium to Establish a Registry for Alzheimer's Disease (CERAD) was published and established common criteria regarding specific information for the diagnosis of AD including standard protocols for inter-laboratory comparisons (66). These protocols include fixing autopsied brain in 10% buffered formalin, use of 6-8 μm paraffin sections, Bielschowsky

stain to detect neuritic plaques and use of additional brain sections common to other dementias to determine an age-related plaque score (none, sparse, moderate, or frequent). This information was then combined with a living clinical diagnosis of dementia to conclude whether a suspected individual was finally confirmed to have been suffering from AD. The CERAD criteria do not utilize tangle formation for this determination. In 1991, Braak and Braak published results that identified a pattern of tangle formation that correlated to a staging system (stages I/II, III/IV, or V/VI) of AD in different brain regions (67). Stages I/II associates with NFTs primarily in the transentorhinol cortex with few in the CA1 subregion of the hippocampus. In addition to stages I/II, stages III/IV are associated with NFTs that are moderately present in the CA1 and subiculum. Also, ghost tangles (dead neurons with uncleared NFTs) are also found in the originally NFT presenting transentorhinol cortex. In the neocortex, a sparse number of NFTs are found in stages III/IV. In addition to stages I-IV, stages V/VI associates with numerous neocortex NFTs while in stage VI is assicated with numerous NFTs that are present in layer V of the primary visual cortex (line of Gennari). The Braak staging system provided additional criteria in the diagnosis of AD that can be used with the same silver stain to determine the presence of neuritic plaques established by the National Institute of Aging and CERAD criteria. In 1997, the National Institute of Aging and Reagan Institute recommended the use of both CERAD and Braak staging systems to improve the diagnosis of AD (68).

1.3.2 Neuropathology

The two major hallmarks of AD are plaques composed extracellular Aβ and NFTs composed of intracellular pTau in areas of brain involved in memory (68). If a neuron contains NFTs and eventually dies, only “ghost tangles” remain because the aggregated filaments of pTau are not

readily cleared from the cerebral extracellular space. In 1980, researchers found that FAD and LOAD share the same pathology and suggest a common pathogenic signaling underlies both types of AD (69). All AD subjects contain plaques that are due to an increase in the production of amyloidogenic Aβ peptide fragment that is derived from the full length APP (70, 71).

APP belongs to the APP gene family consisting of three members APP and amyloid precursor-like proteins 1 and 2 (APLP1 and APLP2) (70, 71). APP proteins do not share sequence homology with Aβ. All three full-length APP proteins contain a large extracellular N-terminal domain (624-700 amino acids), a single transmembrane domain (25 amino acids), and a short cytoplasmic C-terminal domain (46 amino acids). Knock-out mice for each APP member are viable with only subtle neurological deficits. However, a combined knock-out for APP/APLP2 or APLP1/APLP2 results in early postnatal lethality (PO) (72, 73). This suggests a redundant role for at least the APLP2 gene in this family. APP has been shown to be involved in many aspects of cell metabolism including neurite outgrowth, neuronal survival, cell-cell adhesion, axonal transport, cell-proliferation, synaptogensis, transcriptional regulation and cell-ECM adhesion (integrin activation) (74-80). APP has at least 3 known isoforms (695, 751, and 771 amino acids) are generated by alternative splicing (81). APP695 is the predominant isoform and is expressed only in neurons while APP751 and APP771 are expressed in neural and non-neural cells.

APP is proteolytically cleaved by two different pathways producing either the non-amyloidogenic or amyloidogenic peptide (81, 82) . Typically APP is predominantly cleaved by α-secretase between Lys687 and Leu688 to produce the non-toxic/non-amyloidogenic soluble extracellular fragment (sAPPα) leaving the membrane bound C-terminial 83 amino acid (C83) fragment. APP can also be cleaved by β-secretase between Met671and Asp672 to produce the

non-toxic soluble extracellular fragment (sAPPβ) leaving the membrane bound C-terminal 99 amino acid (C99) fragment. In both pathways, the C83 and C99 fragments of APP at the membrane surface can be further cleaved by γ-secretase at Val711 or Ile713 to produce the same APP intracellular domains (AICD) but the remaining peptide fragments have different lengths. The non-toxic small peptide (P3) is derived from the C83 fragment while the toxic Aβ (either 40-42 amino acids) peptide is derived from the C99 fragment. Both APP cleavage pathways operate under normal conditions. However, in AD subjects the toxic amyloidogenic pathway generates a sufficient concentration of Aβ to adopt a stable β-sheet tertiary conformation (83). This β-sheet aggregation of Aβ eventually creates plaques. The current prevailing view is that accumulation of the Aβ, specifically the 42 amino acids fragment, contributes to the progression of AD and is not just a marker of the disease (84).

Not surprisingly, researchers have focused on identifying the mechanism of functional regulation of β-secretase and γ-secretase. The only known protein identified containing β-secretase activities is the β-site APP cleaving enzyme (BACE-1), an aspartic proteinase (85). Both presenilins are members of a complex that determines the activity of γ-secretase. Mutations in either PS1 or PS2, changes the activity of γ-secretase and causes increased generation of the toxic 42 amino acid Aβ fragment (14, 86). The majority of mutations that cause FAD are in the PS1 and PS2 genes (86). Both presenilins contain multiple membrane spanning domains that are found mostly in the endoplasmic reticulum and early Golgi apparatus in neurons (14, 86). Surprisingly, the full-length PS1 (46 kDa) and PS2 (55 kDa) proteins are rarely detected endogenously and are proteolytically cleaved to produce different N-terminal and C-terminal proteins (either 28 and 18 kDa fragments or 35 and 20 kDa fragments) (87).

APP and its proteolytically cleaved Aβ fragment have been implicated in plaque formation found in both FAD and LOAD (88). However, it was once thought that plaques take decades to form and may not account for the progressive memory loss. Transgenic mice that over-express Aβ and PS1 forming genes (APP/PS1) generate an abnormal amount of Aβ and develop plaques in 5-6 months (89). To determine the "birthday" of newly forming plaques, the use of a new imaging technique called multiphoton confocal microscopy was used to image the same area over time in the cortex of a living mouse (89). These studies showed that plaques could develop in a single day. Within a couple of days, activated microglia targeted to the newly formed plaques and adjacent neurons became dystrophic. These results support the hypothesis that plaques form first and adjacent dystrophic neurons form second. In support of these *in vivo* findings for the amyloid hypothesis, APP is located on the human chromosome 21 and duplication of this chromosome (trisomy 21) causes Down's Syndrome (DS) (90, 91). In 1977, Heston and colleagues first published that both AD and DS patients showed the same microtubular pathology in neurons and suggested premature aging was linked in these diseases (92). DS subjects that live past 40 years inevitably develop plaques and AD symptoms years before sporadic cases. These subjects have increased Aβ production at this early age. Thus having a third copy of APP increases one's risk of DS and early plaque formation. Other genes on chromosome 21 may also be involved including superoxide dismutase (SOD1). In light of all of the evidence supporting the cytotoxicity of fully aggregated Aβ, an intermediate form of Aβ (neither soluble or fully aggregated) is now considered the cytotoxic form of Aβ (83). However, it is still possible that yet a fourth globular form of Aβ may contribute to the onset of AD (93).

Tau was originally identified in 1975 as a microtuble-associated protein that normally interacts with tubulin to stabilize axonal microtubules in the cell cytoskeleton and is not present

in the dendrites of neurons (94). This protein is regulated by alternative expression of different isoforms and by phosphorylation. Six tau isoforms are found in brain and contain a different number of C-terminal positively charged microtubule-binding domains (95). The three isoforms with four microtubule-binding domains are believed to stabilize microtubules better than the three isoforms with three microtubule-binding domains (95). Typically phosphorylation of tau disrupts microtubule stabilization (96, 97). However, hyperphosphorylated tau can self-assemble into twisted paired helical filaments forming NFTs resulting in dystrophic neurites associated with AD (98). The tau gene is located on chromosome 17q21 and mutations in this gene have shown a genetic linkage to increased NFT production and cause FTD with PD (99, 100). Subjects with these mutations do not contain a significant number of plaques but they do contain an increase in the number of NFTs and are not considered to be associated with AD. In light of tau mutations, the Braak staging system has shown a strong association with NFTs and AD.

Other less studied hallmarks of AD include intracellular aggregates including granulovacuolar degeneration bodies (GVDs) and Hirano bodies. GVDs were identified in 1911 and are considered the third hallmark of AD pathology that is not typically found in normal neurons (101, 102). Using transmission electron microscopy, GVD bodies are seen as intracytoplasmic double membrane vesicles with a dense central granule (103). They are believed to form from the lysosomal autophagy of cytoplasmic substances containing cytoskeleton proteins including neurofilament, tau, and tubulin (104, 105). This organelle then fails to control normal metabolic pathways in neuropathologic conditions. Other proteins have been shown to localize in GVD bodies including Alz-50, casein kinase-1, β-catenin, and GSK-3α/β (106-109). GVD bodies were hypothesized to be involved in neuronal cell death. Dr. Cotman recently identified both caspase-3 and its caspase-cleaved APP fragment (cAPP) in

GVDs (110). The cAPP fragment was previously found to be a caspase-substrate during apoptosis and is distinct from the C-terminal domains created by secretases (110). These data suggest that cAPP and caspase-3 may be involved in neuronal death with cells containing GVD bodies.

Hirano bodies were first identified as intracellular, paracrystalline, eosinophilic rod shaped structures in neurons of the Guam-Parkinson-dementia complex and later in Guam-ALS subjects (111, 112). Using electron microscopy, Hirano bodies appear to contain alternating rows of actin filaments (111, 113). These crystalline structures are typically found in pyramidal neurons in the hippocampus that are considered a characteristic of normal aging and not specific to AD (114). However, it is believed that Hirano bodies are increased in AD subjects. Hirano bodies are formed after aberrant caspase cleavage to produce an actin filament fragment (fractin) at Asp244 to generate a N-terminal 32 kDa and C-teriminal 15 kDa peptide fragments (115). The 32 kDa fractin fragment crystallizes to form a non-degradable protein complex. Other proteins have been shown to localize to Hirano bodies including α-actinin, actin, ADF/cofilin, cAPP, FAC1, HCNP, Hsp27, iNOS, MAP1, MAP1/2, neurofilament proteins, tau, trypomyosin, and vinculin (116). A mammalian cell culture system has recently been developed to investigate Hirano body formation (117).

The four hallmarks of AD described are now targets for investigation to reveal the mechanism of their formation and clearance from brain and their respective roles in pathogenesis. Both *in vivo* and *in vitro* studies have provided the focal point for investigations that may lead to greater understanding of the mechanisms in the pathogenesis of AD. Biological markers may also be identified aiding in the early diagnosis of AD and monitoring of effective therapies.

1.3.3 Cytoskeletal abnormalities

1.3.3.1 Introduction

In tissue, the ECM regulates many aspects of cellular function. Typically, specific ECM molecules bind to integrin cell surface receptors and activate downstream focal adhesion cell adhesion molecules involved in the regulation of anchorage-dependent cell survival signals (118-123). Focal adhesions are macromolecular protein complexes that link integrin mediated signaling to the actin cytoskeleton (119, 122, 124, 125). Upon cell adhesion, integrins utilize both structural and signaling cell adhesion molecules to impact cellular motility and viability (119, 122, 125, 126). During the initial stage of cell adhesion to the ECM, numerous proteins are required for focal adhesion assembly: the activity of each may be regulated by specific post-translational modifications such as phosphorylation (119, 121, 122, 125, 127-129). For example, integrin activation leads to the phosphorylation and sequestration of LIM domain containing proteins, such as paxillin, which create an intracellular scaffold for many interacting cytoskeleton signaling proteins (124, 130, 131). Paxillin and the closely related protein Hic-5, are members of the group III LIM domain family that contain seven zinc fingers, at least four N-terminus leucine-rich motifs termed LD motifs, and numerous sites modified by phosphorylation (124, 130-135). Hic-5 and paxillin share many interacting partners, hive a high degree of amino acid homology between their LIM domains and can act either competitively or antagonistically in many signal transduction pathways (130, 132, 136-139).

Focal adhesions also assimilate many signaling molecules including growth factor receptors, cadherins, syndecans, and G-protein-coupled receptors, thereby affecting the cellular response to various signals (119, 121, 122, 125, 127, 140). Paxillin is a scaffolding protein and is phosphorylated on tyrosine amino acid residues 31 and 118 (pY31 and pY118) upon the initial

activation of ECM-integrin signaling and the formation of intracellular focal adhesion sites (130, 140-144). Specific phosphorylation of paxillin is required for the activation of distinct downstream signaling pathways (141, 142, 145-147). The integration of a variety of signaling cascades is further influenced by the ability of some focal adhesion proteins to regulate gene expression (126, 131). In fact, both Hic-5 and paxillin have been shown to localize within both cytoplasmic focal adhesions and the nucleus (126). This ability to act both in the nucleus and focal adhesions suggests that intracellular trafficking may impact their biological functions. Hic-5 contains two nuclear export signal sequences within its leucine-rich domains (133). Furthermore, H_2O_2 induces Hic-5 nuclear import in cultured fibroblasts (133). The biological consequences of Hic-5 nucleocytoplasmic shuttling are unclear, although Hic-5 has been shown to be both a positive and negative coregulator of gene expression (148-154).

Integrins and numerous focal adhesion cell adhesion molecules are expressed in all cells throughout the brain and numerous studies indicate a role for integrin signaling in neurite outgrowth during differentiation and in response to the toxic effects associated with neurodegeneration (122, 140, 141, 145, 155, 156). Integrins have now been shown to bind Aβ and activate focal adhesions through integrin clustering, cell adhesion molecule mobilization, and/or cooperatively with growth factor signaling through cell surface growth factor receptors (144, 156-158). Specifically, if fibrillar Aβ is added to cells in culture, both FAK and paxillin are rapidly phosphorylated leading to downstream signaling events that can regulate cell viability (144, 156, 157). The participation of focal adhesion proteins in the pathogenesis of AD has been postulated based upon integrin mediated interactions with Aβ *in vitro* (144, 156-159). Aß induced activation of integrins in AD could trigger downstream signaling events linked to focal adhesion complexes that differentially affect cell function and survival. Neuronal viability and

synaptic loss during the course of AD and potentially other neurodegenerative disorders may be solely mediated through focal adhesion signaling. The role of focal adhesion proteins and downstream pathways in AD warrants further investigation. An analysis of focal adhesion proteins that link integrin activation to downstream signaling cascades should provide insightin helping to identify both upstream early events and downstream late events in cellular responses to various pathological features of AD.

1.3.3.2 Amyloid beta toxicity through integrin signaling

(a) Integrins

Cells adhere to the ECM, basement membrane or connective tissues, to regulate various cellular processes including growth, proliferation, survival, differentiation, morphology, migration, and death (119, 122). The ECM signals through the cell surface integrins, a family of transmembrane subunits including 18 alpha and 9 beta subunits that generate at least 24 different integrins which function as heterodimeric receptors (119, 121, 122). Integrins mediate both cell/ECM and cell/cell adhesions, although they do not contain intrinsic enzymatic activities (119, 126, 160, 161). Instead, integrins associate with numerous intracellular effector cell adhesion molecules.

During the initial stage of cell adhesion to the ECM, numerous cell adhesion molecules are required for focal adhesion assembly, each of whose activity may be regulated by specific post-translational modifications such as phosphorylation (119, 121, 122, 125, 127-129). These cell adhesion molecules assemble into immature less dense peripherially located focal adhesion complexes and mature more dense centrally located focal adhesion complexes associated with actin stress fibers (125, 130, 162). More than 100 cell adhesion molecules are localized to focal

adhesions coupling to the actin cytoskeleton and regulating the structural components of the focal adhesions to efficiently organize multiple signaling pathways. focal adhesions are macromolecular protein complexes that link integrin mediated signaling to the actin cytoskeleton (119, 122, 124, 125). Upon cell adhesion, integrins utilize both structural and signaling cell adhesion molecules to impact cellular motility and viability (119, 122, 125, 126). Structural cell adhesion molecules include actin, α-actinin, α-tubulin, Hic-5, paxillin, Crk associated substrate ($p130^{cas}$), talin, tensin, vinculin, and zyxin (119, 122, 125, 126). Signaling cell adhesion molecules include FAK, Fyn, phosphoinositide-3 (PI-3) kinase, c-Abl, Crk, Csk, Grb-2, Nck, and PYK2 (119-122, 126, 161). Many of these signaling cell adhesion molecules are tyrosine kinases known to be upstream of serine/threonine kinases including members of the mitogen activated protein kinase (MAPK) pathway, cyclin dependent kinase 5 (CDK5), and glycogen synthase kinase-3β (GSK-3β) (119, 121, 122, 126, 130, 155).

Focal adhesions also assimilate many signaling molecules including growth factor receptors, cadherins, syndecans, and G-protein-coupled receptors thereby affecting the cellular response to various signals (119, 121, 122, 125, 127, 140). For example, initial activation of ECM/integin signaling leads to the phosphorylation and sequestration of scaffolding proteins including paxillin, that create an intracellular scaffold for many interacting cytoskeleton signaling proteins and activation of downstream signaling pathways (124, 130, 131, 141, 142, 145-147). The integrin activation of paxillin is discussed in greater detail in Section 3. In addition, protein tyrosine phosphatases (PTP-1D, PTP-PEST, and PTP-1B) have been shown to dephosphorylate cell adhesion molecules upon cell detachment and regulate focal adhesion turnover (119, 120, 122, 126). Cell adhesion molecules localized to focal adhesions have been shown to be involved in bidirectional signaling including the compartmentalization of integrin

activated downstream signaling molecules regulating “outside-in-signaling” and the localization and affinity of integrin receptors to regulate “inside-out-signaling” (118, 119, 121, 122, 161). The integration of a variety of signaling cascades is further influenced by the ability of some focal adhesion proteins to directly regulate gene expression (126, 131). Ultimately, cell adhesion signaling through integrins and focal adhesions can impact the viability of the cell(159).

Integrins are expressed in all cells throughout the brain and influence long-term potentiation in hippocampal neurons, regulate neurite outgrowth induced by growth factors, and regulate survival and death signals (122, 140, 141, 155, 156). Not surprisingly, numerous focal adhesion cell adhesion molecules are also expressed in brain and numerous studies indicate a role for integrin signaling in neurite outgrowth during differentiation and in response to the toxic effects associated with neurodegeneration (144, 145, 155-158). Neurite outgrowth is promoted by the growth of neuronal cells on laminin, an integrin substrate (140, 141, 145, 163). Specific inhibitors of the Src-family kinases can block neurite outgrowth (140, 141, 145). When SH-SY5Y (human), N1E-115 (rat), and Neuro-2a (mouse) cells were plated on laminin and treated with retinoic acid to induce neuronal differentiation, both FAK and paxillin were shown to have increased tyrosine phosphorylation compared to adhesion during active neurite outgrowth (141, 144, 164).

(b) Focal adhesion unit and function

Focal adhesions were originally identified in cultured fibroblast cells (Abercrombie, 1971). FAK is a non-receptor tyrosine kinase that is activated upon integrin clustering forming AD sites (165-167). When cells adhere to the ECM, integrins are activated and FAK is autophosphorylated at position Y397, creating a high affinity-binding site for Src-homology 2 (SH2) domain containing proteins (120, 121, 165-167). Src family kinases (Src and Fyn) contain SH2 domains and

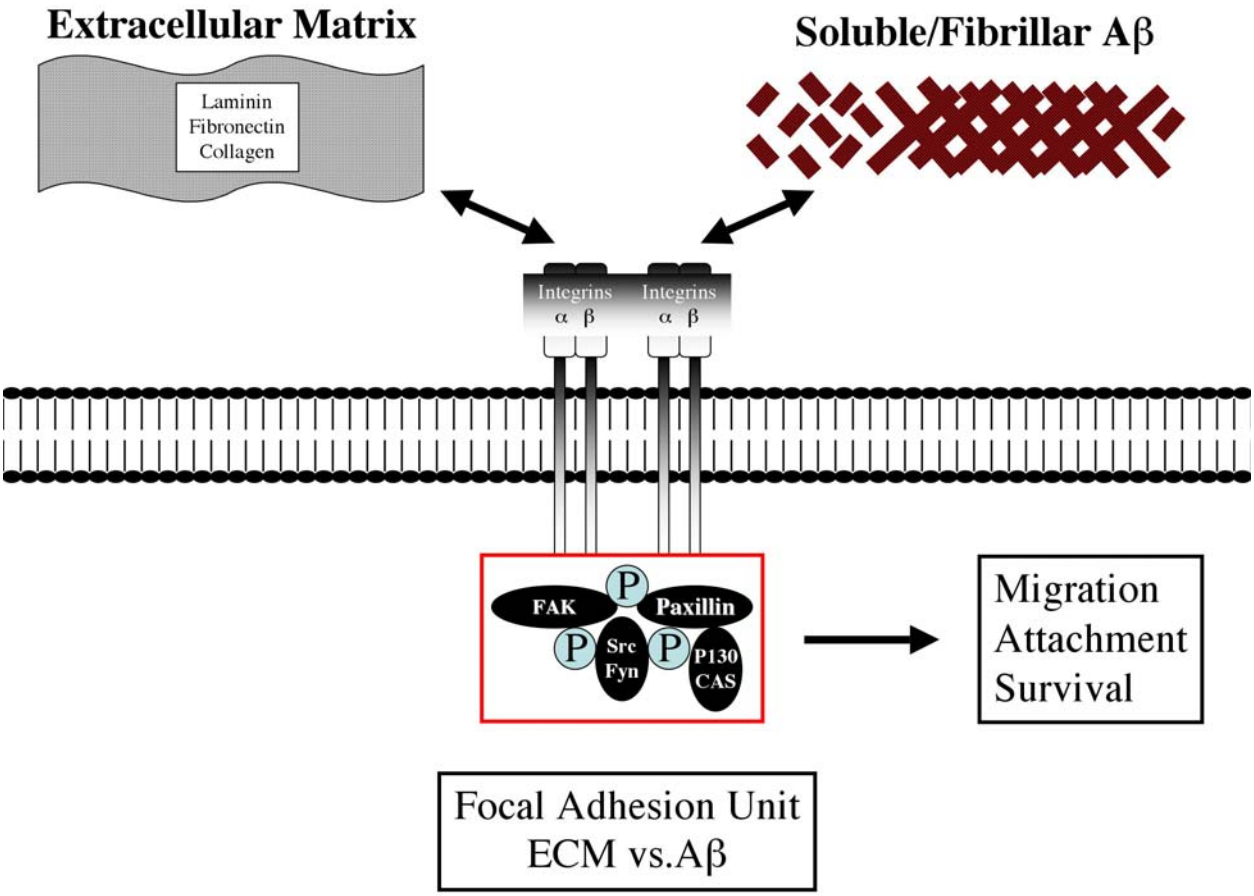

Figure 1. Early signaling pathways mobilized at focal adhesion formation
Integrin activation/adhesion promotes FAK autophosphorylation site recruits SH2 domain proteins including Src and Fyn leading to further FAK phosphorylation and other FA proteins including paxillin. Phosphorylated paxillin then binds to $p130^{CAS}$ forming the FA unit. Integrin receptor binding to fibrillar Aβ mimics early ECM/integrin signaling.

recognize phosphorylated FAK-Y397 (120, 121, 165-167). This complex can further phosphorylate FAK and other focal adhesion structural and signaling cell adhesion molecules including paxillin and $p130^{cas}$ (120, 121, 165-167). The assembly of FAK/Src family/paxillin/$p130^{cas}$ creates the essential four cell adhesion molecules necessary for focal adhesion stabilization and integrin signaling that has been termed "quartenary signaling and structural focal adhesion-unit" (121, 168) (Fig.1). The focal adhesion-unit connects the various signaling cell adhesion molecules mobilized to focal adhesions to coordinate integrin clustering,

cell-cell adhesion, and growth factor signaling (118, 119, 121, 122, 126, 161, 165, 167). In fact, this ECM/integrin/focal adhesion-unit pathway is involved in the regulation of anchorage-dependent cell survival (118-122). Disruption of this pathway, either through the loss of cell adhesion or microinjection of anti-FAK antibodies, results in the activation of an anchorage-dependent cell death pathway called anoikis (greek for "homelessness") (118-122, 161, 167). Expression of constitutively active FAK can prevent anoikis in anchorage independent cells, including cancer cells (118, 120, 165-167). Cell adhesion to the ECM and over-expression of FAK protects cells from oxidative stress by H_2O_2 or ionizing radiation induced apoptosis (120, 121, 167). The anti-apoptotic effect is dependent on FAK Y397-autophosphorylation and the PI3-K/Akt survival pathway (120, 121, 167). Recently, FAK has also been shown to directly interact with and inhibit the tumor suppressor protein p53 induced apoptotic signaling and induced the expression of cdk inhibitor p21 (169, 170). Interestingly, p53 also has the ability to directly regulate the expression of FAK and provide a negative feedback mechanism for p53-induced apoptosis leading to cell survival (169). Therefore, FAK has the ability to regulate multiple survival pathways involved in cell death or survival. These findings support the important role for cell attachment in cell adhesion-mediated drug resistance and resistance to ionizing radiation. Such pathways may also contribute to neuronal cell death/survival pathways during AD.

In addition to regulating cell adhesion and survival pathways, FAK and paxillin also function during neuronal differentiation (140, 141, 145). Nerve growth factor increases the level of paxillin tyrosine phosphorylation during neuronal differentiation in PC-12 cells (145). Two members of the FAK family (FAK and PYK2) regulate neurite outgrowth in both PC-12 and SHSY-5Y cells (171). The c-Jun N-terminal kinase (JNK) pathway has also been shown to

activate paxillin during cell migration in PC-12 cells (147). Finally, during nerve growth factor induced neuronal differentiation p38 MAPK and CDK5/p35 were shown to activate paxillin through serine phosphorylation (145). The role of focal adhesion cell adhesion molecules in neurite outgrowth and neuronal differentiation is now appreciated and investigators are interested in how focal adhesions function in neurodegenerative diseases such as AD.

(c) Amyloid beta binding to integrins and activation of intracellular pathways

Integrins can bind Aβ and activate focal adhesions through integrin clustering, cell adhesion molecule mobilization, and/or cooperatively with growth factor signaling through cell surface growth factor receptors (144, 156-158) (Fig.1). The phosphorylation of tyrosine residues has been shown to be involved in numerous cell signaling pathways leading to Aβ toxicity which have stimulated studies examining how integrins modulate the toxic effects of Aβ (144, 156-158). Both FAK and paxillin were found to be tyrosine phosphorylated after exposure to fibrillar Aβ, well in advance of cell death (144, 156-158). Aβ induced cell death was found to be dependent on cell anchorage and required the treated cells to have a neuronal phenotype, actin cytoskeleton, and Aβ induction of tyrosine phosphorylation (144, 156-158). In a recent report, SHSY-5Y cells treated with fibrillar Aβ failed to exhibit altered FAK or paxillin phosphorylation status until they were differentiated by retinoic acid (141, 144, 164). retinoic acid differentiated SHSY-5Y cells treated with cytochalasin D to disrupt actin polymerization or addition of monomer Aβ did not alter tyrosine phosphorylation of FAK or paxillin nor induce cell death (141). Fibrillar Aβ exposure did not induce changes in the overall protein levels of FAK or paxillin but induces a substantial increase in their tyrosine phosphorylation (FAK-Y397 and

paxillin-Y31/118) and evidence of protein mobilization from the cytosolic fraction to the membrane fraction (144, 156, 157). Specifically, focal adhesion size and proportion of complexes that are positive for paxillin were found to be elevated in fibrillar Aβ treated neurons (157). These results were specific to FAK and paxillin because no changes in the mobilization of another focal adhesion protein, vinculin, were found (157). It has been suggested that in cell culture the early effects of fibrillar Aβ are the induction of FAK and paxillin tyrosine phosphorylation, which mimic early events in integrin signaling during adhesion and/or growth factor signaling (156). Therefore, FAK and paxillin are rapidly phosphorylated by fibrillar Aβ, leading to downstream signaling events that can regulate cell viability.

To investigate the downstream pathways activated by FAK in primary cortical neurons, Williamson *et. al.* used a variety of kinase inhibitors and demonstrated that FAK activated by fibrillar Aβ induces both ERK2 and GSK-3 serine/threonine kinase signaling pathways (156). FAK activation relied on both PI3-K and the Src family member Fyn for downstream signaling. Interestingly, FAK activation did not rely on ERK1, Src, PYK2, PKC, or Ca^{+2} signaling. Fibrillar Aβ causes an increase in the tyrosine phosphorylation of MAP2c and tau that could be blocked with inhibitors specific for Src family kinases and PI3-K (156).. ERK2 activity was sustained for at least 1 hour and tau phosphorylation occurred on serine residues recognized by the paired-helical-filament-1 (PHF-1) antibody (156).. Thus, it is likely that FAK/Fyn/PI3-K activation induces ERK2 and GSK-3 signaling and phosphorylation of tau and MAP2c. In this model system FAK also induced anti-apoptotic signaling via the sequential activation of Fyn/FAK/PI3-K/MAPK pathways (156). However, incomplete activation of these pathways fails to enhance cell survival and may lead to cell death. Fibrillar Aβ does not activate the

complete Fyn/FAK/PI3-K/MAPK pathways and, therefore, the incomplete mimicking of this survival pathway may contribute to neuronal cell death during AD.

1.3.3.3 Integrin mediated cell cycle activation in Alzheimer's disease

(a) Cell cycle activation in Alzheimer's disease

In AD neuronal degeneration predominantly occurs in specific regions of the brain, including the hippocampus, frontal cortex and temporal cortex, which function in learning, memory and language. Typically mature neurons are arrested in the cell cycle G_0 phase to permit the ongoing morphological alteration and synaptic remodeling. Thus, downregulation of G_0 arrest proteins or induction of G_1 entry proteins will result in the unbalance between cell cycle and differentiation control.

Cell cycle progression is controlled by regulating activity of a series of CDKs through the coordinated expression of cyclins and cyclin dependent kinase inhibitors (CDKI) (172). Cyclin D1 is a critical regulator of the cell cycle transition from G_0 to G_1. Accumulation of the cyclin D1/cdk4 complex leads to activation of kinases that phosphorylate and inactivate retinoblastoma protein (Rb), releasing its inhibition of E2F and allowing the transcription of E2F-target genes, such as cyclin E, cyclin A and cdc2 (172). Cyclin E forms a complex with cdc2 and promotes G_1 to S phase transition (172). Both cyclinE and cdc2 have been shown to be upregulated in cell culture models of neuronal cell death (173). The activity of cyclin D1/cdk4 complex and cyclin E/cdc2 complex is regulated by CDKI, p27 and p21, respectively (173). Increased levels of p27 and phosphorylated p27 (Thr187) are present in the cytoplasm of vulnerable neuronal populations in AD brain (174). Phosphorylated p27 (Thr187) colocalizes with dystrophic neurites, neurofibrillary tangles and neuropil threads.

In AD, cyclin D and cdk4 show aberrant expression in the hippocampus and subiculum, but not in the cerebellum (175). Our lab has demonstrated increased phosphorylated Rb (ppRb) and E2F1 immunoreactivity in AD brain compared to control brain, and ppRb was predominantly localized within the nucleus while E2F1 was in the cytoplasm (176). Both ppRb and E2F1 were found in the cells surrounding a subset of Aβ -containing plaques. *In vitro* cell models exhibit similar ppRb and E2F1 distributions in PC12 cells upon Aβ treatment (177). Increased levels of Cyclin D1, cyclin E and ppRb have been demonstrated in the early stage of AD, however, their levels are decreased by late stage AD (178).

MAPK is phosphorylated by its upstream kinase called MAPK-kinase (MAPKK). Both MAPK and MAPKK exhibit increased expression in potentially vulnerable neurons still unaffected by neurofibrillary degeneration during the early stages of AD (179). The subcellular redistribution of MAPK from cytoplasm to nucleus also indicates that MAPK might contribute to AD pathology via activating downstream nuclear signal pathways regulating protein transcription and/or translation. For example, MAPK signaling pathway contributes to neuronal apoptosis by directly phosphorylating the cytoskeleton protein tau or by indirectly activating downstream kinases that consequently phosphorylate tau (180). However, additional evidence indicates that MAPK signaling pathway plays a role in the balance between cell survival and death through its influence on cell cycle progression, as discussed above. Abnormal upregulation of cell cycle regulators and MAPK activation has been found in AD subjects or associated with AD suggesting that MAPK signaling pathway promotes cell death by inappropriatly triggering cell cycle re-entry in AD.

(b) Integrin/focal adhesion kinase activation of the cell cycle

Prior studies indicate that FAK plays an important role in cell cycle progression at the G_1/S transition by regulating the expression and activity of cell cycle proteins including cyclins, cyclin dependent kinases (CDKs) and CDK inhibitors (127). As discussed above, activation of FAK leads to autophosphorylation and binding to intracellular signal molecules including Src and PI3-kinase (165). FAK/Src association activates ERK through two different signal pathways and ERK phosphorylation and activation was associated with neuronal cell bodies and dystrophic neurites around plaques in late AD (181). The first pathway phosphorylates the focal adhesion proteins paxillin and $p130^{cas}$, and leads to activation of MAPK signaling pathway through recruiting focal adhesion adaptor proteins Crk and Nck (128). $P130^{cas}$ has been shown to be functional in central neuronal system disorders, such as hypoxia-ischemia induced neuronal degeneration (182). The other pathway is activated upon binding with focal adhesion adaptor Grb2/SOS and Ras dependent phosphorylation, a family of small G protein including Ras, Rac and Rho proteins, linking growth factor signaling and tyrosine kinases with MAP Kinase, JNK, and p38 MAP kinases (183, 184). After activation of the ERK signaling pathway by FAK, Cyclin D1 is upregulated at the transcriptional level (166).

FAK also interacts with PI3-K to activate the PI3-K signaling pathway, regulating cell survival and cell progression by Akt, Rac and PKC (127). A recent study reported that in tumor cell lines, FAK induced PI3-K/PKC/Akt activation resulted in an induction of cyclin D3 expression and promotion of cell cycle progression from G_1 to S phase (185). The induction of cyclin D3, but not cyclin D1, also has been demonstrated in endothelin treated astrocytes (186). However, cyclin D3 induction in astrocytes is via the small G-protein Rho, and is not dependent on PI3-K and Src. This difference indicates that FAK regulates cell cycle progression through

different signal pathways in different cell types. The signaling pathways involved in the function of FAK on cell cycle regulation in neurons remain unclear. However, FAK activated by amyloid beta peptide 1-42 induced MAPK signaling pathways through its association with Fyn, instead of Src in primary cultured cortical neurons (156). As noted above, Aβ leads to incomplete activation of the FAK/Fyn/PI3-K/MAP kinase pathways that can induce cell death. In addition, FAK activation of ERK kinase pathways may upregulate cyclin D1 and induce cell cycle progression.

However, Guan and his colleagues found that FAK/PI3-K association is insufficient for cell cycle progression but FAK/Src complex plays an essential role (187). Additionally, Src-dependent association of FAK with $p130^{cas}$ and Grb2 are both required for the cell cycle regulation by FAK. Grb2 regulates the cell cycle as an adaptor for cytoskeleton proteins and was recently reported to bind with C-terminal domain of APP (188, 189). This interaction increases in reactive astrocytes of AD, resulting in Ras/MAPK activation (188, 189).

Cyclin D1, a key component of the cell cycle, is regulated by FAK by multiple pathways (165). A recent study demonstrated that FAK upregulates cyclin D1 expression through ERK activation in fibroblast cell lines (166). After the Ras/Raf/MEK/ERK signal pathway is activated by FAK, ERK phosphorylates its downstream target Ets. Ets then binds to the Ets binding consensus site B, EtsB, in the promoter of the cyclin D1 gene to activate its transcription. However, the MEK/ERK pathway not only acts to induce cyclin D1 gene transcription but functions post-translationally to enhance cyclin D1 assembly with CDK4 and sequester p27Kip1 from inhibiting the cyclin E/CDK2 complex (190). In addition, the PI3-K/Akt signal pathway is a downstream target of FAK and regulates the phosphorylation and turnover of cyclin D1 (191). Finally, Rac increases cyclin D1 protein level through stabilizing cyclin D1 mRNA (161).

Integrin mediated FAK activation also results in a decrease of p21 and p27Kip, key CDK inhibitors (165).

In a summary, FAK/Src or FAK/Fyn association upregulates cyclin D1 expression at the transcriptional level through ERK, PI3-K or Rac signaling pathway and can stabilize cyclin D1 mRNA through Rac. FAK also regulates the turnover of cyclin D1 through PI3-K/Akt signaling pathway, and modulates the level of key CDK inhibitors. Thus, FAK contributes to the inbalance between cell cycle and differentiation control and could influence neuronal cell death and memory loss in AD subjects.

1.3.3.4 Integrin mediated transcription

Cell type specificities in the control of the cell cycle by the ECM-integrin-FAK-focal adhesion pathway are most likely dependent on gene expression of cell cycle regulatory proteins. As discussed above, FAK signaling is directly involved in the regulation of cyclin D1 (165, 166). Activation of these transcription factors is dependent on the activities of FAK/Src and FAK/PI3-K complexes and directly targets the promoter of cyclin D1. However, FAK activation can also regulate the expression of transcription factors that can indirectly regulate the expression of cell cycle regulators. Recently FAK was shown to regulate the expression of a member of the Kruppel-like factor (KLF) family of transcription factors (192). The KLF family contains at least 25 members, many of which are important regulators of cell cycle regulators and have been shown to both positively and negatively regulate the cyclin D1 promoter in various cells (192-194). In mouse fibroblast cells, KLF8 was shown to positively regulate cyclin D1 expression and cell cycle progression that is dependent on both FAK/Src and FAK/PI3-K integrin mediated signaling pathways (192). FAK activities were found to coordinate the expression of cyclin D1 promoter element through a “temporal differential manner” of the cell cycle with an early

induction through Ets binding followed by a later induction after FAK up-regulated the expression of KLF8. Numerous types of human cancer have elevated FAK and KLF8 expression levels and their activities are implicated in cell cycle progression during tumorigenesis (192-195). However, other members of the KLF family including KLF1, 4, 6,and 7 have all been shown to be negative regulators of cell cycle progression by decreasing cyclin D1 promoter activity and increasing cdk inhibitor p21 expression levels (193, 194). KLF7 is also believed to control neuronal differentiation and exit from the cell cycle by increasing expression of TrkA, a receptor for nerve growth factor (193). How integrin signaling mediated by FAK regulates the cell cycle progression dynamically either positively (Ets and KLF8) or negatively mediated by members of KLF family in neuronal cells and AD, remains to be determined.

The complex balance of both positive and negative signals for cyclin D1 expression during cell cycle progression at multiple layers as described for FAK is conserved in other well-known pathways that utilize focal adhesions. Wnt signaling through membrane bound frizzled protein family members and β-catenin mediates cell-cell adhesion signaling to the actin cytoskeleton similar to how FAK mediates ECM-cell adhesion signaling (126, 196-198). GSK-3β is an important negative regulator in β-catenin signaling through phosphorylating and targeting β-catenin to the proteosome for removal (197). Not surprisingly, β-catenin is also an important mediator in the signaling of cell cycle events (197). The β-catenin interaction and regulation of T cell factor (TCF) transcription factor has been well characterized in development and regeneration in multiple tissue types (196, 197). Enhanced β-catenin signaling and activation of TCF has been shown to induce cyclin D, bcl-2, and engrailed-1/2 (en-1/2) expression (197, 199, 200). These proteins function during development and favor cell survival and cell cycle progression. In AD the Wnt/β-catenin/TCF pathway is disrupted with subsequent

loss of β-catenin expression and TCF survival signaling (197, 199, 200). However, activation of the Wnt/β-catenin/TCF survival pathway by insulin, protein kinase C (PKC), agonists for PPARγ, and inactivation of GSK-3β all have the ability to protect primary cortical neurons to Aβ induced cell death (195, 197, 199, 200). β-catenin can also mediate cell cycle arrest through enhanced Forkhead box O (FOXO) transcriptional activity (198, 201, 202). Under conditions of oxidative stress, β-catenin interacts with FOXO for translocation into the nucleus to induce the expression of cell cycle inhibitor p27, leading to cell cycle arrest in late G_1 phase (198). Thus, cell adhesion molecules associated with at least two distinctly different adhesion complexes (ECM/integrin and cell/cell) dynamically regulate the progression and arrest of the cell cycle. The mechanism of cell adhesion complexes regulating the cell cycle is redundant, yet specific, for unique signaling inputs. Determining how focal adhesion complexes regulate neuronal viability in AD will lead to novel therapeutic approaches to modulate neuronal survival and synaptic remodeling during AD.

A number of cell adhesion molecules including LIM domain containing proteins (Discussed in Chapter 3) have been shown to shuttle between focal adhesions and the nucleus to regulate expression of numerous genes including: c-Abl, β-cat, CASK, CDK5, ERK, FAK, GSK3β, ILK, JAB1, PINCH, PYK2, and members of the LIM family of proteins (Hic-5, paxillin, Trip6, leupaxin, and zyxin) (126, 130). Many of these targets have been implicated in the molecular pathology of neurodegenerative diseases, though the functional role for each of these proteins in neurodegeneration is not fully understood. This ability to act both in the nucleus and focal adhesions suggests that intracellular trafficking may impact their biological effects.

Our lab and others have shown that Kelch-like Ech Associated Protein (Keap1) is an actin binding protein that has the ability to regulate the subcellular distribution of transcription factors including Fetal ALZ-50 Reactive Clone 1 (FAC1) and Nrf2 in neurons (203-206). Keap1 is localized to periphery focal adhesions containing paxillin, vinculin, and tyrosine phosphylated proteins (204). Keap1, when bound to Nrf2, targets Nrf2 destruction by ubiquitin-mediated pathways (205, 206). However, under conditions of oxidative stress both Keap1 and Nrf2 translocate to the nucleus and nuclear Nrf2 positively regulates promoters containing the anti-oxidant response elements (AREs) (204-206). The induction of Nrf2 mediated survival pathways at the transcription level is considered a conserved function in every cell type (206). FAC1 is a developmentally regulated transcription factor that modulates expression of numerous genes (177, 207). In AD brain and PC-12 cells treated with Aβ, FAC1 exhibits altered expression and subcellular distribution from the cytoplasm to the perinuclear region (177). FAC1 is believed to be an important regulator in Rb and E2F cell cycle activities in response to neurotoxic signals (207). Recently, FAC1 was shown to be an alterantive splice form from a much larger bromodomain PHD transcription factor (BPTF) that is implicated in chromatin remodeling (208). En-1 gene expression was positively regulated by BPTF (208). Since en-1 and en-2 gene expression is required for normal neuronal development, altered expression and subcelluar distribution of factors that associate with their promoter elements could disrupt engrailed expression and activities in AD. How integrin signaling regulates the focal adhesion/Keap1/Nrf2/ARE survival pathway and focal adhesion/Keap1/FAC1/BPTF transcriptional activities in response to toxic neuronal stimuli remains to be determined but the data support a role for altered distribution of cell adhesion molecules in regulating numerous cellular responses to toxic stimuli.

1.3.3.5 Integrins modulate neuronal survival

During early steps of the cell cycle, the ECM/integrin/FAK/focal adhesion pathway regulates anchorage-dependent cell survival (119, 122). Disruption of this cell attachment pathway results in a specific cell death called anoikis and this ECM/integrin/FAK/focal adhesion pathway may actually limit neuronal mitosis (118, 120). Fully differentiated and mature neurons in the adult brain exhibit evidence of cell cycle activation upon oxidative stress or exposure to Aβ fibrils (160, 163, 177, 209, 210). A recent study used a genomic probe for chromosome 11 to identify a pyramidal neuron in the hippocampus of AD brain with four copies of chromosome 11 indicating that this neuron synthesized DNA (210, 211).

As noted above, *in vitro* models of neuronal injury using Aβ and oxidative stress have reproduced the induction of integrin signaling, cell cycle regulators, DNA damage, and apoptosis. Recent models of S-phase induction in neurons include two mouse mutants (stagger and lurcher), overexpression of viral oncogenes and E2F1, targeted disruption of Rb, and a model of stroke all of which show increased levels of BrdU incorporation in neuronal cells indicative of DNA synthesis (163, 209, 212). However, BrdU incorporation is not specific to DNA replication and may also be reflective of DNA repair (210). Post-mitotic cells have increased vulnerablility to DNA damage and repair (210). Growth factor and ECM/integrin signaling appear to inhibit DNA synthesis in neuronal but not in other cell types including glia (163). One hypothesis is that activation of the integrin/FAK/focal adhesion pathway by fibrillar Aβ induces cell death within neurons that concurrently exhibit activation of cell cycle proteins. Loss of ECM/integrin signaling (i.e. loss of cell attachment signaling) may induce anoikis mediated cell death with concurrent dis-inhibition of DNA synthesis. Therefore, the appearance of DNA synthesis in some neurons during AD may result from altered focal adhesion signaling.

1.4 CURRENT THERAPIES AND THERAPEUTIC TARGETS

Currently there is no cure for AD and current therapeutic strategies only target symptoms and not AD pathogenesis. Though AD has many etiologies, the pathogenesis is similar in all cases, including loss of information transfer at the synapse, loss in number of synapses, and selective neuronal cell death. AD is associated with the loss of cholinergic neurons in the nucleus basalis and increased levels of glutamate (213-215). Thus, early drug discovery targeted both neurotransmitter pathways seeking to elevate acetylcholine levels by inhibiting the enzyme known to degrade acetylcholine, acetylcholine esterase, or decrease glutamate signaling through NMDA receptors to protect from glutamate toxicity.

Table 4. Standard Drug Treatments for AD

Drug	Target	Side Effects	Source
Donepezil (Aricept)	Acetylcholinesterase inhibitor	Nausea, vomiting, loss of appetite, increased frequency of bowel movements.	Eisai Inc. Pfizer
Galantamine (Razadyne) (Reminyl) (Nivalin)	Acetylcholinesterase inhibitor, Nicotinic receptor actions	Nausea, vomiting, loss of appetite and increased frequency of bowel movements.	Johnson & Johnson's
Rivastigimine (Exelon)	Acetylcholinesterase inhibitor, Butyrylcholinesterase inhibitor	Nausea, vomiting, loss of appetite and increased frequency of bowel movements.	Novartis Pharm. Corp.
Tacrine (Cognex)	Acetylcholinesterase inhibitor	Used rarely due to liver damage, nausea, and vomiting.	
Memantine (Namenda) (Akatinol) (Axura) (Ebiza)	Glutamate regulation, NMDA-noncompetitive antagonist	Headache, constipation, confusion and dizziness.	
Derived from the Alzheimer's Association and package inserts.			

Table 5. Alternative AD drug and diet therapies

New Drugs	Target	Source
Flurizan (Tarenflurbil) (MPC-7869) (R-flubiprofen)	Plaque formation. Gamma secretase modulator, lowers Aβ 1-42 levels	Myriad
Bapineuzumab (AAB-001)	Plaque formation	Elan/Wyeth
Xaliproden	Reduce neurodegeneration in animal studies	Sanofi-Synthelabo Inc.
Tramiprosate (3APS) (Alzhemed)	GAG-mimetic binds soluble Aβ reducing plaques	Neurochem Inc.
Leuprolide	Reduce luteinizing hormone levels	DOR BioPharma

The only medications approved for AD by the United States Food and Drug Administration target cognitive deficits and include cholinesterase inhibitors and enhancers of glutamate signaling (Table 4). These drugs are most effective when AD symptoms first appear and slow its progression for one year in 20% of patients (216). Typically, physicians determine which cholinesterase inhibitor the patient responds positively by initially administering the drug with a lowtitration to help the patient develop a tolerance to the known side effects. When this class of drugs is no longer effective the physician switches the patient to memantine (a glutamate enhancer) and when the patient no longer responds to glutamate enhancers, the patient is then prescribed a combination of both drug classes simultaneously (217). However, current guidelines recommend cessation of these drug treatments when dementia becomes severe (218).

Alternative drug treatments or diets have been proposed that target the cause of cognitive impairment and memory loss due to synaptic and neuronal losses in AD. These include lowering cholesterol (statins), lowering homocysteine (folic acid), vitamin E, monoamine oxidase inhibitors, steroids (estrogen), anti-inflammatory agents, ginko bilobo, curry, fish oil, fresh fruit,

and huperzine-A (219) (220-226). However, conflicting reports necessitate further investigation into the effectiveness of these alternative treatments. There are a number of drugs in clinical trials that target AD pathogenesis mechanisms and some have indicated early successes (Table 5). Vaccines or immunotherapy has also been used to treat already diagnosed AD patients by adapting the immune system to remove Aβ. Initial studies were promising in 20% of those treated but increased encephalitis was fouind in 6% of the trial participants and led to a halt in the study. Second generation vaccines are currently in production that hopefully will not cause an encephalitic response in patients (Table 6).

Table 6. New AD drug candidates in clinical trials

New Drugs	Target	Source
Flurizan (Tarenflurbil) (MPC-7869) (R-flubiprofen)	Plaque formation. Gamma secretase modulator, lowers Aβ 1-42 levels	Myriad
Bapineuzumab (AAB-001)	Plaque formation	Elan/Wyeth
Xaliproden	Reduce neurodegeneration in animal studies	Sanofi-Synthelabo Inc.
Tramiprosate (3APS) (Alzhemed)	GAG-mimetic binds soluble Aβ reducing plaques	Neurochem Inc.
Leuprolide	Reduce luteinizing hormone levels	DOR BioPharma

During AD progression, memory loss is not the only symptom and often changes in behavior may be unhealthy or put the patient at risk for injury. Drugs used to treat behavioral deficits include antidepressants, anxiolytics, and antipsychotics (Table 7). Non-drug treatments target the behavior of the patient and include environmental modifications (noise or light levels),

changes in activity demand (introduce routines and reduce complexity), and interpersonal approaches (focus on patient's wishes, interests, and concerns) (227).

Table 7. Behavioral drugs used during AD drug treatments

Antidepressants	Anxiolytics	Antipsychotics	Seizure/mood stabilizer
low mood, irritability	anxiety, restlessness, agitation, aggression, verbally disruptive behavior and resistance	hallucinations, delusions, aggression, agitation, hostility and uncooperativeness	agitation
Citalopram (Celexa) Fluoxetine (Prozac) Paroxeine (Paxil) Sertraline (Zoloft) Trazodone(Desyrel)	Lorazepam (Ativan) Oxazepam (Serax)	Aripiprazole (Abilify) Clozapine (Clozaril) Haloperidol (Haldol) Olanzapine (Zyprexa) Quetiapine (Seroquel) Risperidone (Risperdal) Ziprasidone (Geodon)	Carbamazepine (Tegretol) Divalproex (Depakote)

1.5 SPECIFIC AIMS

The overall hypothesis tested in this thesis is whether changes in the expression and localization of focal adhesion proteins paxillin and Hic-5 occur during AD. Both Hic-5 and paxillin are expressed in numerous regions of rat brain. However, no study to date has addressed the expression profile of these proteins in specific human brain regions. Thus, my studies may be particularly relevant in cases of altered redox state where Hic-5 and paxillin trafficking and genomic function may be affected. Furthermore, the expression patterns and functional interactions of Hic-5 and paxillin with its various partners at both the plasma membrane and the nucleus could impact neuronal cell responses to toxic insults in AD. The ability to detect distinct phosphorylated isoforms of paxillin with specific antibodies allowed for an indirect assessment

of signaling pathways that may be altered in AD. Western Blot (WB), IHC and immunofluorescence (IF) analysis was used to determine the tissue specific expression and subcellular localization of Hic-5, paxillin, and phosphorylated isoforms of paxillin in specific regions of human brain and stages of AD. My findings demonstrate the subcellular distribution of Hic-5, paxillin and phosphorylated isoforms of paxillin within particular regions of hippocampus including pathological hallmarks found in AD brain. Functional interactions between two group III LIM domain proteins, Hic-5 and paxillin, have direct consequences on paxillin's role in Aß-induced neuronal toxicity. Thus, intracellular signaling molecules that have both genomic and non-genomic effects are responding to distinct extracellular cues in AD versus normal brain. Understanding the consequences in neurons of subcellular localization and/or phophorylation of paxillin and Hic-5 may provide insights into the cellular signaling pathoways that contribute to AD pathogenesis. These studies have generated novel hypotheses regarding intracellular signaling events important for regulating neuronal response and survival during AD.

2.0 DETAILED DESCRIPTION OF LIM DOMAIN PROTEINS

Focal adhesions are essential protein complexes involved in signal tranduction pathways that generally amplify input from various upstream activators. For example, the ECM signals through the cell surface integrins to efficiently organize multiple signaling pathways mediated by the assembly of more than 100 intracellular effector cell adhesion molecule to form components of focal adhesions (119, 121, 122). Ultimately, signal transduction by cell adhesion signaling through integrins and focal adhesions impact the viability of the cell.

2.1 LIM DOMAIN PROTEINS

LIM domain family proteins associate with focal adhesions and regulate numerous signal transduction pathways through their protein interacting domains. The LIM domain proteins are a family of proteins that share a common motif comprised of two zinc finger structures with the consensus sequence $CX_2CX_{16-23}HX_2CX_2CX_2CX_{16-21}CX_2$(C/H/D) (Fig. 2) (124, 228-231). The LIM family was originally named after the three originally identified homeodomain proteins Linl-1, Isl-1, and Mec-3, and LIM now refers to the Zinc finger domains within each family member (232, 233). This family is diverse but can be divided into four groups based on the location of the LIM domains including N-terminal, LIM only, C-terminal, and functionally diverse LIM domain proteins (131). However, most LIM domain proteins in the four groups

contain specific functions based on other protein interacting domains. In fact, other protein interacting domains within the LIM family members impact the specificity in downstream signal transduction pathways (Fig. 3). The integration of a variety of signaling cascades is further

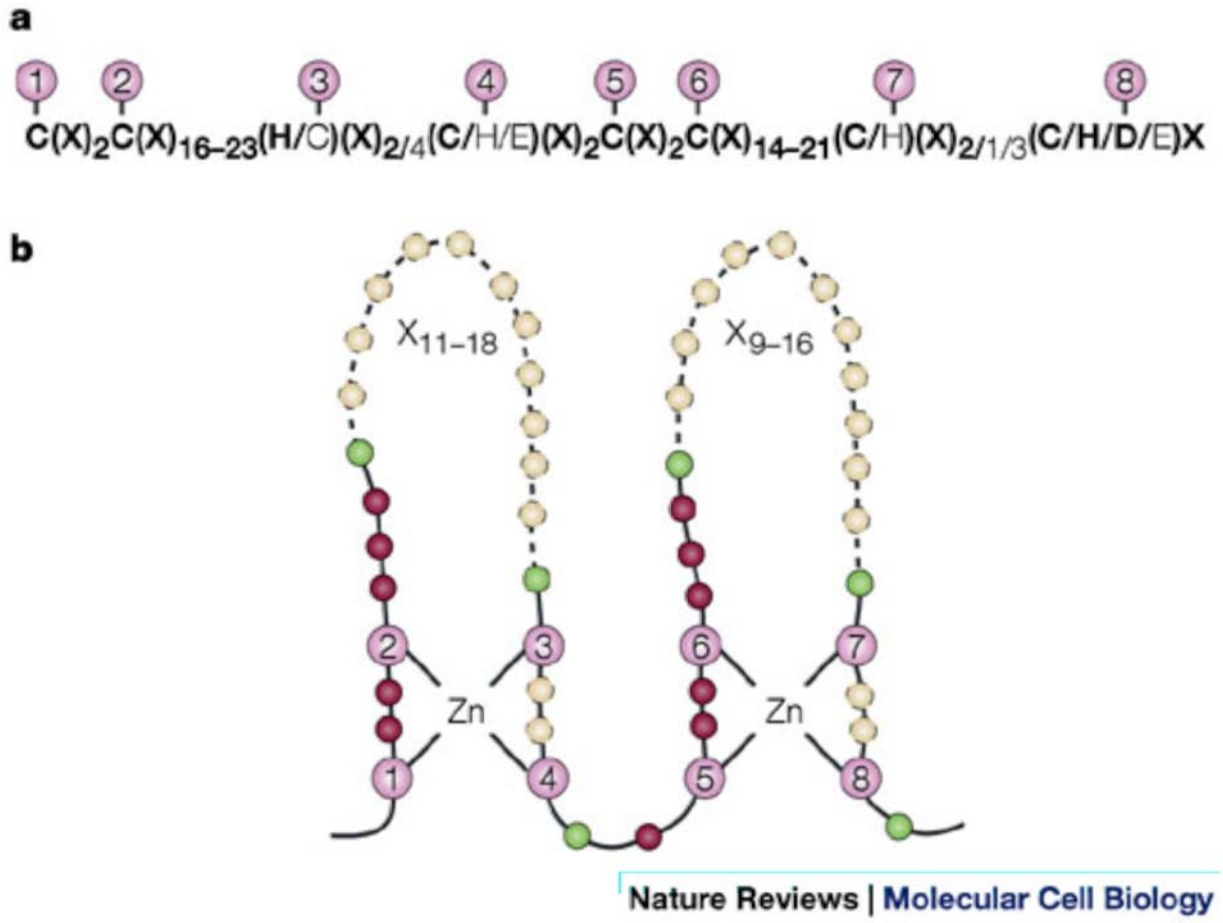

Figure 2. Schematic representation of LIM domain
The spacing and identity of the eight zinc-binding residues (1–8) based on an analysis of 135 human LIM sequences. Infrequently observed patterns (which are seen in <10% of cases) are denoted by text that is not bold. X denotes any amino acid. b | Topology of zinc coordination. Purple circles indicate the zinc-binding residues. Semi-conserved aliphatic/bulky residues are shown as green spheres. Non-conserved residues with invariant spacing are represented as magenta spheres. Dashed yellow circles indicate a variable number of residues (X) that are possible within the sequence. Reprinted by permission from Macmillan Publishers Ltd: [Nature Reviews Molecular Cell Biology] (131), copyright 2004.

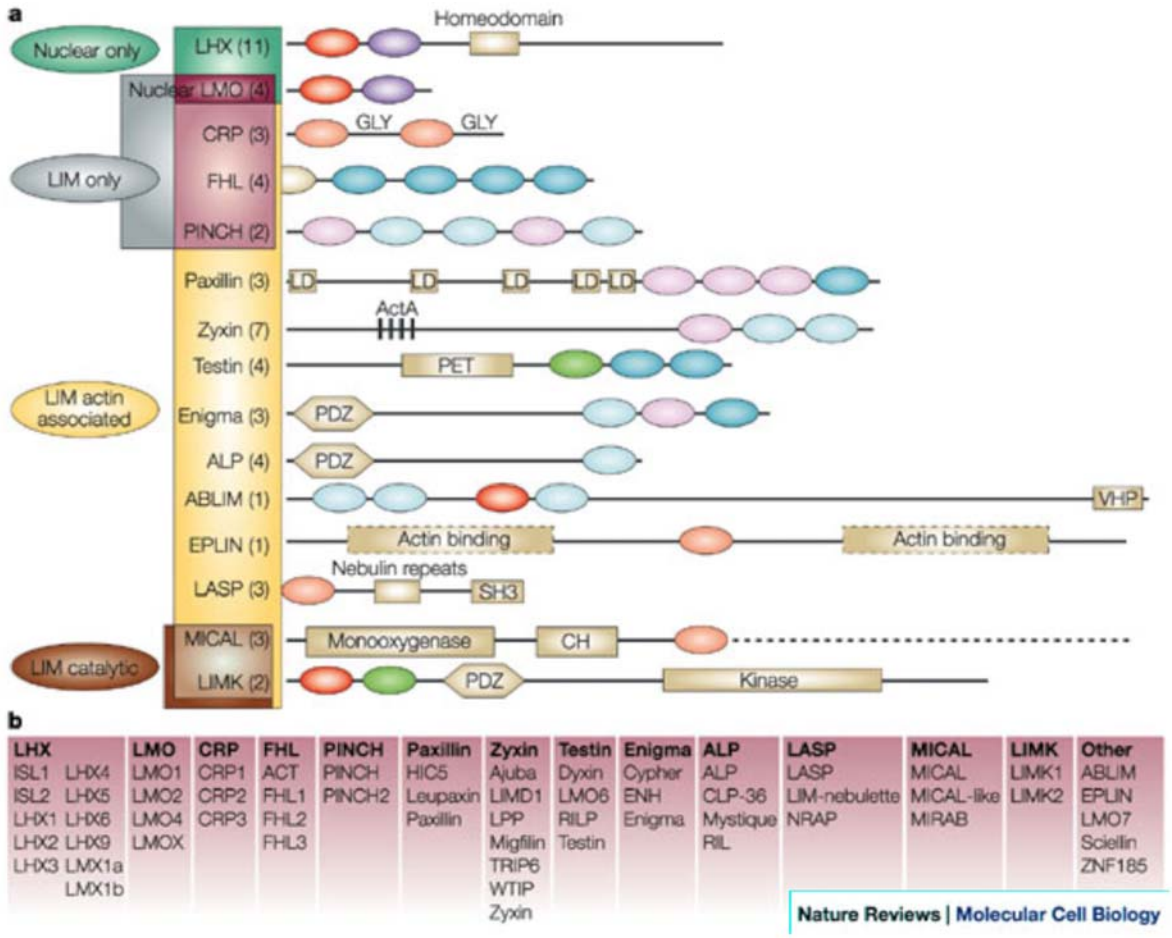

Figure 3. LIM domain family classification

The domain structures of the founding member and/or the most characterized example of the main LIM-protein families are shown. The number of known members of each family is indicated in parentheses. The coloured boxes represent several commonly used categorization schemes. Individual LIM domains are shown as coloured ovals that have been subjectively grouped according to the similarity within the LIM sequence. Heterologous domains such as the LD motif, the monooxygenase domain and actin-binding domains are described in the main text. Domains with boundaries that are not precisely defined are shown as dashed boxes. Dashed lines indicate that scale is not preserved. b | A list of the identified members of each LIM family. ABLIM, actin-binding LIM protein; ACT, activator of cyclic AMP response element modulator (CREM) in the testis; ALP, alpha-actinin-associated LIM protein; CH, calponin homology; CRP, cysteine-rich protein; EPLIN, epithelial protein lost in neoplasm; FHL, four-and-a-half LIM; GLY, glycine-rich region; LASP, LIM and SH3 protein; LHX, LIM-homeodomain protein; LIMK, LIM kinase; LMO, LIM only; MICAL, molecule interacting with CASL protein-1; PDZ, postsynaptic density-95, Discs large, zona occludens-1; PET, prickle, espinas and testin; PINCH, particularly interesting new cysteine and histidine-rich protein; SH3, Src-homology-3; VHP, villin head piece. Reprinted by permission from Macmillan Publishers Ltd: [Nature Reviews Molecular Cell Biology] (131), copyright 2004.

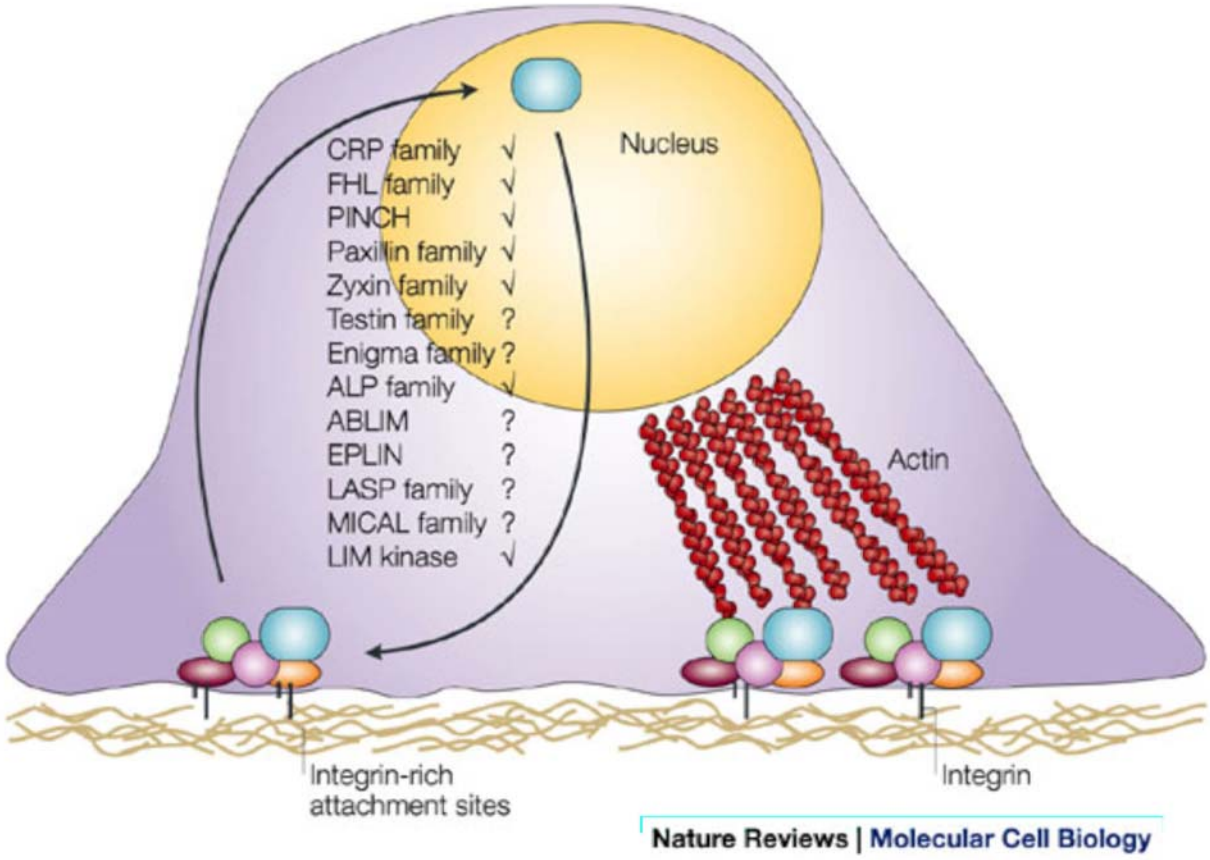

Figure 4. LIM domains shuttle between focal adhesions and nucleus
LIM proteins that have been observed at focal adhesions, muscle-attachment sites or other analogous integrin-rich attachment structures are listed. Many of these proteins can also be found in the nucleus (radic), although a nuclear localization for other proteins in this group has not yet been examined (?). Dual localization might function in communication between these cellular compartments. ABLIM, actin-binding LIM protein; ALP, alpha-actinin-associated LIM protein; CRP, cysteine-rich protein; EPLIN, epithelial protein lost in neoplasm; FHL, four-and-a-half LIM; LASP, LIM and Src-homology-3 protein; MICAL, molecule interacting with CASL; PINCH, particularly interesting new cysteine and histidine-rich protein. Reprinted by permission from Macmillan Publishers Ltd: [Nature Reviews Molecular Cell Biology] (131), copyright 2004.

influenced by the ability of some focal adhesion proteins to regulate gene expression (131, 133, 136, 139, 148-154, 195, 228, 234). Surprisingly, numerous LIM domain proteins including ALP, CRP, Hic-5, FHL, leupaxin, LHX, LIM kinase, LMO, paxillin, PINCH, Trip6, and zyxin have been shown to localize within both cytoplasmic focal adhesions and the nucleus (Fig. 4)

(126). This ability to act both in the nucleus and focal adhesions suggests that intracellular trafficking may impact their biological effects and separate different targets including short-term (adaptive) vs. long-term (gene expression).

2.2 STRUCTURE OF THE LIM DOMAIN

The LIM domain structure has been determined by multidimensional NMR spectroscopy and by X-ray crystallography (235). The number and spacing of cysteine and histidine residues indicated to researchers that LIM domains are metal-binding structures (236). LIM domains are characterized by the presence of zinc finger that consists of two anti-parallel β strands and a α helix. Further studies showed LIM domains preference for zinc compared to iron; the sequesters two zinc ions that are crucial for stability of LIM structure (228).

2.3 GROUP III LIM DOMAIN PROTEINS

2.3.1 Introduction

Integrin activation leads to the phosphorylation and sequestration of LIM domain containing proteins, such as paxillin, which create an intracellular scaffold for many interacting cytoskeleton signaling proteins and the formation of focal adhesions (124, 130, 131). Paxillin and the closely related protein Hic-5, are members of the group III LIM domain family that contain seven zinc fingers, at least four N-terminal leucine-rich motifs termed LD motifs, and numerous potential

phosphorylation sites (124, 130-135). Paxillin is a scaffolding protein and is phosphorylated on tyrosine amino acid residues 31 and 118 (pY31 and pY118) upon the initial activation of ECM-integrin signaling and the formation of intracellular focal adhesion sites (130, 140-144). Specific phosphorylation of paxillin is required for the activation of distinct downstream signaling pathways that can further amplify the original input by the association of the other protein interacting domains within paxillin (141, 142, 145-147).

In humans the genes for paxillin and Hic-5 were identified on chromosome 12q24.31 and 16p11.2, respectively (237, 238). Paxillin, was first identified in 1989 as a substrate for tyrosine kinases in Rous sarcoma virus-transformed fibroblasts (239). In 1990 paxillin was characterized as a scaffolding protein due to the numerous protein interacting motifs and proposed function to link actin and membrane integrins through its interaction with focal adhesions and actin binding protein vinculin (240). Paxillin is evolutionarily conserved across species including human, mouse, rat, zebra fish, Drosophila/fruit fly, slime mold, and yeast (238, 241-249).

In higher eukayotes, paxillin alternative splice forms have been identified. A splice variant that encodes the C-terminal portion of paxillin (PDLP) has been identified in Drosophila (243, 244). In humans, at least 4 alternative splice forms (paxillin-α, -β, -γ, and -δ) have been identified (130, 247, 248). Paxillin-α is a 559-amino acid protein that is expressed only in extraembryonic tissue during murine gastrulation (250). Later in midgestation, both paxillin-α and -β are expressed in mesodermal and endodermal tissue (251). Paxillin-γ expression is further restricted and limited to myeloid cells and differentiating promonocytic cells express both paxillin-β and -γ (252). Paxillin-β and -γ are generated by the addition of 34 and 48 amino acid insertions into the 277/278 amino acid site in paxillin-α (130). In addition to developmental differences in the expression of paxillin-α, -β, and -γ, isoforms -β and -γ have gained additional

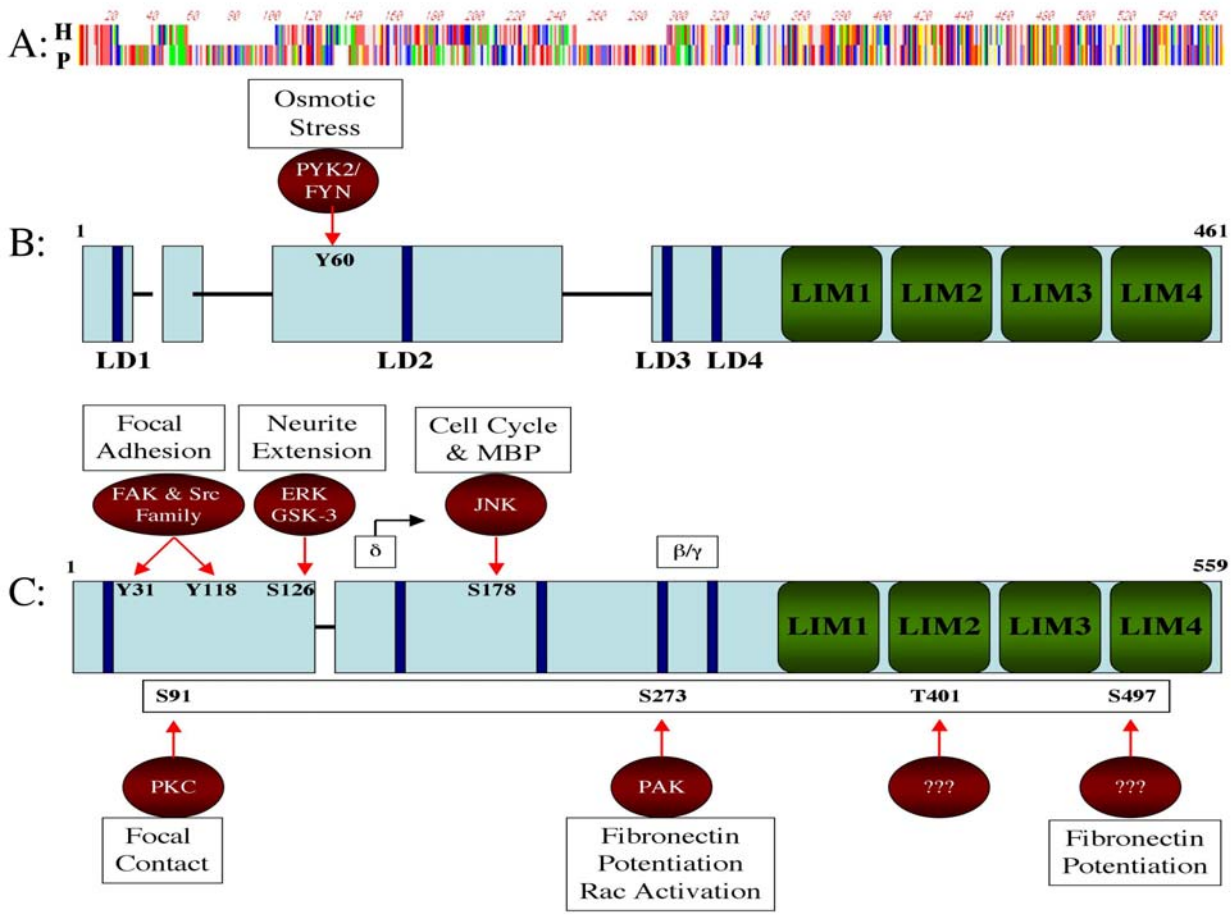

Figure 5. Protein alignment comparing full-length human Hic-5 and paxillin
Full length Hic-5 (NM 001042454) and paxillin (U14588) proteins aligned for similarities based on both chemical type and amino acid compositions. Hic-5 and paxillin have 50% amino acids homology based on 220 (39%) conserved amino acids identities and 64 (11%) similar amino acids based on chemical composition. Major structural differences are observed between Hic-5 and paxillin including four gaps between paxillin and Hic-5 exist including three groups at varying lengths (16, 42, and 44 amino acids) that are not found in Hic-5 at paxillin sites (21-36, 56-97, and 240-283). Red: Acidic (DE), White: Hydrophic (AGILV), Aqua: Amido (NQ), Orange: Aromatic (FWY), Blue: Basic (RHK), Pink: Hydroxyl (ST), Green: Proline (P), Yellow: Sulfur (CM). Sequences were aligned using MacVector v10.0: ClustalW v1.83 multiple sequence alignment.

structural and signaling functions compared to -α (130). These translated paxillin isoforms compete with one another and regulatory molecules to determine phenotypic outcomes (130). In fact, studies focusing on TGF-β1 induced epithelial-mesenchymal transformation have identified antagonist roles for paxillin-α and paxillin-δ proteins critical for the regulation of cell migration

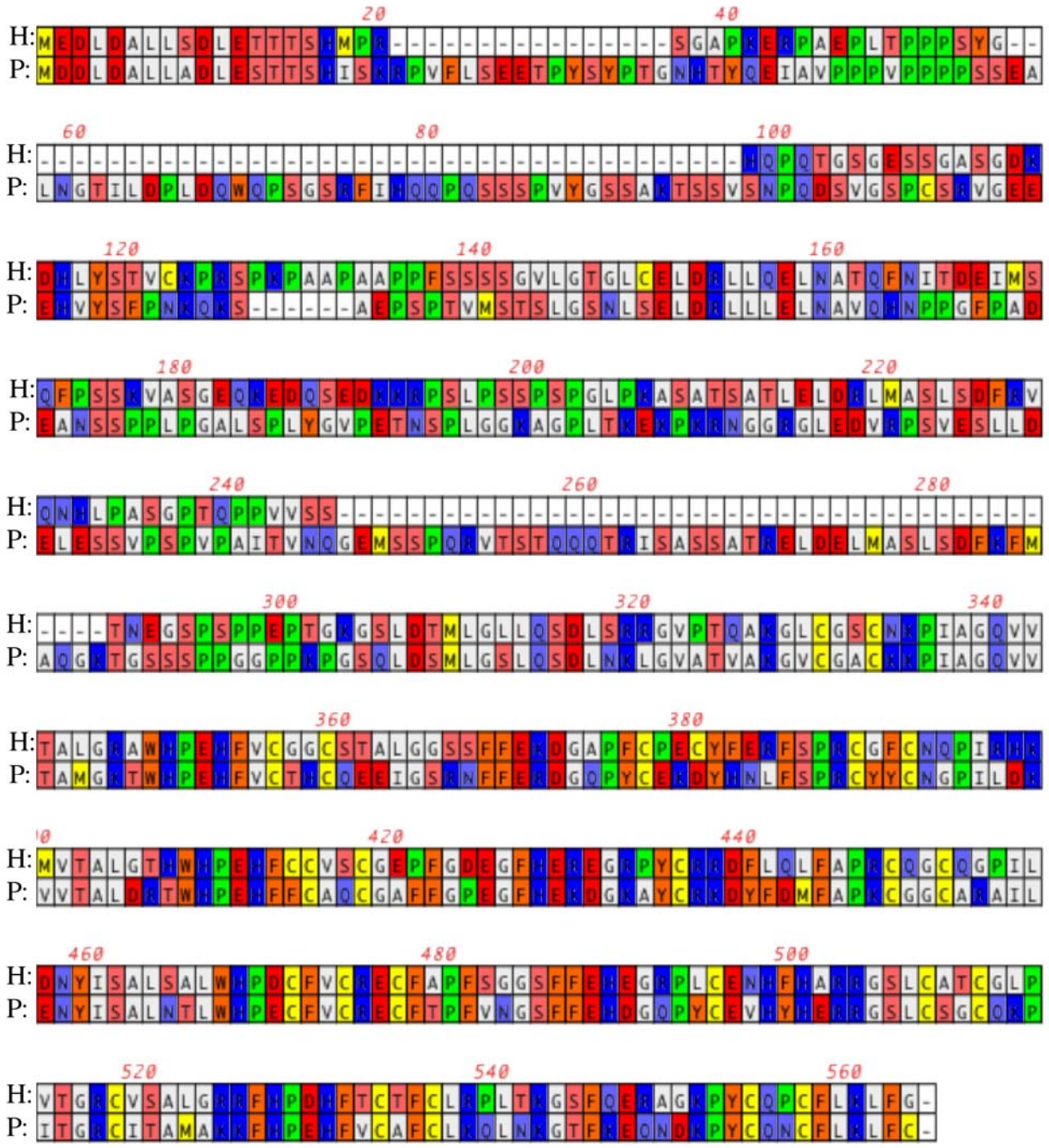

Figure 6. Structural differences between Hic-5 and paxillin

Hic-5 (NM 001042454) and paxillin (U14588) primary structures and known phosphorylation sites were aligned. **(A):** Linear representation of Fig. 5 to determine gaps in the primary amino acids sequence between Hic-5 and paxillin. **(B):** A schematic of Hic-5 is shown. Hic-5 contains 461 amino acids, four LD motifs in the N-terminus, and four tandem LIM domain double zinc finger located on the C-terminus. Hic-5 is phosphorylated on Y60 by PKY2 and Fyn is response to osmotic stress. **(C):** A schematic of paxillin-α is shown. Paxillin contains 559 amino acids,

five LD motifs in the N-terminus, and four tandem LIM domain double zinc finger located on the C-terminus. Alternative splice forms of paxillin are indicated. β/γ isoforms of paxillin are due to the addition of amino acids between LD4/5. δ isoform of paxillin is due to an alternertive Kozak translation start site and does not include the first 133 amino acids found in α/β/γ isoforms of paxillin. Paxillin is phosphorylated on many sites by many kinases including Y31, Y118, S91, S126, S178, S273, T401, and S497. Y: tyrosine, S: serine, T: threonine.

(248). Paxillin-δ utilizes an internal and alternative translation site from a Kozac sequence and an AUG codon at the amino acid site 132 that is present in all three paxillin -α, -β, and -γ isoforms (248). TGF-β1 was found to induce cell migration through the reduction of paxillin expression and ultimately the loss of the N-terminus amino acids known to be critical in the initial activation of ECM-integrin signaling. The formation of intracellular focal adhesion sites are responsible for the loss of migration linked to paxillin-δ (248). The same study further showed that while paxillin and paxillin-δ were expressed mainly in epithelial cells, Hic-5 expression enhanced epithelial-mesenchymal transformations(248).

In vitro paxillin and Hic-5 have been shown to compete in many signaling pathways that may be due to their sequence, structure, or functional similarities and may serve bioloigically relevant roles *in vivo* (130, 132). In fact, paxillin and Hic-5 are 50% similar amino acid sequence with the highest similarity in the protein interaction motifs (Fig. 5). However, major structural differences are observed in paxillin and Hic-5 (Fig. 6). Each shared motif is thought to be antagonistic modules for interacting signaling molecules that compete for either paxillin or Hic-5 (Fig. 7 and 8). The LD motifs are responsible for specific protein interactions and the LD1 motif observed in paxillin-α is not found in Hic-5 and paxillin-δ. Paxilin-α and Hic-5 contain the LD2 motif while leupaxin does not. The LD3, 4, and 5 motifs are conserved among LIM III family members including paxillin, Hic-5 and leupaxin. The LIM domains contain the

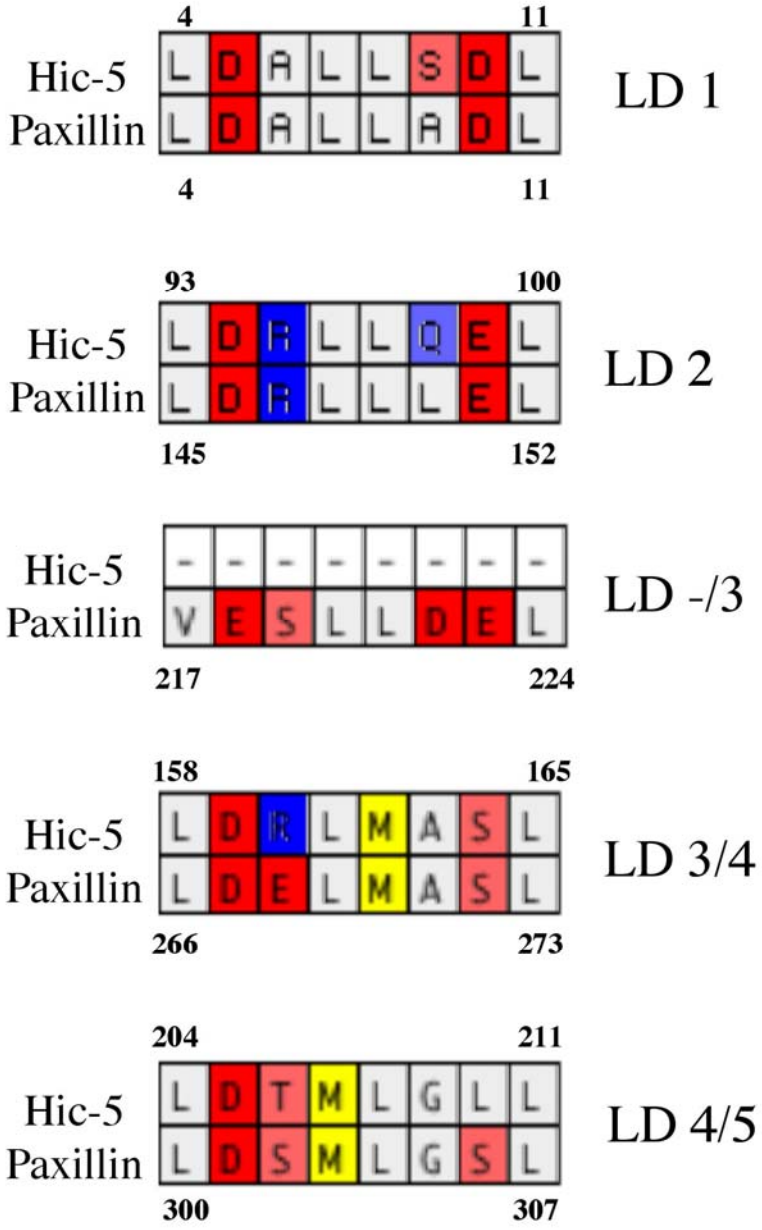

Figure 7. Schematic representation of the distribution of LD motifs within human Hic-5 and paxillin.

Hic-5 (NM 001042454) and paxillin (U14588) have a high percentage of homology in the LD motifs. The LD motifs are localized on the N-terminous in both Hic-5 and paxillin. The appropriate location of amino acids for each LD motif is indicated for both Hic-5 and paxillin. Paxillin has five LD motifs and Hic-5 contains four LD motifs. Hic-5 does not have the paxillin LD 3 motif. Red: Acidic (DE), White: Hydrophic (AGILV), Aqua: Amido (NQ), Orange: Aromatic (FWY), Blue: Basic (RHK), Pink: Hydroxyl (ST), Green: Proline (P), Yellow: Sulfur (CM). Sequences were aligned using MacVector v10.0: ClustalW v1.83 multiple sequence alignment.

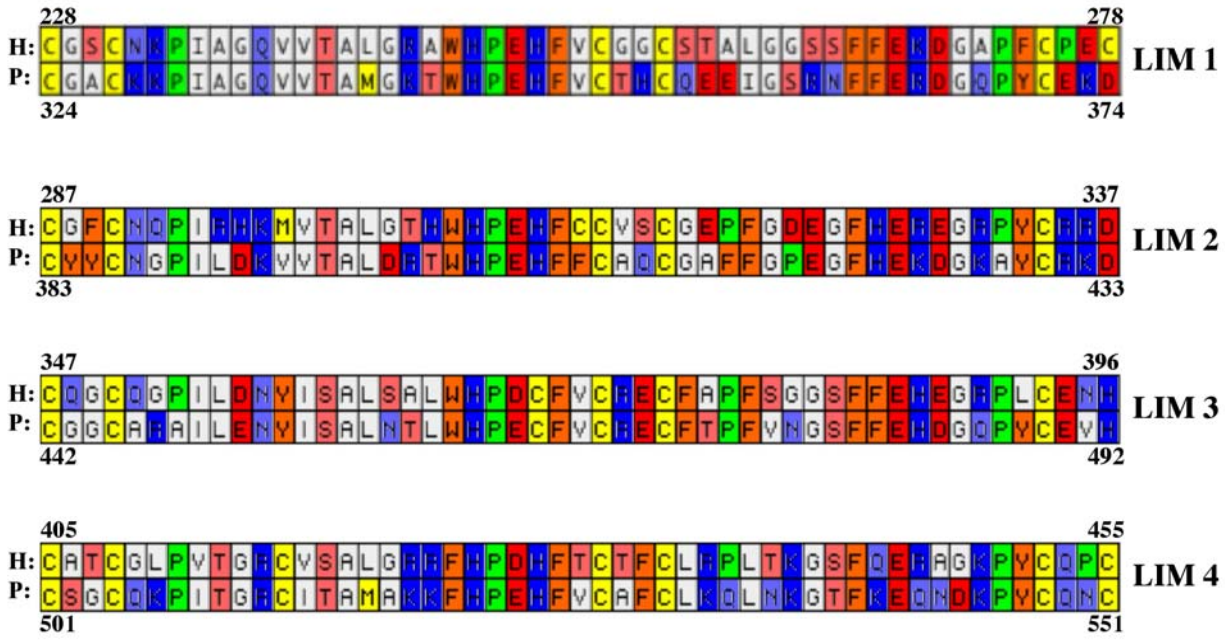

Figure 8. Schematic representation of the distribution of LIM domain within human Hic-5 and paxillin.
Hic-5 (NM 001042454) and paxillin (U14588) have a high percentage of homology in the LIM domain. Both Hic-5 and paxillin have four tandem LIM domain double zinc fingers located on the C-terminous. The appropriate location of amino acids for each LIM domain is indicated for both Hic-5 and paxillin. H: Hic-5, P: paxillin. Consensus LD motif: LDX(L,M) = X{2,2}X{2,2}L. Red: Acidic (DE), White: Hydrophic (AGILV), Aqua: Amido (NQ), Orange: Aromatic (FWY), Blue: Basic (RHK), Pink: Hydroxyl (ST), Green: Proline (P), Yellow: Sulfur (CM). Sequences were aligned using MacVector v10.0: ClustalW v1.83 multiple sequence alignment.

highest similarities throughout the paxillin subfamily (124, 130). The LIM3 domain in paxillin and Hic-5 determine their localization to focal adhesions (253, 254). The LIM2/3 domains in paxillin were found to bind directly to tubulin (255). PTP-PEST was also found to bind to the LIM3/4 domains of paxillin and the LIM4 domain of Hic-5 (256, 257).

Hic-5 is a 444 amino acid protein that was first identified as a mouse osteoblast TGF-β1 and H_2O_2 induced gene (258). Hic-5 was later identified in human cells by a yeast two-hybrid screen through its interaction with androgen receptor (AR) (259). To date, no alternative splice isoform of Hic-5 have been published (130). However, earlier reports suggested the existence of

an alternative Hic-5 isoform containing an additional 17 amino acids was due to a cloning error and not a true alternative splice variant of Hic-5 (137). Hic-5 orthologs are present in human, dog, chimpanzee, rat mouse, Drosophila/fruit fly, worm, and yeast (130, 259).

As stated earlier, the ability to act both in the nucleus and in focal adhesions suggests that intracellular trafficking may impact paxillin and Hic-5 biological effects. Zinc finger domains have historically been shown to bind to DNA. The use of the nuclear export inhibitor, leptomycin B, demonstrated that both Hic-5 and paxillin cycle between the cytoplasm and nucleus, indicating these proteins contain a functional nuclear export sequence (153). Indeed, Hic-5 contains two nuclear export signal sequences within its leucine-rich domains LD2 and LD3 (133). Furthermore, Hic-5 nuclear export seems to be influenced by the redox state of cells as Hic-5 was found to be sequestered into the nucleus of cultured fibroblast cells treated with H_2O_2 (133). While no putative nuclear import signal was found within the primary amino acid structure of Hic-5, the LIM domains are required for its nuclear import (133). The LIM domains of paxilin and Hic-5 have been found to target these proteins to the nuclear matrix (NM) and the LIM domains in Hic-5 shown to bind DNA (151, 154, 260). Though the relevance of this binding is unclear, our lab has shown that Hic-5 targets glucocorticoid receptor (GR) to the NM (149).GR is a member of the steroid nuclear receptor family of transcription factors that is activated upon binding glucocorticoid (261). Once GR is bound to specific enhancer gene elements, these GR domains associate with many primary transcriptional coactivators including members of the p160 family (SRC-1/NcoA, GRIP-1 and ACTR) (261). These primary coactivators in turn associate with secondary coactivators including histone acetytransferases (HATs) (CBP/p300, TIF-1, and RIP-140) and methyltransferases (CARM-1 and PRMT-1). Secondary coactivators then recruit the basal transcriptional machinery and the transcriptional

pre-initiation complex to the promoter of targeted genes directly or indirectly by remodeling chromatin structure using ATP dependent SWI/SNF complexes, HATs, and methyltransferases (154). Other members of the steroid receptor family have been shown to associate with the NM through acceptor proteins that are believed to be responsible for cell and tissue specific NM composition. A minimal NM targeting signal (NMTS) for GR has been identified and shown to include the DNA-binding domain and the tau-2 transactivation domain (154). Using a yeast two-hybrid screen, the DeFranco lab has shown that the NMTS of GR interacts with the LIM domains of Hic-5 (154). The DeFranco lab further showed that at least 10% of total paxillin and Hic-5 protein are localized to the nuclear matrix, potentially recognizing repetitive A-T rich matrix attachment regions (MARs) (149, 151). The NM and associated matrix proteins may also participate in GR regulated gene expression. Transiently transfected Hic-5 potentiated the transactivation activity of a glucocorticoid response element (GRE)-linked promoter using a transiently transfected reporter gene (154). Despite the high amino acid sequence similarity between paxillin and Hic-5, the amino acids known to responsible for transactivation are distinct and located in the carboxyl terminus for paxillin and the amino terminus for Hic-5 (154). The amino terminus and the LIM domains are required for the targeting of paxillin to the nuclear matrix while only the LIM domains are required for Hic-5.

The biological consequences of Hic-5 nucleo-cytoplasmic shuttling are unclear, although Hic-5 and paxillin are both a positive and negative coregulators of gene expression for nuclear steroid hormone receptors AR, GR, and peroxisome proliferators-activated receptor γ (PPARγ) and other transcription factors including SMAD3 (TGFβ receptor substrates), lymphoid enhancer factor/T-cell factor (LEF/TCF)-1 & -4, and Sp1 (Fig. 9) (148, 150). Interactions with cofactor proteins may also affect paxillin and Hic-5 function in the nucleus. In support of cofactor

interactions, our lab has shown specific Hic-5 and GR complexes with TIF-2, RAC3, CBP, and

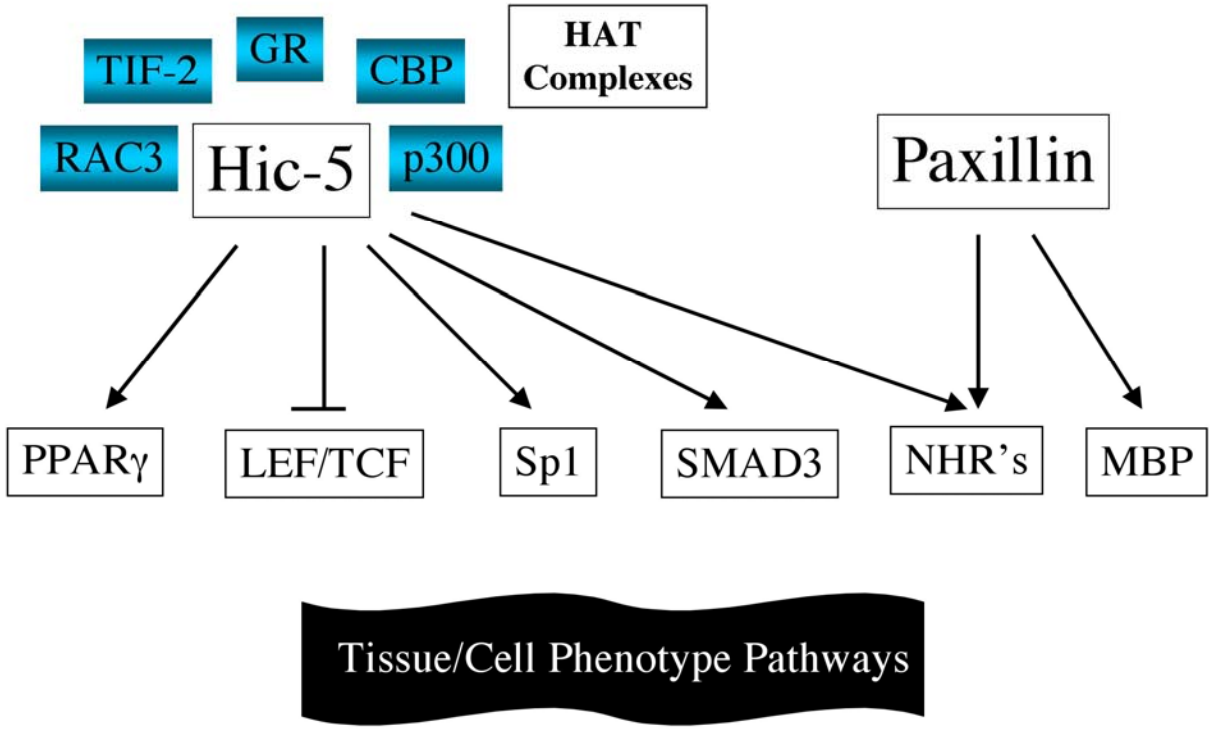

Figure 9. A schematic of known nuclear targets for both Hic-5 and paxillin
Hic-5 and paxillin are known to be both a positive and negative co-regulators of gene expression for nuclear steroid hormone receptors AR, GR, and peroxisome proliferators-activated receptor γ (PPARγ), SMAD3 (TGFβ receptor substrates), lymphoid enhancer factor/T-cell factor (LEF/TCF)-1 & -4, and Sp1 transcription factors. Hic-5 bound to GR also complexes with TIF-2, RAC3, CBP, and p300 co-regulators. Specific phosphorylation on pS178-paxillin was found to regulate myelin basic protein (MBP) expression.

p300 coregulators (150). Recently, specific phosphorylation on pS178-paxillin was found to regulate the differentiation of oligodendrocyte precursor cells through a sequential JNK and CDK5 kinase activities to ultimately regulate myelin basic protein (MBP) expression (262).

Overall it is clear that LIM domain proteins function as intracellular scaffolds that link many, if not all, aspects of cell signaling including those near the cell surface and in the nucleus.

Determining how LIM domain proteins impact biological effects in normal and various diseases conditions will aid in understanding the most basic concepts of biological sciences.

3.0 MATERIALS AND METHODS

3.1 HUMAN BRAIN TISSUE

The Committee for Oversight of Research Involving the Dead (CORID) at the University of Pittsburgh School of Medicine approved the use of human tissue from the University of Pittsburgh Tissue Bank. A blinded retrospective cross-sectional study involving age-matched postmortem brains was performed using 5 cases with no clinical history of a neurodegenerative disease or AD pathology, 5 cases with pathologically defined “early-stage” AD, and 5 cases pathologically defined “late-stage” AD (Table 8). Brain tissue samples from mild cognitive impairment were not available. Using cases of “late-stage” AD (Braak-stage VI) and “early-stage” AD (frequent neocortical neuritic plaques and Braak-stage II or III) the study consisted of 10 patients who were clinically diagnosed as having “probable AD” using the National Institute of Neurological and Communication Disorder and Stroke/Alzheimer’s Disease and Related Disorders Association (NINCDS-ADRDA) criteria at the Pittsburgh Disease Research Center and pathological AD using the Consortium to Establish a Registry for AD (CERAD), Braak criteria, and the National Institute of Aging/Reagan Institute (National Institute of Aging-Reagan Institute) criteria (66, 67, 228, 263, 264). A Bielschowsky stain was performed on all cases.

Table 8. Subject Demographics

CASE	AGE	SEX	BRAAK	BW	PMI
1	51	F	0 = Normal*	1400	5hrs
2	51	M	0= Normal	1310	6hrs
3	57	M	I= Normal	1450	2hrs
4	68	M	II= Normal	1380	27hrs
5	70	F	Nd= Normal	1200	6hrs
6	56	F	II= Early-stage AD	1190	19hrs
7	66	F	II= Early-stage AD	1160	9hrs
8	71	M	II= Early-stage AD	1340	15hrs
9	72	F	II= Early-stage AD	1120	9hrs
10	76	M	III= Early-stage AD	1545	13hrs
11	57	F	VI= AD	900	9hrs
12	58	M	VI= AD	1250	7hrs
13	69	F	V= AD	960	5hrs
14	70	M	VI= AD	1240	3hrs
15	71	F	VI= AD	1030	4.5hrs

Clinical data for subjects used in this study consisting of: 5 subjects with no neurodegenerative disease (control), 5 subjects with early-stage AD (Braak stages II and III) and 5 subjects with late-stage AD (Braak stages V and VI). Nd: no dementia. BW: brain weight in grams. PMI: post mortem interval. F: female. M: male. *: Metastatic adenocarcinoma of the cerebellum.

3.2 WESTERN BLOT

3.2.1 Hic-5 and paxillin expression levels compared in different stages of Alzheimer's disease subjects

Tissue extracts were prepared essentially as previously described (265). Briefly, fresh frozen human CB, cerebellum (AD stages I and VI); HP, hippocampus (AD stages IV and VI); MF, midfrontal cortex (AD stages II and VI) was homogenized in 10% w/v of ice-cold lysis buffer (1x Tris-buffered saline with protease (Sigma, St. Louis, MO) and phosphatase (Calbiochem, LaJolla, CA) inhibitors. The homogenate was centrifuged at 27,000 x g for 15 min. at 4°C to remove unbroken cells, membrane, large organelles, and nuclei to generate the soluble (S2) fraction. S2 fractions were quantitated using the BCA Protein Assay Kit (Pierce). 40 μg protein/lane for each brain region was separated on a 10% SDS-PAGE and transferred to nitrocellulose membrane for immunoblot analysis.

3.2.2 Hic-5 and paxillin expression levels in control vs. Alzheimer's disease subjects

Tissue extracts were prepared essentially as previously described (265). Briefly, fresh frozen human hippocampi from control and AD subjects were homogenized in 20% w/v of cold Tris-Triton X-100 (TX-100) buffer with protease (Sigma, St. Louis, MO) and phosphatase (Calbiochem, LaJolla, CA) inhibitors. The homogenate was centrifuged at 500 x g to remove debris and then centrifuged at 100,000 x g at 4° C. The supernatant was saved containing the TX-100 soluble fraction. The pellet containing the TX-100 insoluble fraction was resuspended in TX-100 buffer and saved. The protein concentration for TX-100 soluble and insoluble

Table 9. Antibody Information

Antibody	Host	Dilution	Source	Specificity*
Hic-5/ ARA55	Rabbit	1:300	GenWay, SanDiego, CA	Negative growth molecule, cell adhesion, FA turnover, TX co-regulator, redox sensitive, and localizes to nuclear matrix
Paxillin	Rabbit	1:300	Epitomics, Burlingame,CA	Pro-growth molecule, cell adhesion, and FA turnover
pY31 Paxillin	Rabbit	1:300	Epitomics	Modified during initial FA formation by Crk/Src and FAK after integrin and growth factor stimulation
pY118 Paxillin	Rabbit	1:100	Biosource, Camarillo, CA	Modified during initial FA formation by Crk/Src and FAK after integrin stimulation
pS126 Paxillin	Rabbit	1:100	Biosource	Modified after Raf stimulation MEK → ERK → GSK3 pathway
pS178 Paxillin	Rabbit	1:100	Biosource	Modified by cdc2 kinase during mitosis, JNK during migration
Beta-Amyloid	Mouse	1:300	Dako,Carpinteria, CA	Plaque component
AT8	Mouse	1:300	Pierce, Rockford, IL	Hyperphosporylated Tau and Neurofibrilliary Tangles
GFAP	Mouse	1:1000	Dako	Activated astrocytes
CD68	Mouse	1:100	Dako	Mature & Immature Microglia
TO-PRO-3	Chemical	1:300	Invitrogen, Carlsbad, CA	Nuclei
* As reported on the company's data sheet				

fractions was quantitated using the BCA Protein Assay Kit (Pierce). 50 μg protein/lane for each subject was separated on a 10% SDS-PAGE and transferred to nitrocellulose membrane. Non-specific antigens were blocked with 5% dry milk for 1 hour at room temperature, and incubated overnight at 4° C with primary antibodies (Table 9). Immunoblots were then incubated with horseradish peroxidase-conjugated secondary antibodies (Chemicon International, Temecula, CA) and developed using ECL (PerkinElmer Life Sciences, Boston, MA). Protein levels were quantified after scanning the appropriate molecular weight on the film using NIH Image 1.63. Specifically, the "mean gray value" for pixels within each lane was obtained. Each lane was normalized to actin and the most intense band was arbitrarily set to 100%.

3.3 IMMUNOHISTOCHEMISTRY AND IMMUNOFLUORESCENT LASER SCANNING CONFOCAL MICROSCOPY

Tissue was immersion-fixed in 10% buffered formalin and embedded in paraffin. Human hippocampal tissue sections (8 µM) were heated to 60°C for 1 hour prior to deparaffinization with three incubations of 100% xylene for 10 minutes each. The tissue was then rehydrated with two incubations of 100% and 90% alcohol followed by water for 5 minutes each. Endogenous peroxidase activity in the tissue was blocked with 0.3% hydrogen peroxide for 30 minutes. To expose antigenic epitopes, tissue was steamed for 20 min. in target retrieval solution (Dako, Carpinteria, CA). To reduce nonspecific primary antibody labeling for endogenous biotin, biotin receptors, and avidin binding sites in tissue, the avidin/biotin blocking kit was used according to company specifications (Vector Laboratories, Burlingame, CA). To block general nonspecific tissue antibody binding sites in tissue, SuperBlock (ScyTek Laboratories, Logan, UT) was added to tissue for 10 minutes. For each series of immunostaining, a no-primary antibody control slide was used to determine nonspecific immunoreactivity associated with the secondary antibodies. Blocking peptides commercially available for phosphorylated Y118 (pY118) and pS126 paxillin were utilized to demonstrate specificity of the immunostaining. For the blocking peptides, brain tissue was incubated with antibody and 100-fold molar excess of either specific blocking peptides or non-specific blocking peptides. Immunoreactivity on the tissue slides were visualized with Nova-Red chromagen (Vector Laboratories), dehydrated and mounted with permount (Fisher, Pittsburgh, PA). Immunofluorescent staining was carried out as previously stated except after primary antibody slides were incubated with goat anti-mouse or rabbit secondary antibodies conjugated to Alexa Fluor-488 and –568. Triple labeling was performed by incubation with the far-red fluorescent nucleic stain TO-PRO-3 (Invitrogen, Carlsbad, CA).

Pyramidal neurons in human brain are known to contain elevated levels of lipofuscin granules typically localized within the soma, which exhibit significant autofluorescence at longer wavelengths. Therefore, to minimize the contribution of autofluorescence to LSCM signals, secondary antibodies conjugated to Alexa Fluor –488 were used for Hic-5 or paxillin while Alexa Fluor –568 were used for colabeling with well-characterized markers for AD pathology.

3.4 PRIMARY CORTICAL CULTURES

The Institutional Animal Care and Use Committee (IACUC) at the University of Pittsburgh approved all animal protocols. Primary cortical cultures were prepared as previously described (Kress et al., 2002) to limit glial cell population to < 5% (266). Primary cortical neurons were derived from E17 pregnant female Sprague Dawley rats (17 days in gestation). Pups were decapitated and whole brains removed. Meninges were removed from each cortical lobe. Isolated cortical lobes were digested with 0.0375% Trypsin-EDTA (Gibco) at 37° C for 30 minutes. Digested brain tissue was titurated approximately 15 times followed by the deactivation of Trypsin-EDTA with the addition of sterile filtered plating media (DMEM with 10% FBS and 1% penicillin/streptomycin (Gibco). Cells were filtered with a 40 µM cell strainer (BD Falcon). Dissociated cells (10 ul) were added treated with trypan blue (90 µl) for cell counting. 1-1.2 x 10^6 cells/ml were then plated on to polyornithine (3 µg/ml) and laminin (5 µg/ml) coated glass coverslips for 5 hours. Plating media was completely removed and cells were then grown continuously in sterile filtered B27-NB media (Neurobasal media-Gibco, 10 ml of B27-Gibco supplement minus antioxidants, 0.5% penicillin/streptomycin). Cells were provided 1/3 fresh B27-NB media on day 3 and 7. Constructs for GFP-Hic-5 and GFP-paxillin

(gift from Dr. Rick Horwitz) were added to 5/6-day neuronal cultures after incubated with Lipofectamine 2000 (Invitrogen) at a ratio of 1ug DNA: 1μl reagent yielding approximately 3-5% transient transfection efficiency at 24-48 hours post transfection. Nuclei were labeled with TO-PRO-3 (Molecular Probes).

3.5 IN VITRO SUBCELLULAR LOCALIZATION

Two whole cell extraction buffer systems (WCE and RIPA) were compared with two different soluble vs. nuclear extraction buffer systems (A and B). For each buffer system used, primary cortical cultures were grown on four 10 cm plates and then harvested at 8 days in culture. Extracts from each buffer system were analyzed by immunoblot using antibodies for paxillin, hic-5, and actin. 30 ug for each brain region was loaded on a 10% SDS-PAGE. WCE: 50 mM Tris pH 7.5, 2 mM EDTA, 100 mM NaCl, 1% NP-40, protease (Sigma) and phosphatase (Calbiochem) inhibitors. RIPA: 50 mM Tris HCL pH 7.4, 150 mM NaCl, 1% Triton X-100, 1% sodium deoxycholate, 0.1% SDS, protease (Sigma) and phosphatase (Calbiochem) inhibitors. The protocol for buffer A the extracts were prepared similarily to previous published (267). A: cytoplasmic: 10 mM Pipes pH 6.8, 100 mM NaCl, 300 mM sucrose, 3 mM $MgCl_2$, 1 mM EGTA, 1 mM DTT, 0.5% Triton-X-100, protease (Sigma) and phosphatase (Calbiochem) inhibitors. A: nuclear pellets were adjusted to 0.25 mM ammonium sulfate and pelleted. The protocol for buffer B: cytoplasmic and nuclear fractions were performed using the manufacture's recommendations (Pierce NE-PER Kit).

3.6 IMMUNOPRECIPITATION

Fresh frozen human hippocampus from control and AD subjects were homogenized in 5 volumes of cold lysis buffer (50 mM Tris HCL pH 7.4, 150 mM NaCl, 1% Triton X-100, 1% sodium deoxycholate-stage, 0.1% SDS, protease (Sigma) and phosphatase (Calbiochem) inhibitors in a glass-teflon homogenizer (500 rpms, 10 strokes). 100 μl of total homogenate from control and AD subjects were preincubated with 4ul primary antibodies of interest for 2 hours. The tissue lysate was then mixed with Protein G Magnetic Microbeads for 30 minutes. To activate the μMACS columns (Miltenyi Biotec, Auburn, CA), 200 μl of lysis buffer was added before the immunoprecipitates were captured using the magnetic field. After the tissue lysate flowed through the columns, they were washed 4X 200 μl lysate buffer, 1 X 200 μl high salt buffer (500 mM NaCl, 1% NP-40, 50 mM Tris HCL pH 8.0, and 1X 200 μl low salt buffer (20 mM Tris HCL pH 7.5). To elute the bound complexes, 20 μl of pre-heated (95° C) 1X sample buffer (200mM Tris HCL 6.8, 0.2% SDS, 10% glycerol, 0.01% bromphenol blue) was added to the columns for 5 minutes. 80 μl of 1X sample buffer was then added and the flow through was saved. A control for nonspecific binding of protein to μMACS columns was determined by running control and AD subject lysate combined with Microbeads through the columns without prior incubation with primary antibodies in a same manner.

3.7 RANK ORDER AND STATISTICAL ANALYSIS

The number of subjects utilized for this study was 15. Statistical tests involving sample sizes of less than 100 without knowledge of variables/parameters require the use of nonparametric

methods for analysis. Tests based on ranked data are nonparametric and rank "intensity" order test were utilized in this study (268). The intensity of protein expression was ranked from lowest to highest based on blinded qualitative observations and assigning them values of 1 to 15. The rank "intensity" order was then divided into groups based on the un-blinded information (Table 10). The Mann-Whitney (U) test was used when comparing intensity differences in control vs. AD subjects and the Kruskal-Wallis (ANOVA) test was used when comparing control, early-stage AD and late-stage AD subjects (GraphPad Prism 4.0a).

4.0 RESULTS

4.1 IN VITRO SUBCELLULAR LOCALIZATION

The cellular expression and subcellular localization of Hic-5 and paxillin proteins was examined using WB analysis of extracts from embryonic rat cortical cultures. Two whole cell extraction buffer systems (WCE and RIPA) were compared with two different soluble vs. nuclear extraction buffer systems A and B (Cytoplasmic and Nuclear). For each buffer system used, primary cortical cultures were grown on four 10 cm plates and then harvested at 8 days in culture. To limit variability between buffer systems, cell pellets were combined and 30 ug from each fraction was used for WB analysis. Specific Hic-5 and paxillin immunoreactive bands of the appropriate molecular mass were evident in all subcellular fractions analyzed (Fig. 10). As shown in Fig. 10, paxillin was readily detected in whole cell and soluble fractions (WCE, RIPA, A: cytoplasmic, and B: cytoplasmic). However, paxillin was not easily detected in nuclear fractions for either A or B. These results suggest that paxillin is very soluble and support a number of reports showing limited localization of paxillin in the nucleus. In contrast, Hic-5 shows strong nuclear localization in both nuclear fraction buffer systems. Although antibodies for actin were used to control for protein gel loading, additional controls should be used to establish the purity of the various subcellular fractions including Na/K-ATPase for membrane, HSP-90 or GAPDH for cytoplasmic and HDAC, SP1, c-fos, or lamin B1 for nuclear fractions.

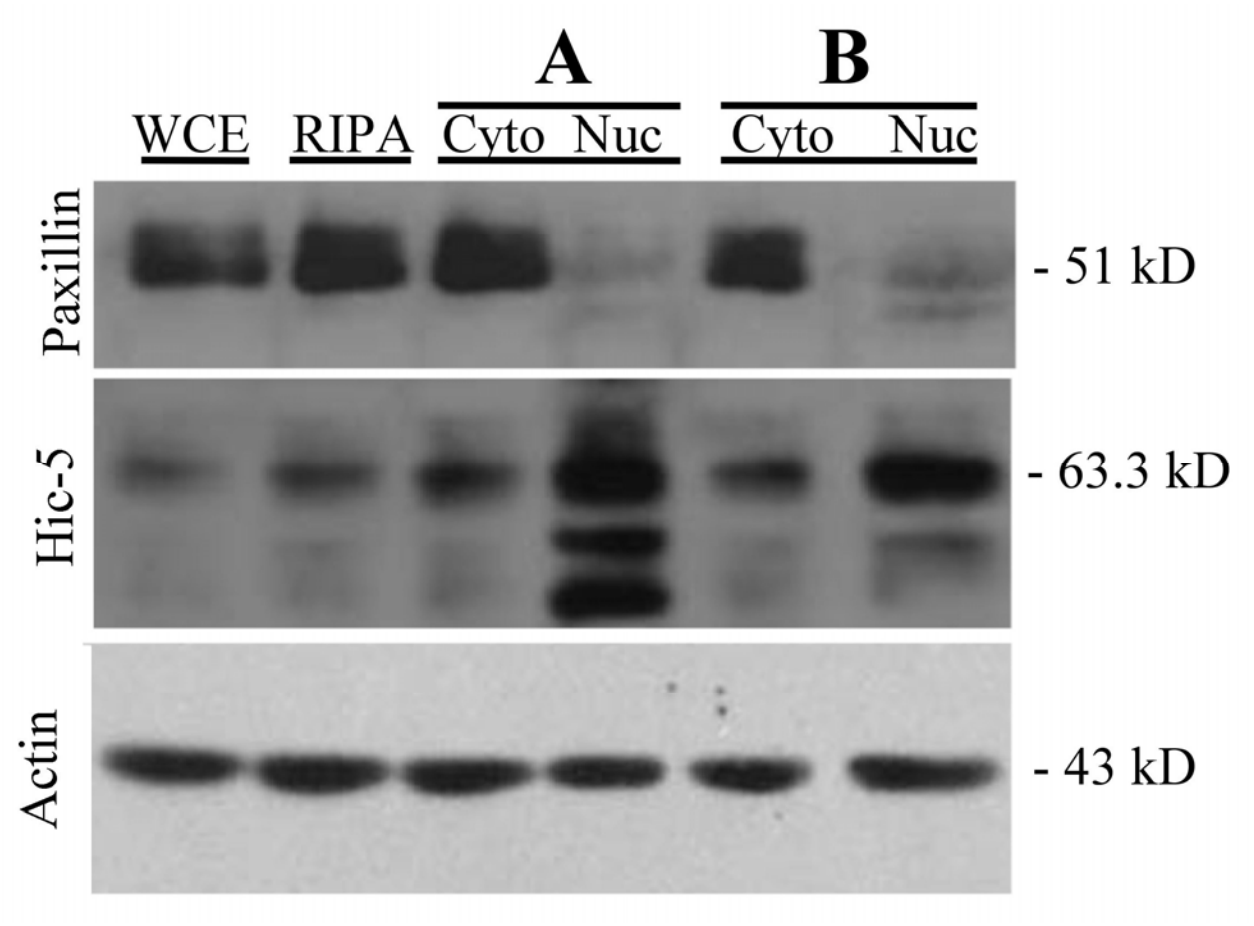

Figure 10. Immunoblot analysis to determine the in vitro subcellular localization of Hic-5 and paxillin
Two whole cell extraction buffer systems (WCE and RIPA) were compared with two different soluble (Cyto.) vs. nuclear (Nuc.) extraction buffer systems A and B. For each buffer system used, embryonic cortical cultures were grown on four 10 cm plates and then harvested at 8 days in culture. Extracts from each buffer system were analyzed by immunoblot using antibodies for paxillin, Hic-5, and actin. 30 ug for each brain region was loaded on a 10% SDS-PAGE.

4.2 IN VITRO NUCLEAR LOCALIZATION

Hic-5 and paxillin have previously been demonstrated to shuttle into and out of the nucleus of non-neuronal cell lines after treatment with leptomycin B (133, 269). Both Hic-5 and paxillin have been shown to function in the cytoplasm of cultured neurons and neuronal cell lines; these

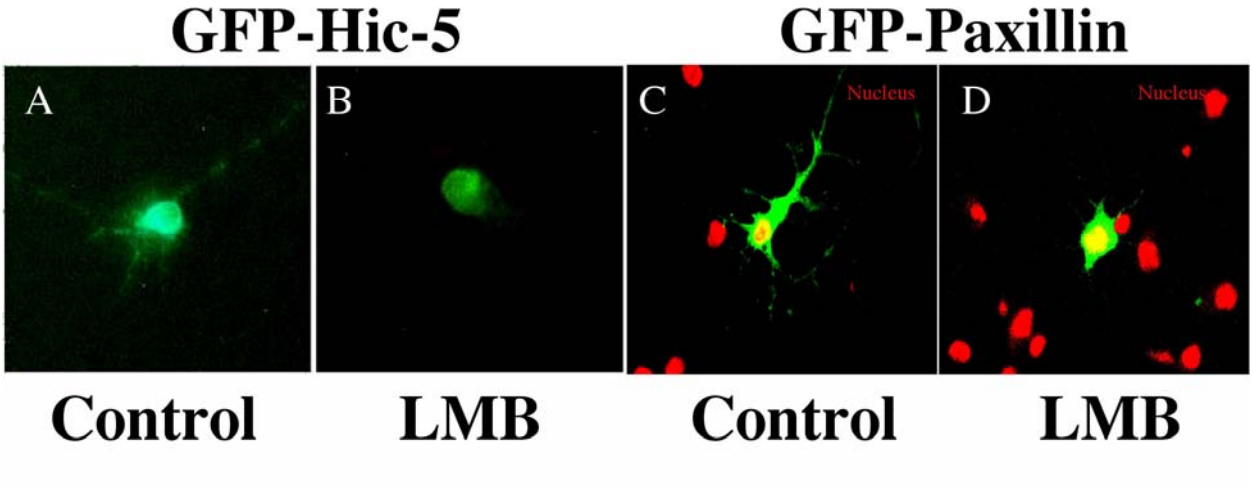

Figure 11. In vitro nuclear localization of Hic-5 and paxillin in embryonic cortical cultures Constructs for GFP-Hic-5 and GFP-paxillin were added to 5/6-day primary neuronal cultures after incubated with Lipofectamine 2000 (Invitrogen) at a ratio of 1ug DNA: 1μl reagent yielding approximately 3-5% transient transfection efficiency at 24-48 hours post transfection. Nuclei were labeled with a nuclear dye (TO-PRO-3). **(A):** GFP-Hic-5, control. **(B):** GFP-Hic-5, leptomycin B. **(C):** paxillin, control. **(D):** paxillin, leptomycin B.

studies did not address potential genomic roles of these proteins (158, 270). To establish whether Hic-5 or paxillin had the capacity to accumulate in the nuclei of neurons, embryonic cortical cultures were transfected for 24 hr with GFP tagged Hic-5 or paxillin. Transfection conditions were optimized to maximize the number of cells expressing these two proteins. In order to clearly establish shuttling of either protein, cultures were then treated with leptomycin B and changes in localization were observed by LSCM. Exogenously expressed GFP-Hic-5 protein is localized throughout neuronal processes and appeared localized in the nucleus of primary cortical brain cultures even in the absence of leptomycin B (Fig.11 A). Leptomycin B treatment led to a reduction in GFP-Hic-5 fluorescence in neuronal processes but it was not possible to assess the presumed enhanced nuclear accumulation under these conditions (Fig. 11 B). GFP-paxillin protein is also localized throughout the neuronal processes and nucleus (Fig. 11 C). A reduction of GFP-paxillin expression in the soma and neuronal processes were

observed in primary cultures incubated with leptomycin B (Fig.11 D). These *in vitro* results indicate that nuclear import of Hic-5 and paxillin occurs in neurons.

4.3 HIC-5 AND PAXILLIN EXPRESSION IN BRAIN

Both Hic-5 and paxillin are expressed in numerous regions of the rat brain. However, no study to date has addressed the expression profile of these proteins in specific brain regions. Furthermore, Hic-5 and paxillin expression and function have not been assessed in a human disease in which cells are exposed to conditions that may impact Hic-5 and/or paxillin function (i.e. oxidative stress). Numerous reports have made a connection between oxidative stress and AD. Therefore, the tissue specific expression and subcellular localization of Hic-5, paxillin, and phosphorylated isoforms of paxillin were examined in multiple human brain regions and stages of AD.

4.3.1 Hic-5 and paxillin expression levels compared in different stages of Alzheimer's disease subjects

Immunoblot analysis was performed to detect Hic-5, paxillin, and phophorylated isoforms of paxillin using soluble homogenates of fresh frozen tissue extract (27,000 x g) supernatants from cerebellum, hippocampus, and midfrontal cortex of human subjects. Specifically, monoclonal antibodies directed to Hic-5 and paxillin and polyclonal antibodies directed against pY31 paxillin, pS126 paxillin, or pS178 paxillin isoforms were used. In the soluble fractions of cerebellum, hippocampus, and midfrontal cortex, a specific immunoreactive band of the

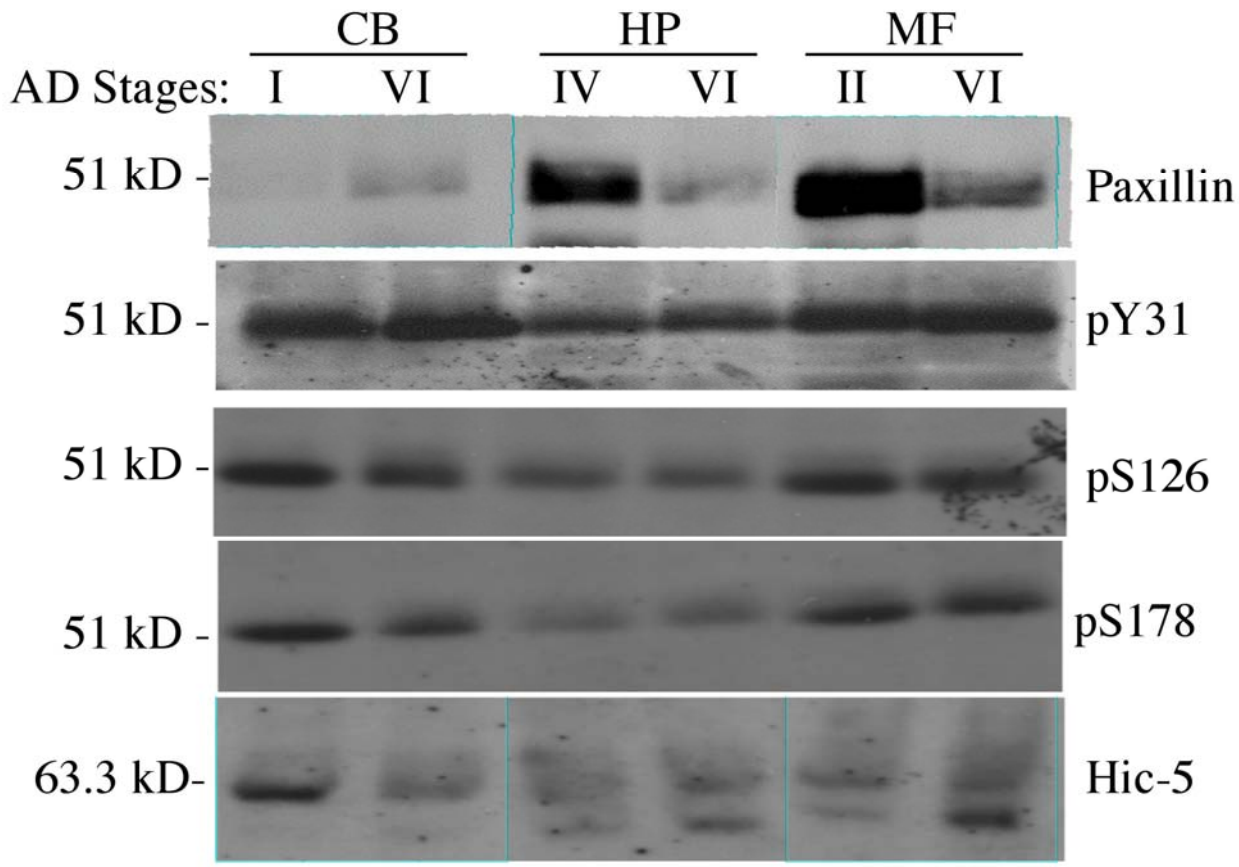

Figure 12. Expression levels compared in different stages of Alzheimer's disease
Fresh frozen CB= cerebellum, HP= hippocampus, and MF= mid-frontal cortex from different stages of AD were homogenized as described in Methods to generate S2 fraction. Equal amounts of protein from each total homogenate were loaded in gel lanes and immunolabeled using antibodies specific to Hic-5 or paxillin, pY31 paxillin, pS126 paxillin, and pS178 paxillin.

appropriate molecular mass was present for Hic-5, paxillin, pY31 paxillin, pS126 paxillin, and pS178 paxillin immunoblots (Fig. 12). Paxillin is highly expressed in the early stages of AD in the hippocampus (stage IV vs. VI) and midfrontal cortex (stage II vs. VI). Paxillin expression was barely detectable in the cerebellum although relatively weak expression of paxillin was detected in the later stage of AD (stage VI vs. I). The immunoblots for Hic-5, pY31 paxillin, pS126 paxillin, and pS178 paxillin did not indicate a readily observable difference in expression levels for these three brain regions or different AD stages tested. These experiments need to be

repeated with multiple subjects and disease stages to establish whether overall expression of paxillin or Hic-5 is altered in specific brain regions of AD subjects.

4.3.2 Immunoblot analysis to determine the specificity of antibodies

To establish the specificities of antibodies, immunoblot analysis was performed to compare either whole cell extracts from control cells: prostate stromal cells (WPMY-1) with small interfering RNA (siRNA) ablation of Hic-5 or mouse embryonic fibroblast cells (MEF) with genetic ablation of paxillin, and fresh frozen human hippocampus with either TX-100 soluble (100,000 x g) or insoluble tissue extracts (271, 272). Individual gels were performed for each antibody tested and molecular weights were determined by a linear regression plot of log [molecular weight] vs. migration from molecular weight protein standards. The blot was then probed with actin antibodies for a loading control.

Antibodies directed towards Hic-5 detected a specific band that migrated approximately 63.3 kDa in both whole cell extracts from WPMY-1 cells and TX-100 insoluble fractions in both control and AD hippocampus (Fig. 13 A). This band was barely detected in cells that were Hic-5 ablated. A doublet of higher molecular weights was also detected in WPMY-1 cells that were not present in human hippocampus (Fig. 13 A). Antibodies directed towards paxillin (Fig B), pY31 paxillin (Fig. 13 C), pY118 paxillin (Fig. 13 D), pS126 paxillin (Fig. 13 E), and pS178 paxillin (Fig. 13 G) detected a specific band that migrated approximately 51 kDa in both whole cell extracts from MEF cells and TX-100 soluble fraction in both control and AD hippocampus. This band was barely detected in the paxillin ablated MEF cells but was not entirely absent (Fig. 13 B). A larger molecular weight band migrating approximately 78 kDa was detected in both MEF cells and human hippocampus for pY31, pS126, and pS178 immunoblots (Fig. 13 D – F).

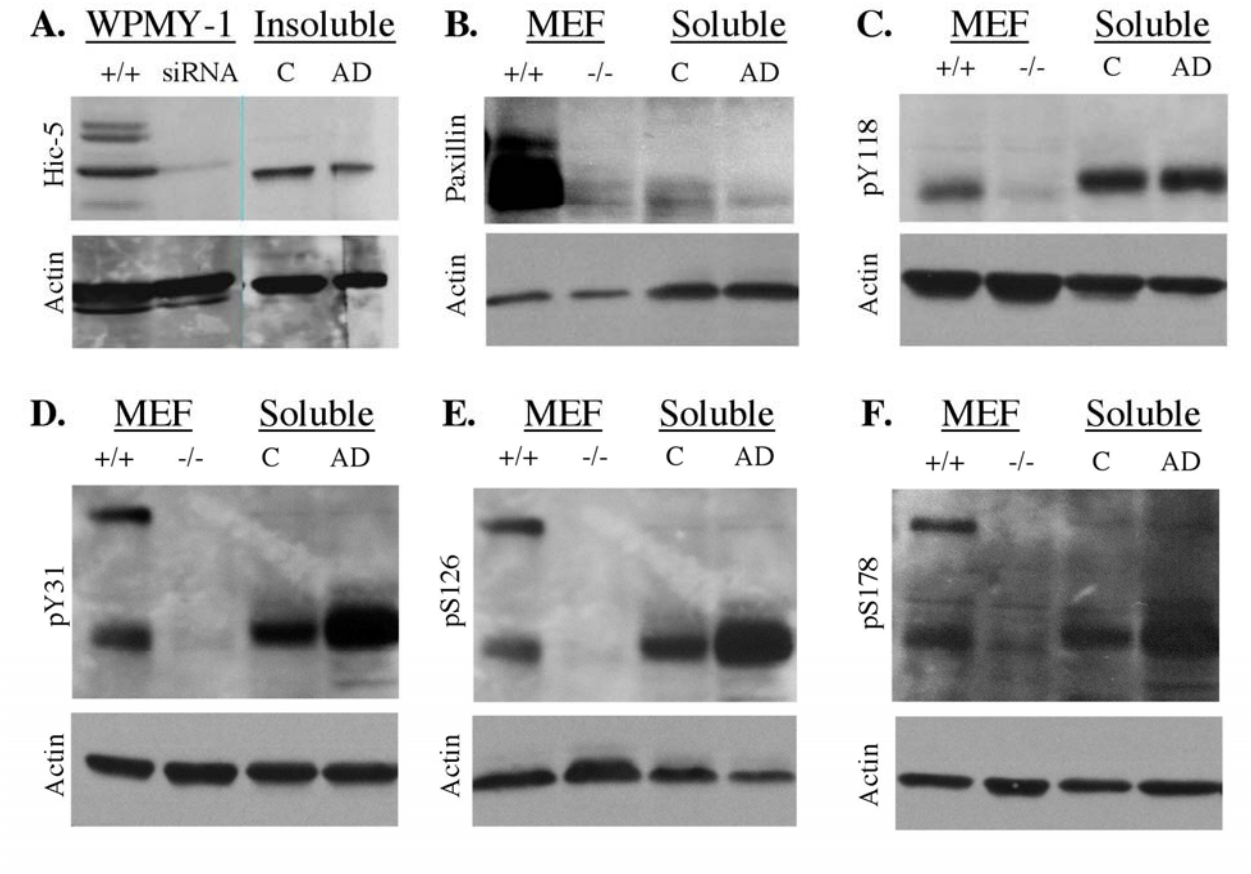

Figure 13. Immunoblot analysis to determine the specificity of antibodies
Individual gels were performed for each antibody tested and molecular weights were determined by a linear regression plot of log [molecular weight] vs. migration from molecular weight protein standards. The blot was then probed with actin antibodies for a loading control **(A):** Immunoblot with Hic-5 antibodies for whole cell extracts from control prostate stromal cells (WPMY-1) with small interfering RNA (siRNA) ablation of Hic-5 and fresh frozen human hippocampus with either TX-100 soluble (100,000 x g) or insoluble tissue extracts. **(B-F):** Immunoblot with paxillin **(B)**, pY118 paxillin **(C)**, pY31 paxillin **(D)**, pS126 paxillin **(E)**, and pS178 paxillin **(F)** antibodies for whole cell extracts from control mouse embryonic fibroblast cells (MEF) with genetic ablation of paxillin, and fresh frozen human hippocampus with either TX-100 soluble (100,000 x g) or insoluble tissue extracts.

4.3.3 Hic-5, paxillin, and activated isoforms of paxillin expression in control vs. Alzheimer's disease subjects

Initially, hippocampal tissue was the focus for examination of Hic-5 and paxillin expression as this region undergoes dramatic and well-defined pathologic changes during the progression of AD. Immunoblot analysis was performed using TX-100 soluble and insoluble fractions of fresh frozen tissue extract (100,000 x g) from hippocampus. In both TX-100 soluble and insoluble fractions of hippocampus a specific immunoreactive band of the appropriate molecular mass was present for Hic-5, paxillin, and activated isoforms of paxillin immunoblots in both control and AD hippocampus (Fig. 14 and 15). Molecular weights for specific bands detected by each antibody used were determined by a linear regression plot of log [molecular weight] vs. migration from molecular weight protein standards. The blot was then probed with actin antibodies for a loading control. Protein levels in the TX-100 soluble fraction immunoblots for Hic-5, paxillin, and activated isoforms of paxillin tested did not change significantly in early-stage AD or late-stage AD compared to control subjects (Fig. 14). However, Hic-5 levels did trend to be significantly decreased ($p < 0.087$) in early-stage AD and late-stage AD compared to control subjects (Fig. 14). However, Hic-5 protein levels in the TX-100 insoluble fraction were significantly decreased ($p < 0.012$) in early-stage AD compared to control and late-stage AD subjects (Fig. 15). This result is shown graphically in Fig. 16.

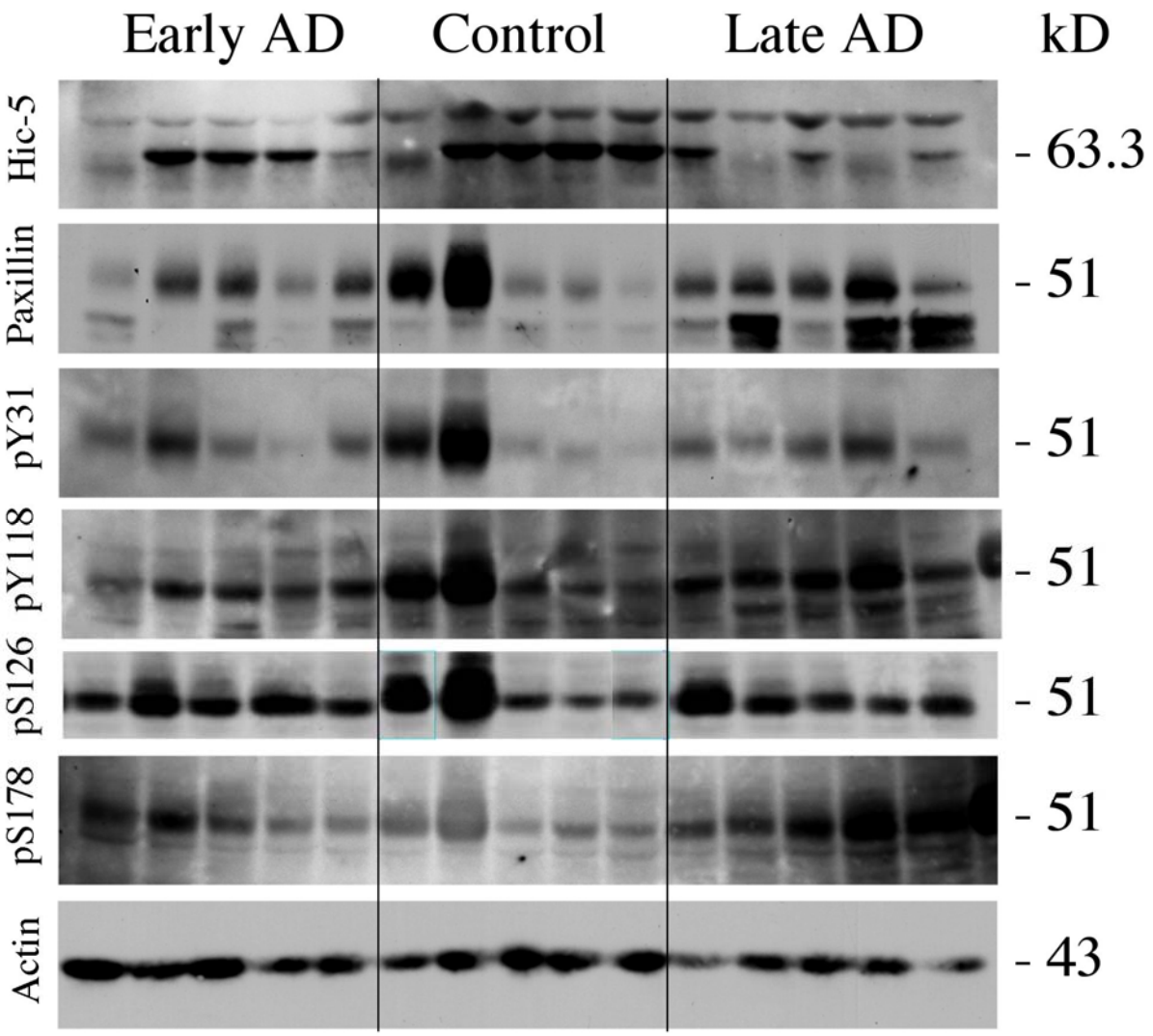

Figure 14. Immunoblot analysis for Hic-5, paxillin, and activated isoforms of paxillin protein in TX-100 soluble fraction of human hippocampus

Fresh frozen hippocampus from 5 non-neurologic disease controls, 5 early-stage AD, and 5 neuropathologically confirmed late-stage AD cases were homogenized as described in Methods to generate TX-100 soluble fraction. Equal amounts of protein from each total homogenate were loaded in gel lanes and immunolabeled using antibodies specific to Hic-5, paxillin and activated isoforms of paxillin. Antibody to actin was used as a loading control. Lanes 1-5 are from early-stage AD, lanes 6-10 are from control subjects and lanes 11-15 are from late-stage AD subjects. Quantitative measurements for each lane were normalized to actin and the most intense band was arbitrarily set to 100%. The Kruskal-Wallis statistical test was performed to compare control vs. early-stage AD vs. late-stage AD subjects: Hic-5 = $p < 0.087$, paxillin = $p < 0.763$, pY31 = $p < 0.613$, pY118 = $p < 0.249$, pS126 = $p < 0.512$, pS178 = $p < 0.134$.

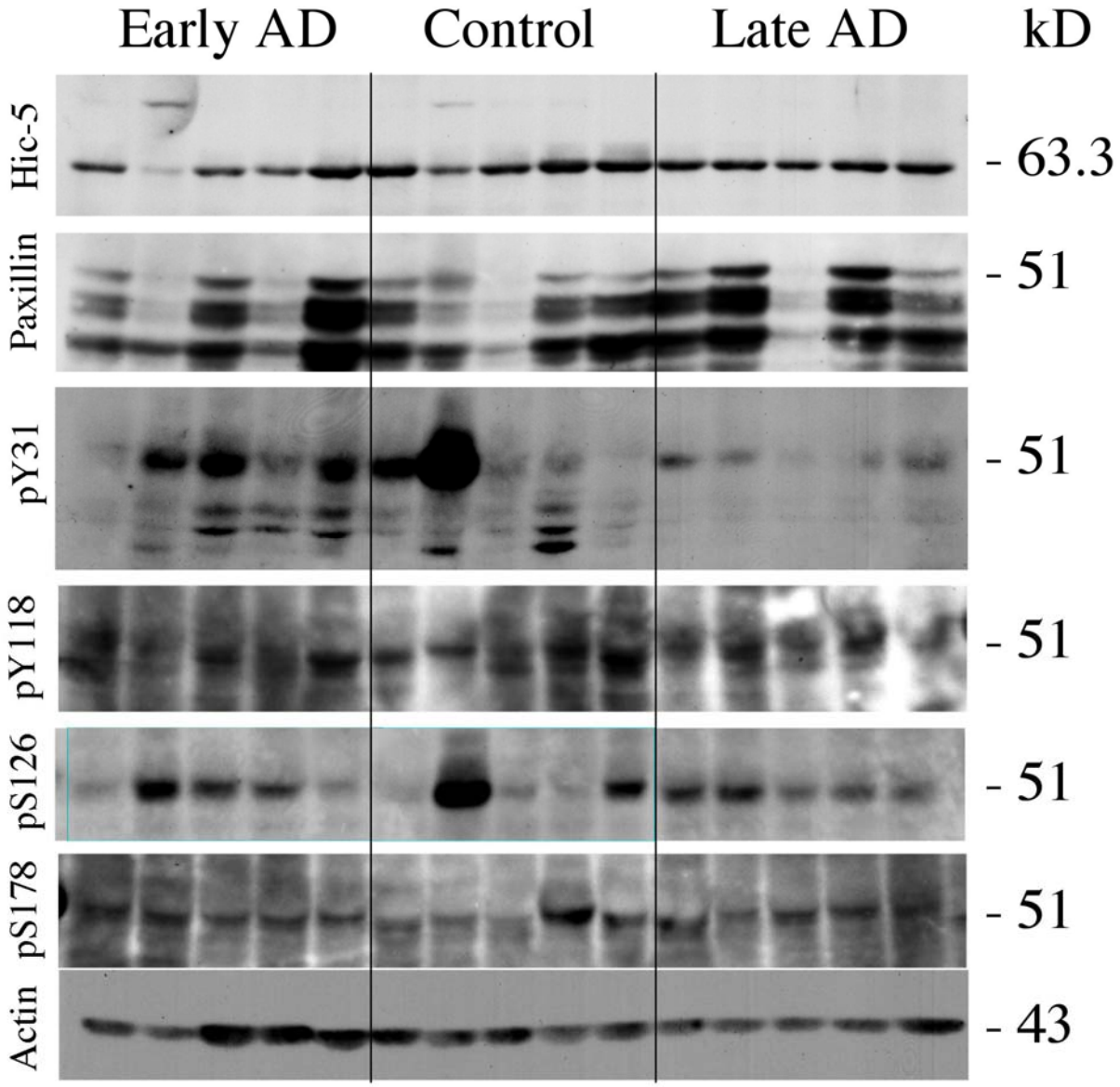

Figure 15. Immunoblot analysis for Hic-5, paxillin, and activated isoforms of paxillin protein in TX-100 insoluble fraction of human hippocampus

Fresh frozen hippocampus from 5 non-neurologic disease controls, 5 early-stage AD, and 5 neuropathologically confirmed late-stage AD cases were homogenized as described in Methods to generate TX-100 insoluble fraction. Equal amounts of protein from each total homogenate were loaded in gel lanes and immunolabeled using antibodies specific to Hic-5, paxillin and activated isoforms of paxillin. Anti-actin antibodies were used as a loading control. Lanes 1-5 are from early-stage AD, lanes 6-10 are from control subjects and lanes 11-15 are from late-stage AD subjects. Quantitative measurements for each lane were normalized to actin and the most intense band was arbitrarily set to 100%. Kruskal-Wallis statistical test was performed to compare control vs. early-stage AD vs. late-stage AD subjects: Hic-5 = $p < 0.012$, paxillin = $p < 0.691$, pY31 = $p < 0.99$, pY118 = $p < 0.075$, pS126 = $p < 0.33$, pS178 = $p < 0.21$.

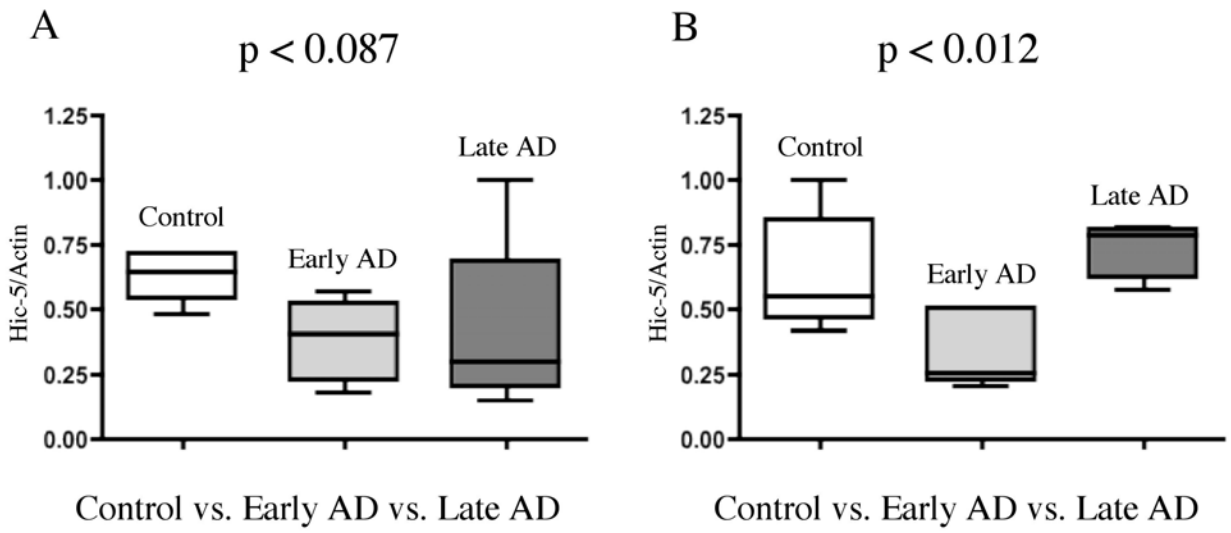

Figure 16. Graphical representation of Hic-5 immunoreactivity in AD
The results of the Kruskal-Wallis statistical test are shown comparing Hic-5 protein levels in the hippocampus for control vs. early-stage AD vs. late-stage AD. **(A)**: Hic-5 levels in TX-100 soluble fraction = $p < 0.087$ **(B)**: Hic-5 levels in TX-100 insoluble fraction = $p < 0.012$.

4.3.4 Distribution of hic-5 and paxillin in hippocampus

WB analysis of brain extracts can only provide limited information about Hic-5 and paxillin expression since this tissue contains many distinct cell types. Furthermore, biochemical fractionations from frozen human brain tissue are inherently inefficient. Therefore, to more precisely investigate the subcellular distrubution of Hic-5 and paxillin, light and LSCM was used to assess Hic-5 and paxillin expression and subcellular distribution within the hippocampus of control, early-stage AD and late-stage AD subjects (Table 8). IHC of human hippocampus was performed with polyclonal antibodies directed against Hic-5, paxillin, and phosphorylated isoforms of paxillin that distinguish various activated forms of the proteins (Table 9). Tissue

slides were for each antibody were performed simultaneously and were also not counterstained so as to accurately interpret the observed staining patterns. Classical plaques are composed of a heterogeneous population of extracellular Aβ deposits, dystrophic neurites, NFTs, activated astrocytes and microglia (84, 273). Therefore, LSCM with markers specific to plaques (β-amyloid), NFTs (AT8), activated astrocytes (GFAP) and microglia (CD68) were used to determine the localization of Hic-5, paxillin, and phosphorylated isoforms of paxillin in AD pathology.

4.4 HIC-5 DISTRUBUTION IN HIPPOCAMPUS

Hic-5 localizes to cells of the vascular system including smooth muscle cells surrounding arteries and large capillaries (Fig. 17, panel a) as well as arterial/capillary endothelial cells (Fig. 17, panels b and c). Hic-5 stained the walls of the vascular system indicative of endothelial cells and showed clear nuclear staining (Fig. 17, panels b and c). Further, ependymal cells that line the ventricles that do not have a basement membrane are positive for Hic-5 (data not shown). Throughout control and AD hippocampus, the majority of Hic-5 immunoreactivity was observed in dentate gyrus neurons (Fig. 18, panel a), pyramidal neurons throughout the stratum pyramidale layer (Fig. 19, panels a - f), and small round cells of the stratum oriens layer between the alveus and stratum pyramidal layers (Fig. 18, panel b). Hic-5 immunoreactivity was also observed in neuronal processes of the alveus/fimbria layer that contains the major output of pyramidal neurons in the hippocampus (Fig. 18 A, panel c) and cells of the choroid plexus (Fig. 18, panel d). Hic-5 protein within reactive astrocytes in control subjects was not observed. Hic-5 immunoreactivity was compared between control and AD hippocampus and significantly

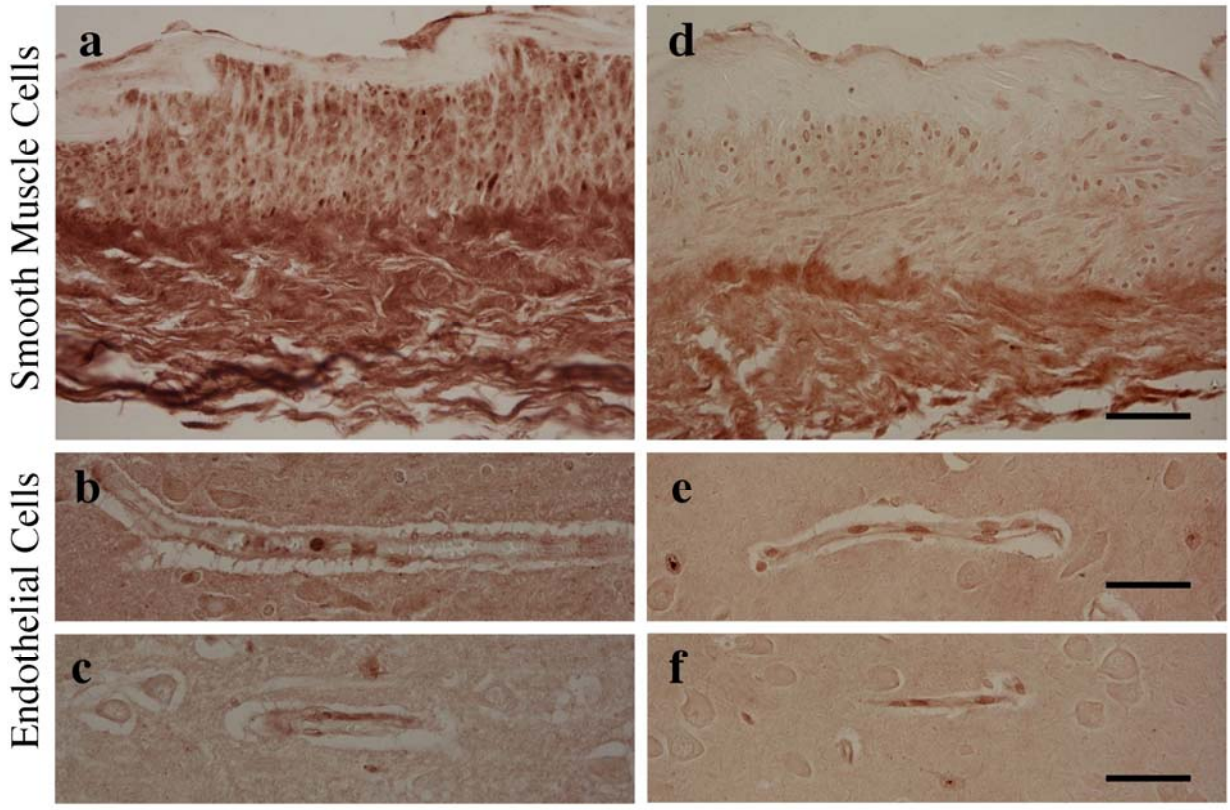

Figure 17. Hic-5 and paxillin immunoreactivity in cells of the vascular system
Tissue sections from control hippocampus immunostained with **(a):** anti-Hic-5 and **(d):** anti-paxillin antibodies reveals protein expression in smooth muscle cells surrounding arteries and large capillaries. **(b and c):** Hic-5 and **(e and f):** paxillin stained arterial/capillary endothelial cells. Scale bars = **(a and d)** 100μm: **(c, b, e, f)** 50 μm.

elevated levels of Hic-5 in CA1 pyramidal neurons in AD subjects (Fig. 19, panels e and f; Table 10, Row 1) were noted. Hic-5 immunostaining was statistically different between control, early-stage AD and late-stage AD subjects by rank order analysis (Fig. 19, panels d - f; Table 10, Row 2). The results of these significance tests are shown by graphical representation in Fig. 20. Hic-5 immunoreactivitywas predominantly located within the cell body and was excluded from the nucleus in the majority of pyramidal neurons in the hippocampus (Fig. 19; Fig. 21, panel f). This observation contradicts those shown *in vitro* where Hic-5 was premoniantly in the nuclear

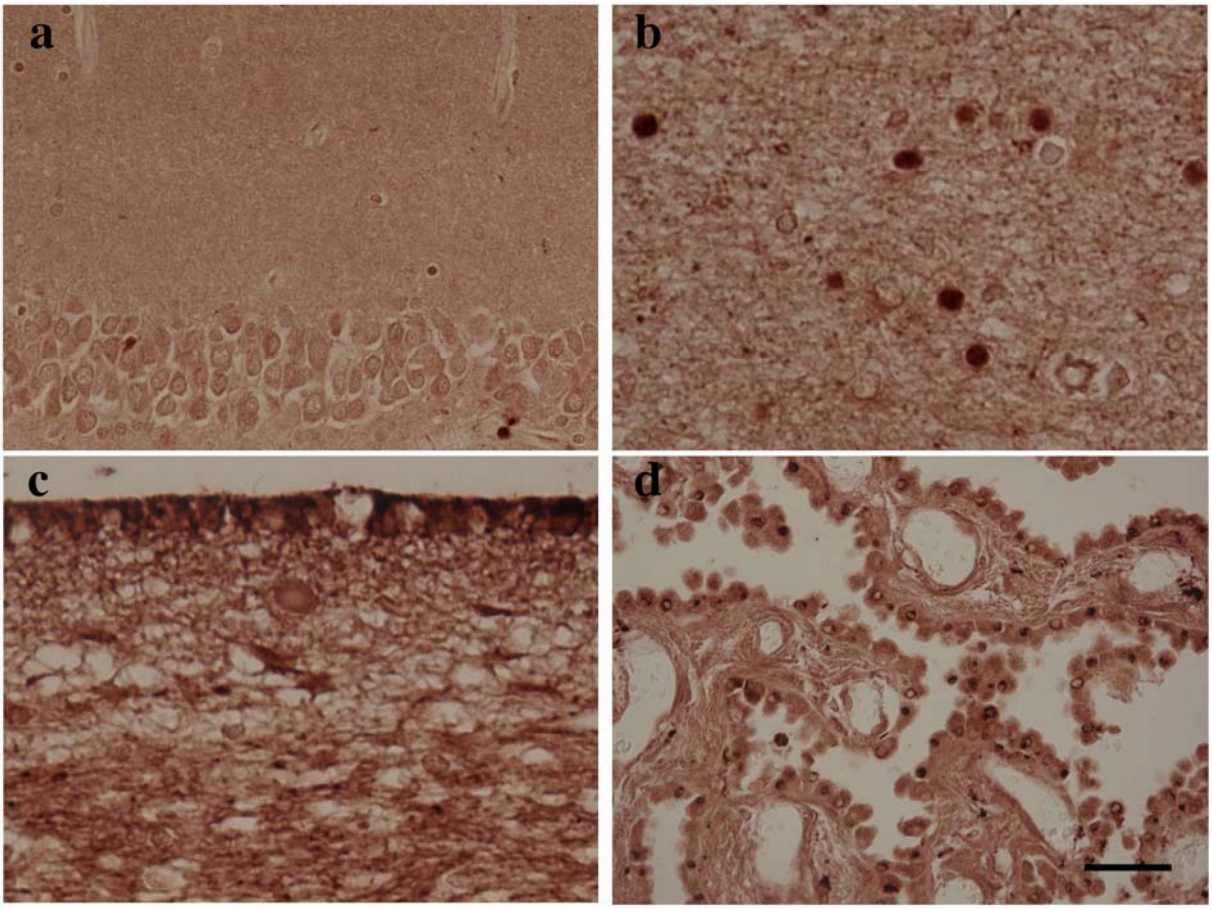

Figure 18. Hic-5 immunoreactivity in human hippocampus
(A): Tissue sections from control hippocampus immunostained with anti-Hic-5 antibody reveals protein expression in the soma of dentate gyrus granular and pyramidal neurons **(a)**; nuclei of glial cells **(b)**; alveus/white matter tracts **(c)**; cells of the choroid plexus (**d**). Scale bars = **(a - d)** 25 μm.

fraction or nucleus. However, a subset of CA3 and CA1 pyramidal neurons of both control and AD subjects exhibited Hic-5 immunoreactivity in the nucleus (Fig. 21, panels a – e). Hic-5 immunoreactivity was significantly increased in extracellular plaques within the hippocampus in all AD subjects compared to controls, and statistically significant when comparing all three subject groups to each other (Fig. 21, panel g; Table 10, Row 2). Specifically, Hic-5 distribution in plaques was greatest in late-stage AD subjects. Within plaques Hic-5 was located within

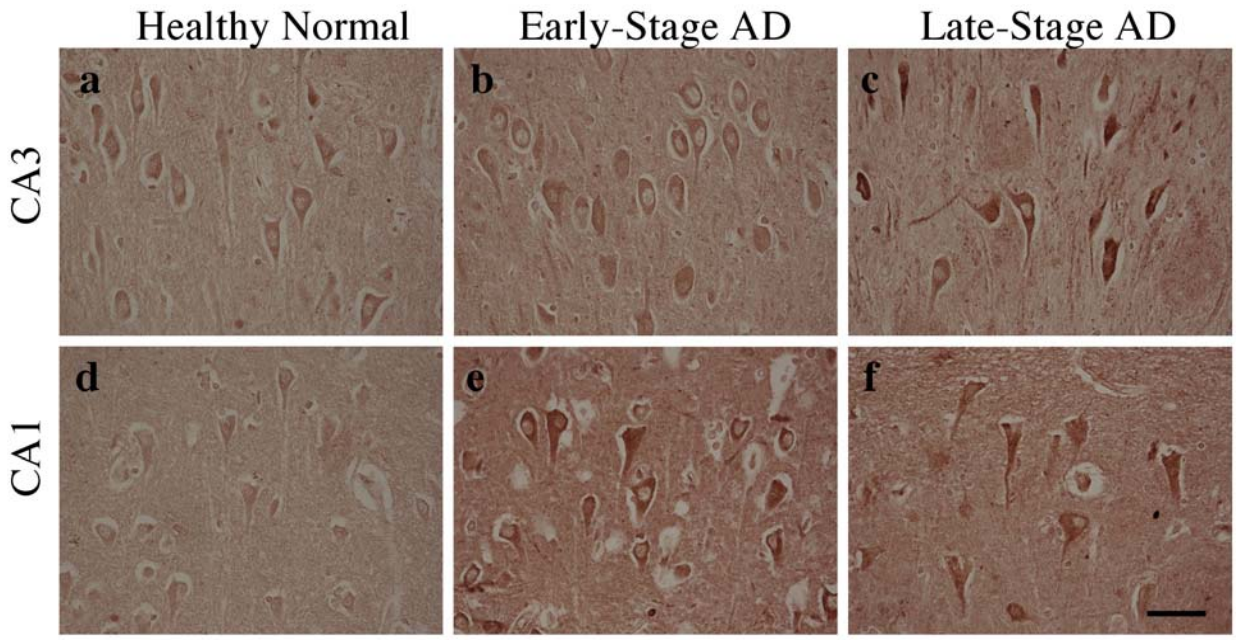

Figure 19. Hic-5 localization and relative expression in the CA3 and CA1 subfields
(a - c): Hic-5 immunoreactivity in CA3 pyramidal neurons in control, early-stage AD, and late-stage AD subjects. **(d - f):** Hic-5 immunoreactivity in CA1 pyramidal neurons in control, early-stage AD, and late-stage AD subjects. Scale bars = **(a - f)** 50 μm.

morphologically diverse structured including nuclei, neuropil and punctate aggregates (Fig. 21, panel g). Hic-5 was also present in the soma and nuclei of choroid plexus (Fig. 18, panel d).

The major synaptic inputs to the hippocampus occur on the projecting dendrites from the dentate gyrus in the outer molecular layer (OML) from the ipsilateral (same side) entorhinal cortex and the inner molecular layer (IML) from the contralateral (opposite side) entorhinal cortex. In many subjects, Hic-5 immunoreactivity was observed to be elevated in the OML compared to the IML (Fig. 22, panel a). At the light level, it is difficult to determine whether the observed staining is derived from dendrites or axons. As stated earlier, FAK is activated in the presence of Aβ in cell culture. Though FAK distribution was not examined in all cases, immunostaining was also performed with antibodies directed to FAK and its activated

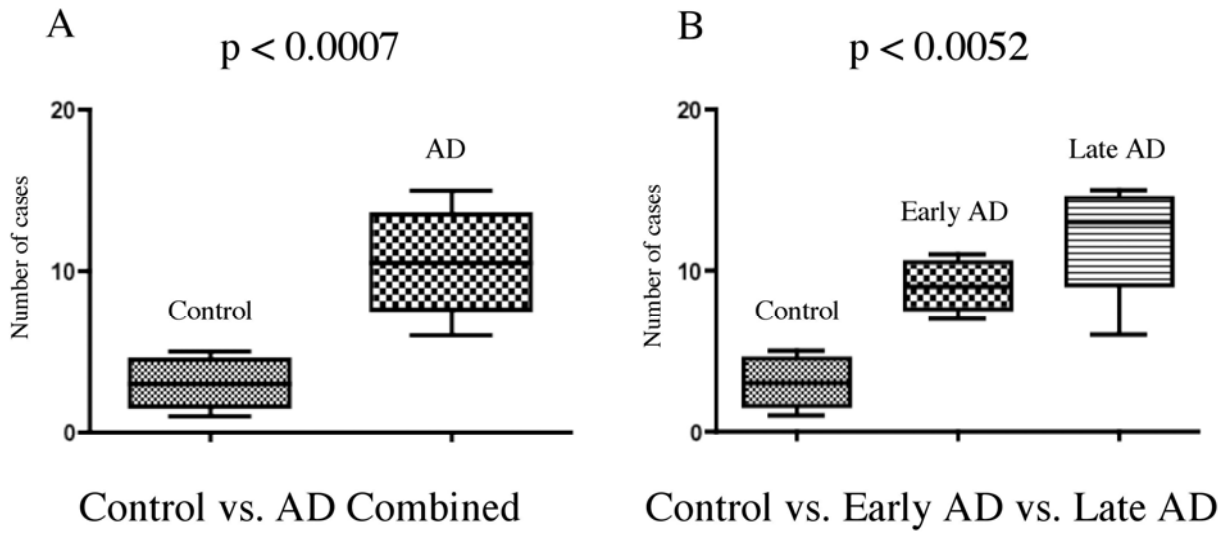

Figure 20. Graphical representation of Hic-5 immunoreactivity in AD
The results of the significance tests for Hic-5 expression levels in Table 10 are shown by graphical representation. (A): Mann Whitney statistical test comparing Hic-5 immunoreactivity in control vs. AD subjects, (B): Kruskal-Wallis statistical test comparing Hic-5 immunoreactivity in control vs. early-stage AD vs. late-stage AD subjects.

autophosphorylated isoform (pY397 FAK) in some cases. In serial sections of hippocampus, immunoreactivity for FAK was not as easily detected compared to pY397 in the hippocampus (data not shown). However, in both the IML and OML FAK was observed in clusters of granules that are not as evident in the surrounding hippocampus (data not shown). Immunoreactivity for pY397 FAK was elevated in the OML compared to the IML (Fig. 22, panel b). The pY397 FAK staining was observed in dense granules that were only present in the OML and not in the IML or surrounding hippocampus. Neither the cluster of granules or dense granule staining observed with FAK or pY397 FAK was detected with Hic-5 (Fig. 22). FAK is a known upstream regulator of Hic-5 and paxillin (130) . Colocalization of FAK/pY297 FAK and Hic-5/paxillin/phosphorylated isoforms of Hic-5 combined with a third label for either axons

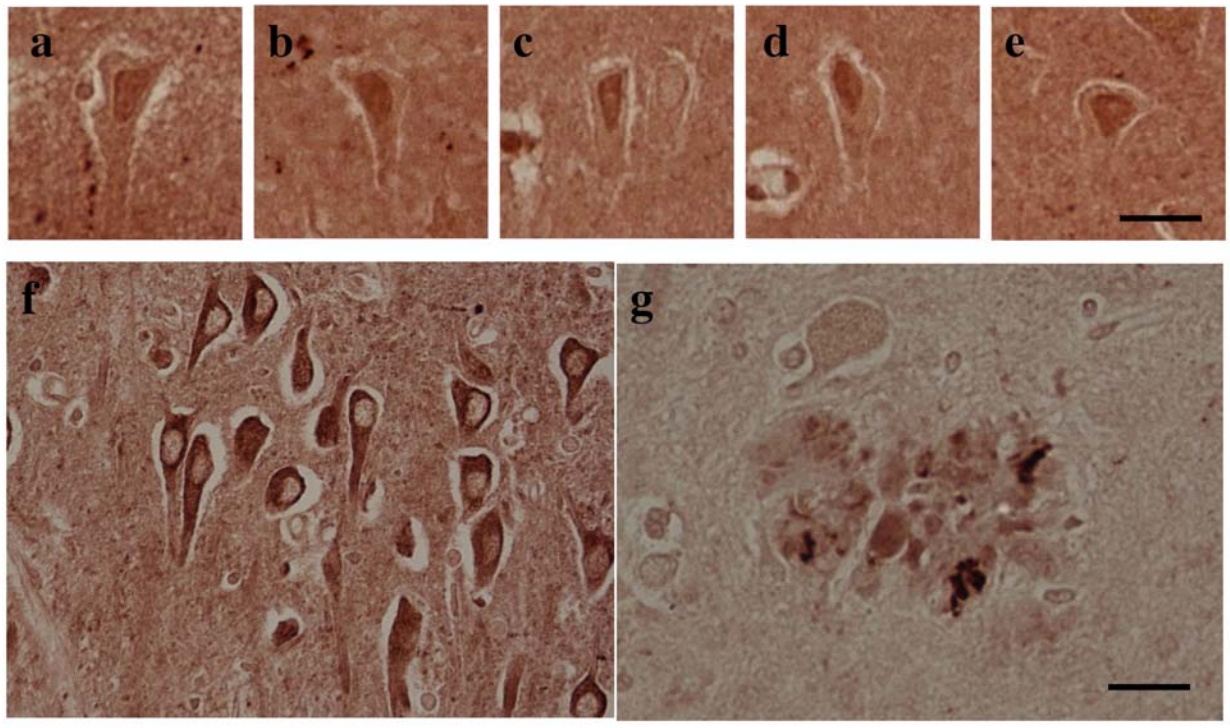

Figure 21. Hic-5 immunoreactivity localizes in the nucleus of CA1 pyramidal neurons and neuritic plaques throughout the AD hippocampus
(a – f): Hic-5 was detected in the nucleus of a number of CA1 pyramidal neurons. **(g):** Hic-5 was detected in neuritic plaques throughout the AD hippocampus. Scale bars = **(a - e)** 30 μm, **(f and g) 25** μm.
.

(tubulin or tau) or dendrites (MAP2) would confirm if these proteins are colocalizing in the OML.

Hic-5 immunofluorescence was observed in pyramidal neurons throughout the hippocampal within neurites, the cell body and nucleus (Fig. 23). Hic-5 positive pyramidal neurons were also observed adjacent to β-amyloid containing plaques (Fig. 23, panels a – c). The presence of Hic-5 immunofluorescence in beaded processes projecting throughout the hippocampus and a subset of plaques (Fig. 23, panels a and j) were noted. Hic-5 immunofluorescence was also observed in the majority of AT8 labeled NFTs, including those

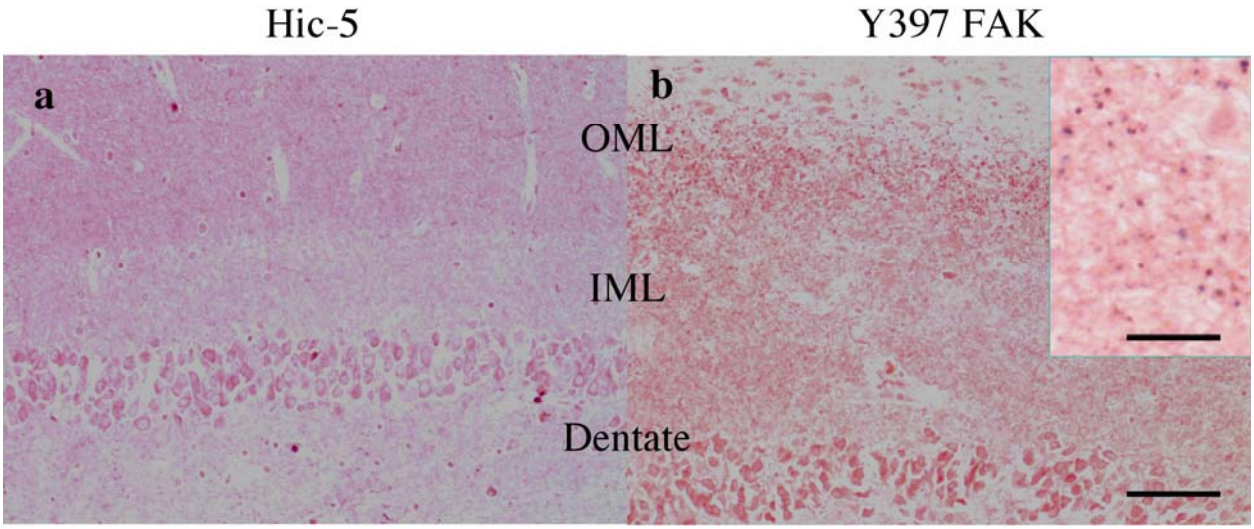

Figure 22. Hic-5 and FAK y397 immunoreactivity in the outer molecular layer of the dentate gyrus of AD subjects
Tissue sections from AD hippocampus immunostained with **(a):** anti-Hic-5 antibodies reveal increased immunoreactivity in the outer molecular layer compared to the inner molecular layer of the dentate gyrus in AD subjects. **(b):** FAK y397 antibodies reveal increased immunoreactivity in the outer molecular layer compared to the inner molecular layer of the dentate gyrus in AD subjects. Aggregates were positive for y397 FAK **(b):** inset. Scale bars = **(a and b)** 100 μm, **(b)** inset = **25** μm.

adjacent to plaques in AD hippocampus (Fig. 23, panels d – i). Colocalization of Hic-5 in AT8 positive NFTs was evident in the perinuclear region or limited to large processes proximal to the cell body (Fig. 23, panels d – i). Neuropil threads recognized by AT8 were negative for Hic-5 (Fig. 23, panels d – i). Many Hic-5 containing pyramidal neurons lack AT8 positive NFTs, and Hic-5 was not observed in extracellular ghost tangles (Fig. 23, panels d – i). Hic-5 immunofluorescence was consistently observed within the plaque core (Fig. 23, panels a – f). These results mimic the diversity of Hic-5 immunoreactivity observed by light microscopy. Hic-5 was not localized to activated astrocytes (GFAP positive cells) (data not shown) but exhibited colocalization in CD68 positive microglia within plaque pathology (Fig. 23, panels j – l).

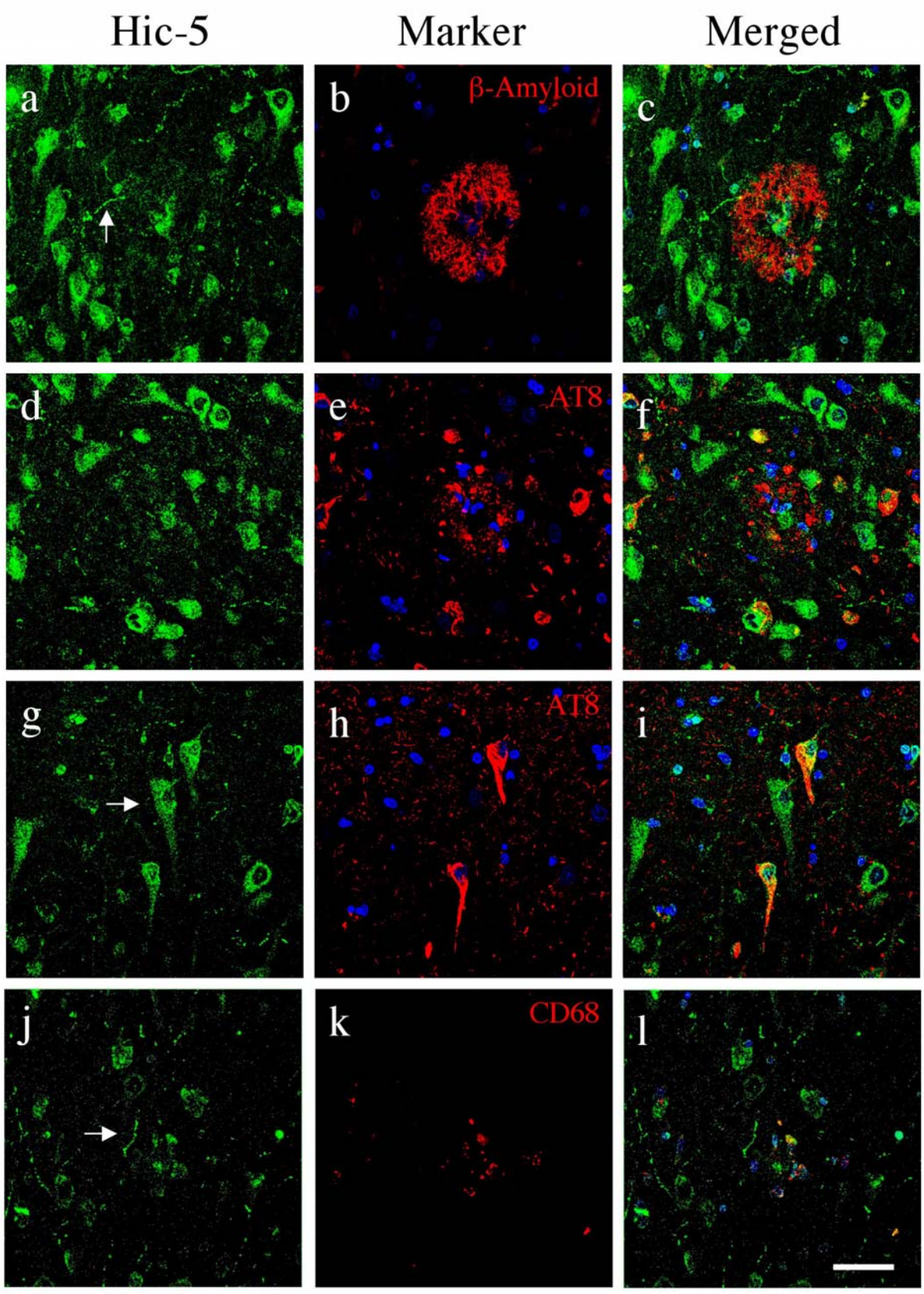
Hic-5
Marker
Merged
a
b
β-Amyloid
c
d
e
AT8
f
g
h
AT8
i
j
k
CD68
l

Figure 23. Hic-5 distribution in Alzheimer's disease pathology
LSCM with Hic-5 (green), nucleus (blue) and plaque components (red) representing β-amyloid, pTau, or microglia. Hic-5 immunofluorescence was localized to pyramidal neurons in the hippocampus, as well as processes and plaque cores within β-amyloid positive plaques **(a – c)**. Arrow **(a)** indicates beaded process projecting through plaque in panel **(c)**. In AT8 labeled NFTs, Hic-5 immunofluorescence was found surrounding and co-localizing within plaques **(d – f)**. A subset of AT8 positive NFTs exhibit colocalization with Hic-5 in the perinuclear region and proximal neuritic processes of pyramidal neurons **(d – i)**. Arrow in **(g)** indicates Hic-5 immunofluorescence in a pyramidal neuron negative for NFTs **(g – i)**. Arrowheads in **(g)** denote examples of Hic-5 co-localization in DAPI labeled nuclei **(g – i)**. Hic-5 immunofluorescence was co-localized in CD68 positive microglia within plaques **(j – l)**. Scale bars = **(a - l)** 50 μm.

Hic-5 immunofluorescence was detected in dystrophic neurons thoughout the hippocampal subfields. In the subiculum/entorhinal cortex subfield, Hic-5 immunofluorescence was detected in dystrophic neurons that were both positive and negative for AT8 (Fig. 24, panels a and b). Other investigators have reported that FTD patients have different types of intracellular inclusions based on the presence or absence of pTau (274). However, all inclusions specific to FTD subjects are positive for ubiquitin. Further studies with Hic-5, pTau, and ubiquitin are needed to establish whether Hic-5 labels FTD inclusions. Hic-5 IF was detected in a cell cluster surrounding the lateral ventricle and appear to be similar to those seen in periventricular heterotopia (275). These nodules are believed to due to a defect in migration from radial glial cells but could also be due to a defect in migration within the cells that use radial glial cells for migration. In granular ependymitis, the eppendymal lining is damaged and the cells are replaced by reactive astrocytes. Hic-5 is partially colocalized with MAP-2 neuronal processes in these nodules (Fig. 24).

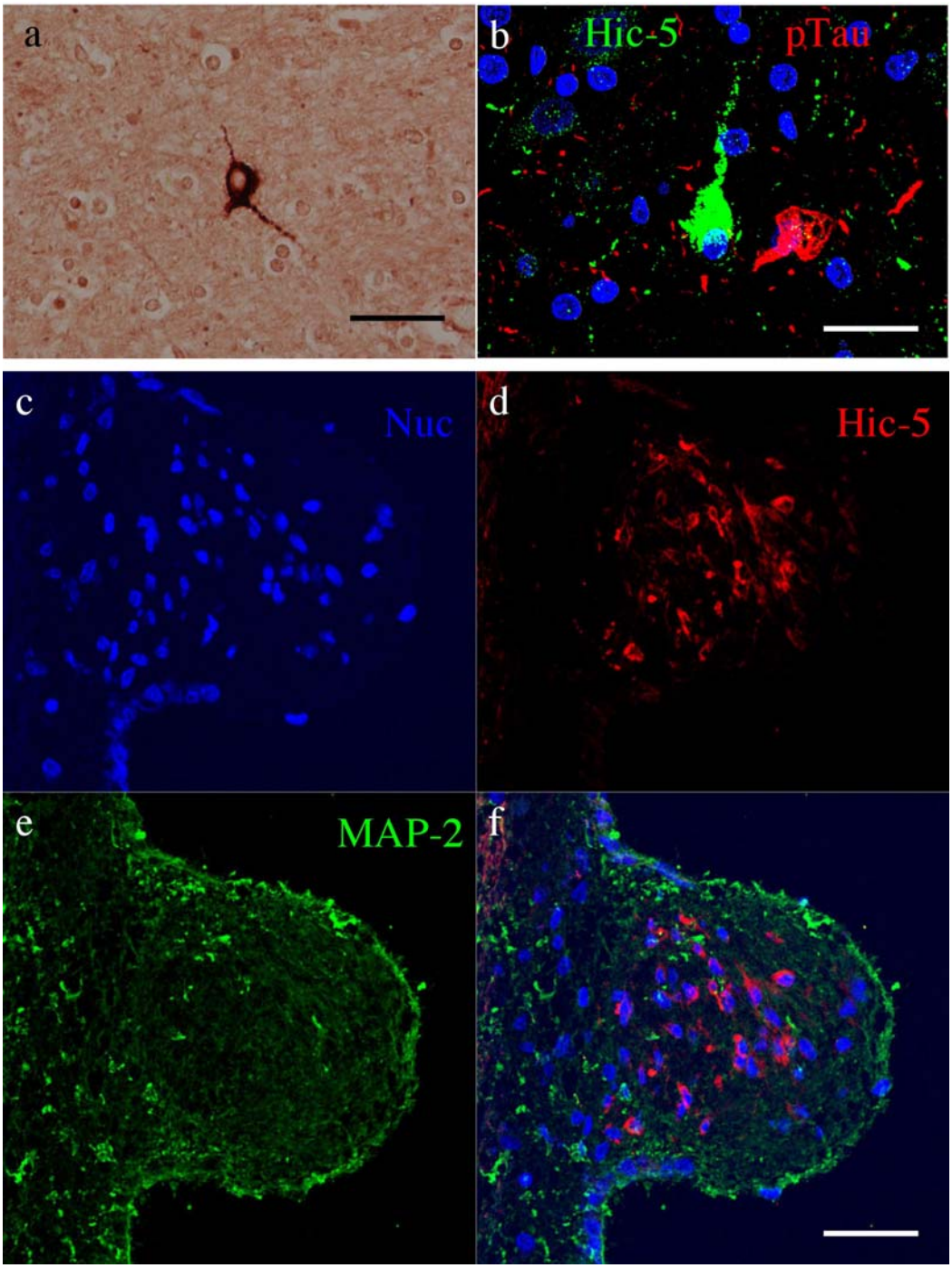

Figure 24. Hic-5 localization within intraneuronal inclusions and periventricular heterotopias.
Hic-5 immunoreactivity was localized within intraneuronal inclusions **(a).** Hic-5 immunofluorescence was localized in pTau negative intraneuronal inclusions **(b).** Hic-5 immunofluorescence was co-localized with MAP-2 in periventricular heterotopias **(c - f).** Scale bars = **(a)** 37.5 μm, **(fb) 25** μm, **(c – f)** 100μm.

4.5 PAXILLIN DISTRIBUTION IN HIPPOCAMPUS

Paxillin localizes to cells of the vascular system including smooth muscle cells surrounding arteries and large capillaries (Fig. 17, panel d) as well as arterial/capillary endothelial cells and (Fig. 17, panels e and f). Paxillin stained the walls of the vascular system indicative of endothelial cells and showed clear nuclear staining (Fig. 17, panels e and f). Further, ependymal cells that line the ventricles that do not have a basement membrane are also positive for paxillin (data not shown). Paxillin immunoreactivity in control hippocampus was predominately located to the outer white matter closest to the lateral ventricle and the stratum lacunosum (Fig. 25, panels a and b). Paxillin immunoreactivity was detected in the nucleus and cytoplasm of reactive astrocytes and neuropil within the hilus/CA4 region of all cases (Fig. 25, panels a – d). However, paxillin immunoreactivity was significantly increased in reactive astrocytes and neuropil throughout the CA3, CA2 and CA1 hippocampal subfields in AD subjects compared to control subjects (Fig. 25, panels b and d; Table 10, Row 3). The highest paxillin protein levels were detected in late-stage AD subjects but this observation did not reach significance compared to control and early-stage AD subjects (Figure 26, Table 10, column B, Row 3). Although there was ae lack of statistical significance observed when comparing all three groups due to the presence of paxillin in astrocytes of the hilus/CA4 in both control and early-stage AD subjects, paxillin immunoreactivity was increased in AD and tended toward significance (Fig. 26, panel c). Although paxillin was predominately expressed in reactive astrocytes, paxillin immunoreactivity was observed localized in focal nuclear granules of CA1 pyramidal neurons in control subjects (Fig. 27, panel a). Rank order analysis showed a significant loss in the nuclear distribution of paxillin in CA1 pyramidal neurons of all AD subjects compared to controls was

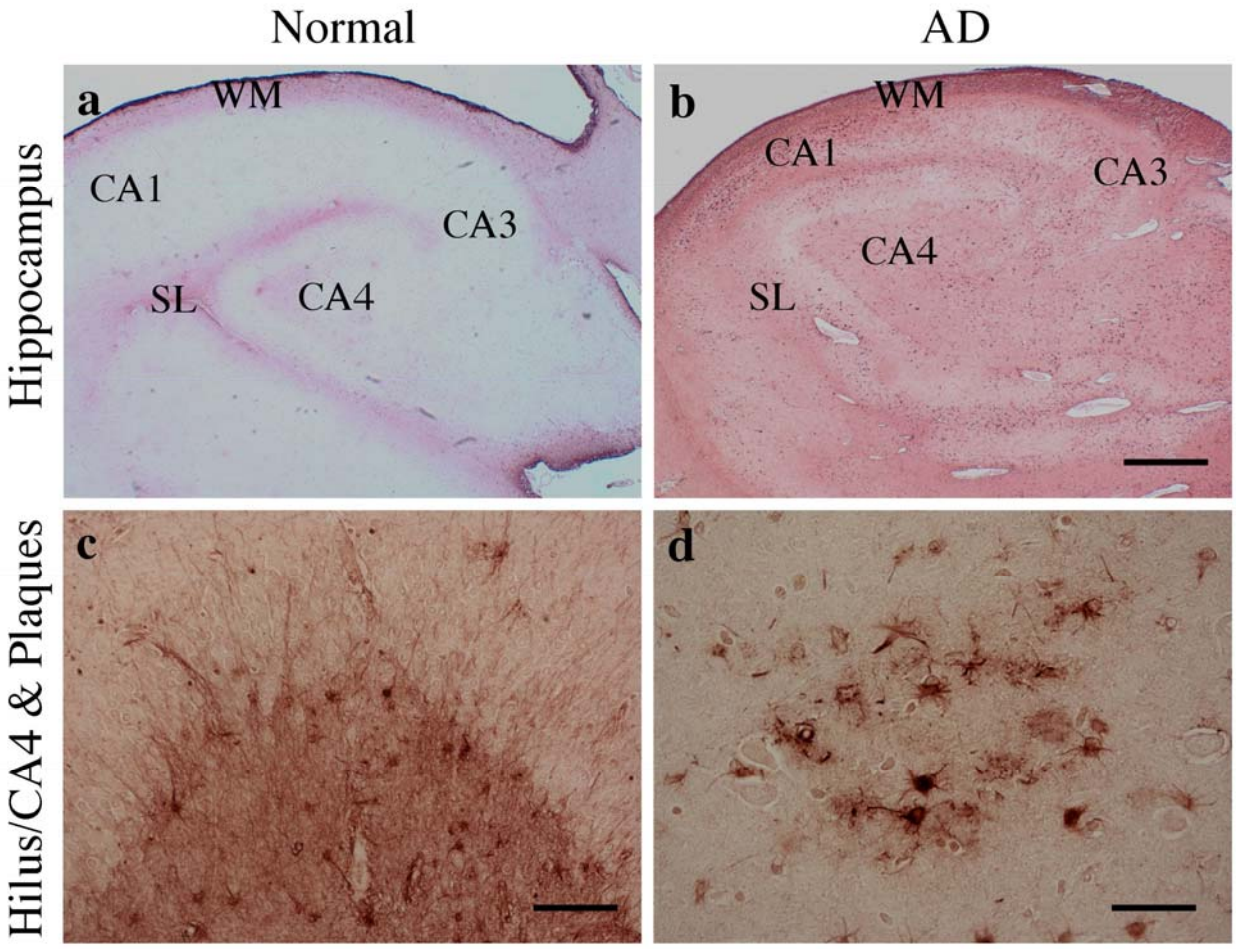

Figure 25. Paxillin expression in control and Alzheimer's disease hippocampus
Low power magnification reveals paxillin immunoreactivity in the alveus/white matter (WM) tracts and the stratum lacunosum (SL) layer in both control **(a)** and AD **(b)** subjects. In the hilus/CA4 of control subjects, paxillin is localized to reactive astrocytes and neuropil **(c)**. AD hippocampus exhibits elevated paxillin immunoreactivity in reactive astrocytes throughout the hippocampus and within plaques **(d)**. Scale bars = **(a and b)** 500μm, **(c) 100**μm, **(d)** 50μm.

also observed (Fig. 27 panel b; Table 10, Row 4). Though control subjects did have the highest number of CA1 pyramidal neurons with paxillin distributed in focal nuclear granules, upon counting at least 100 pyramidal neurons in each section the nuclear distribution of paxillin only trended towards significant loss in CA1 pyramidal neurons during AD progression ($p < 0.167$). A statistically significant loss in nuclear paxillin within the choroid plexus of AD patients was

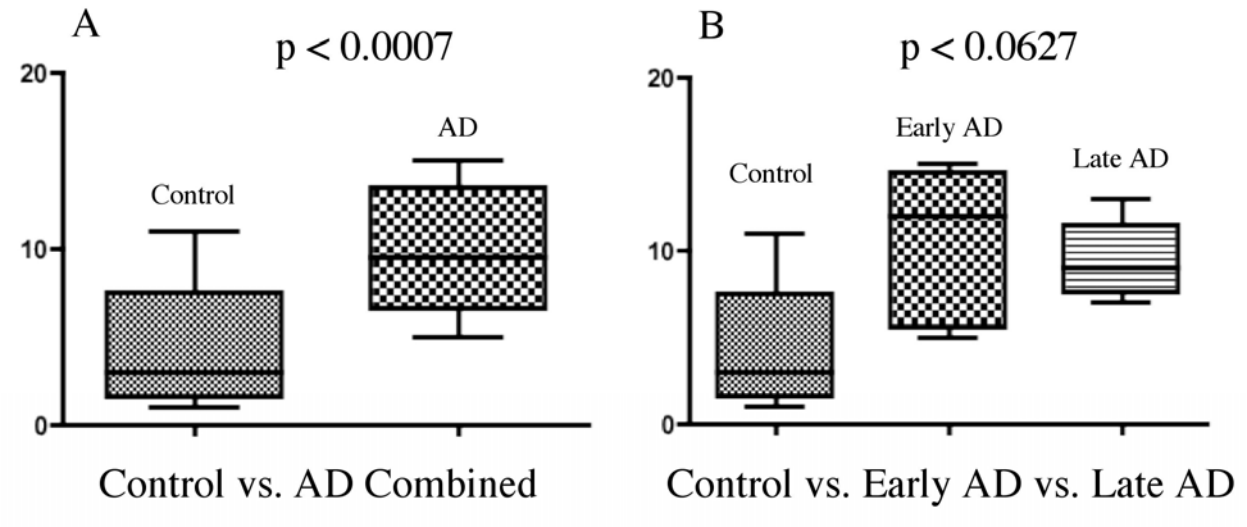

Figure 26. Graphical representation of paxillin immunoreactivity in AD
The results of these significance tests for paxillin expression levels in Table 10 are shown by graphical representation. **(A)**: Mann Whitney statistical test comparing paxillin levels in control vs. AD subjects, **(B)**: Kruskal-Wallis statistical test comparing paxillin levels in control vs. early-stage AD vs. late-stage AD subjects.

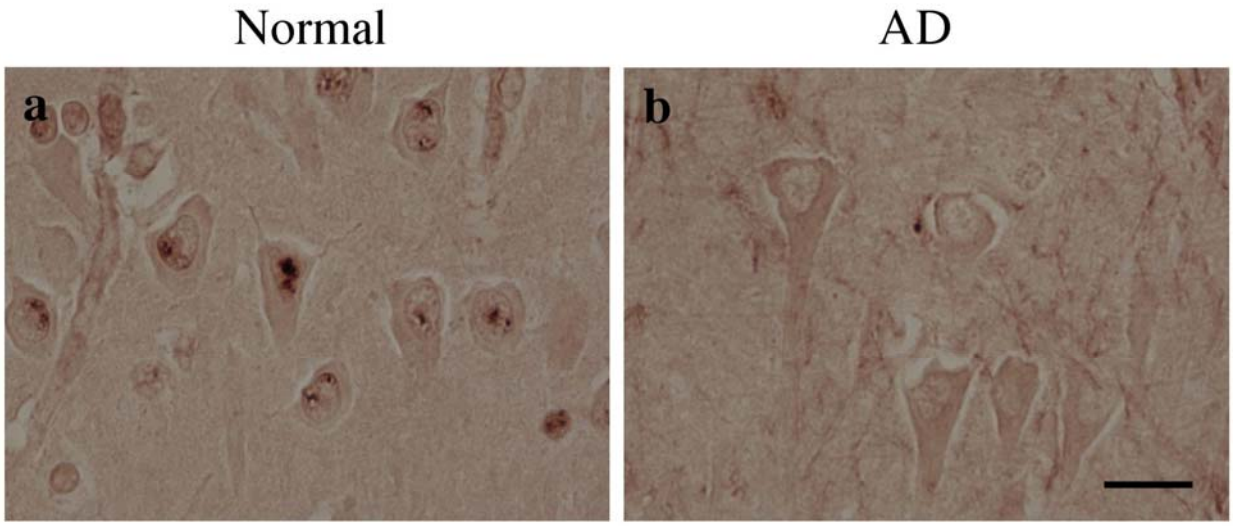

Figure 27. Paxillin localization in CA1 pyramidal neurons
CA1 pyramidal neurons in control subjects display paxillin predominantly in nuclei **(a)**. Paxillin is predominately in the cytoplasm of CA1 pyramidal neurons in AD subjects **(b)**. Though control subjects contained the majority of nuclear paxillin CA1 pyramidal neurons, the observed losses of paxillin the nuclei of AD subjects did not reach a level of statistical significance (Kruskal-Walllis statistical test). Scale bars = **(a and b)** 25μm.

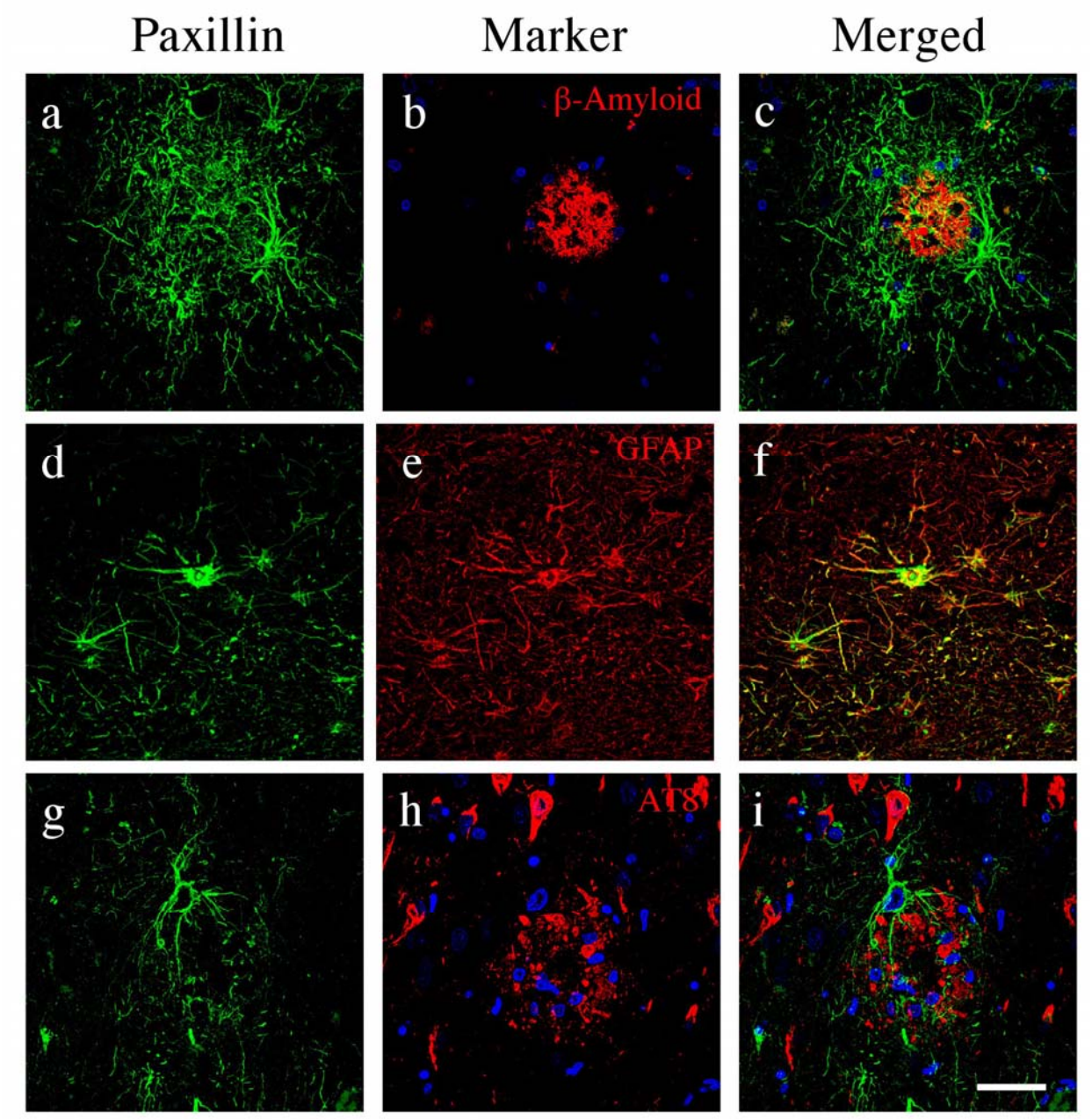

Figure 28. Paxillin localization in Alzheimer's disease pathology
LSCM of AD hippocampus with paxillin (green), nucleus (blue) and plaque components (red): β-amyloid, hyperphosphorylated tau, activated astrocytes **(a – i)**. Paxillin immunofluorescence was elevated in reactive astrocytes and numerous processes surrounding and penetrating β-amyloid positive plaques throughout the AD hippocampus **(a – c)**. Paxillin immunofluorescence was observed in the majority of GFAP positive reactive astrocytes surrounding plaques **(d – f)**. Paxillin was not detected in AT8 immunoreactive NFTs **(g – i)**. Scale bars = **(a - i)** 50μm.

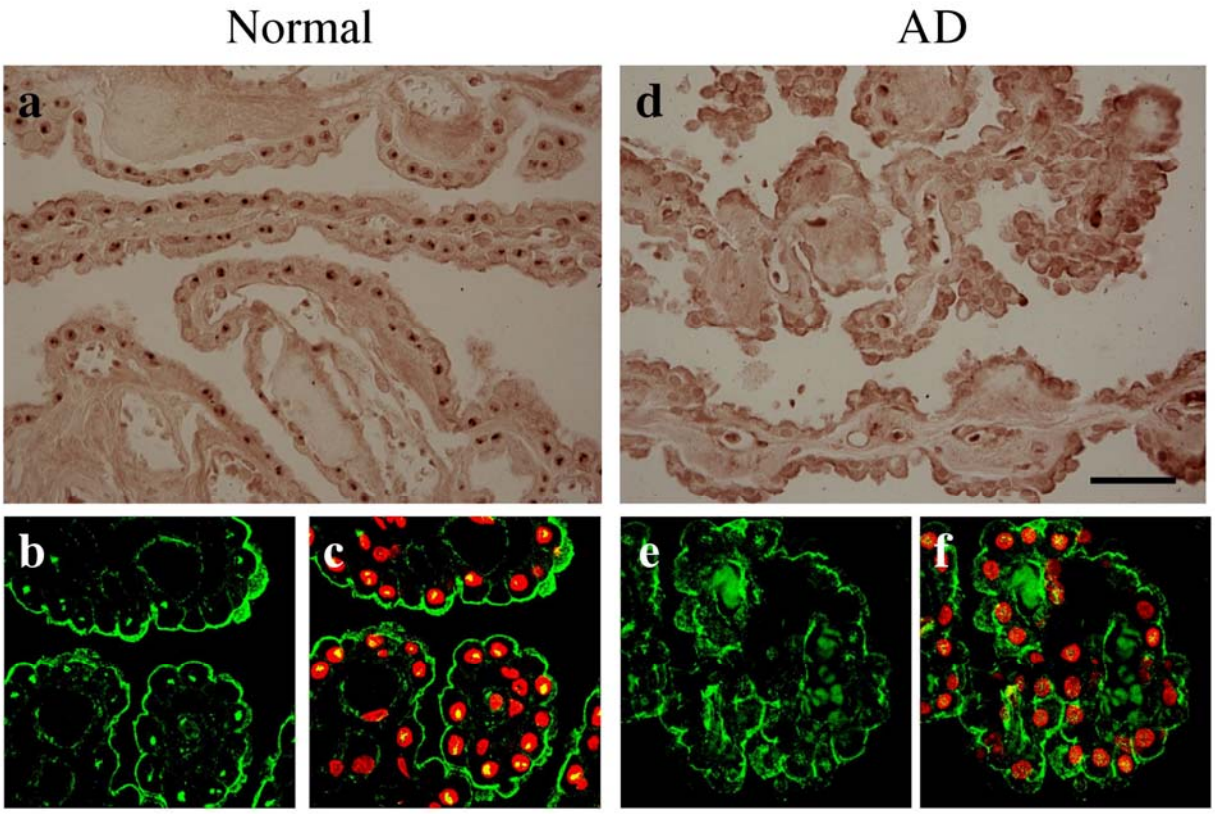

Figure 29. Paxillin localization in cells of the choroid plexus
Paxillin immunoreactivity was also observed in the choroid plexus of control **(a)** and AD **(d)** subjects. Note loss of nuclear immunoreactivity in AD subjects **(d)**. LSCM of control and AD choroid plexus for paxillin (green) and cell nuclei (red) **(b and c; e and f)**. Paxillin immunofluorescence was predominantly expressed in the nucleus of the choroid plexus in control subjects **(b and c)** but reduced in nuclei of AD subjects **(e and f)**. Scale bars = **(a – f)** 50μm.

noted (Fig. 27, panels a and b; Table 10, Row 5). Therefore, in AD paxillin immunoreactivity is elevated in reactive astrocytes and decreased in the nuclei of CA1 pyramidal neurons and choroid plexus cells. To further define cell types expressing paxillin associated with AD pathology, LSCM with cell type specific markers were used. Paxillin immunofluorescence was elevated in cells containing numerous processes surrounding and penetrating β-amyloid containing plaques in AD hippocampus (Fig. 28, panels a – c). Colocalization of paxillin and a

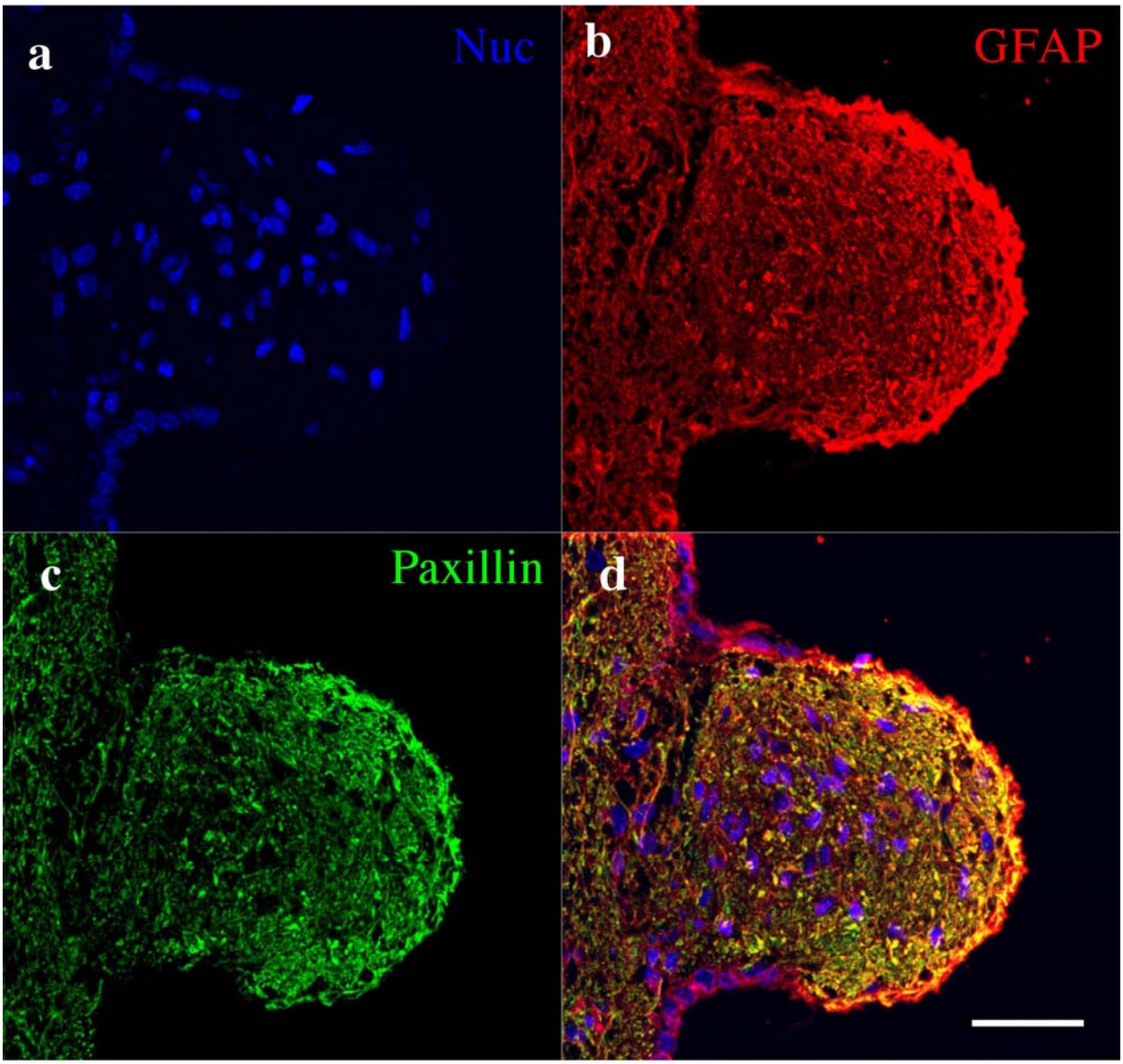

Figure 30. Paxillin localization in periventricular heterotopias
Paxillin immunofluorescence was colocalized with GFAP in periventricular heterotopias **(a - d).** Scale bars = **(a – d)** 100μm.

subset of GFAP labeled reactive astrocytes surrounding plaque pathology in AD were detected (Fig. 28, panels d – f). This result is consistent with observations by light microscopy showing paxillin in reactive astrocytes (Fig. 28, panel d). Colocalization of paxillin and GFAP immunofluorescence was not evenly distributed and appeared in discrete locations within the

glial processes though it is posible that antibody hindrance by unknown methods may have reduced the apparent colocalization (Fig. 28, panel f). Paxillin immunofluorescence was not detected in AT8 labeled NFTs (Fig. 28, panels g – i). Paxillin in nuclei of choroid plexus cells in control subjects was also detected (Fig. 29, panels a - c), with loss of nuclear immunostaining in AD (Fig. 29, panels d - f). These results are also consistent with those observed from light microscopy (Fig. 29, panels a and d). Paxillin IF was detected in a cluster of cells that surround the lateral ventricle (Fig. 30). In granular ependymitis, the eppendymal lining is damaged and the cells are replaced by reactive astrocytes (275). Paxillin is predominantly colocalized with GFAP positive cells in these nodules (Fig. 30).

4.6 DISTRIBUTION OF ACTIVATED ISOFORMS OF PAXILLIN

To further determine the cell types that exhibit these phosphorylated forms of paxillin, performance of both light microscopy and LSCM of control and AD tissue sections were conducted. In control subjects, pY31 paxillin immunoreactivity was distributed throughout the soma, processes and well-defined nuclear localization in hippocampal pyramidal (Fig. 31 A, panel a) and dentate neurons (data not shown). In AD, pY31 paxillin was observed in the cytoplasm, punctate structures within the soma, and reduced levels within nuclei of CA1 pyramidal neurons (Fig. 31 A, panel b). pY31 recognized both Hirano bodies and plaques in the hippocampus of AD subjects (Fig. 31, panels c and d). pY31 paxillin immunofluorescence was observed by LSCM in pyramidal neurons and colocalized with AT8 immunopositive soma and neuritic processes (Fig. 31 B, panels a – f). Within plaques, pY31 paxillin was present in both AT8 positive and negative neuritic processes (Fig. 31 B, panels d – f). Serial hippocampal

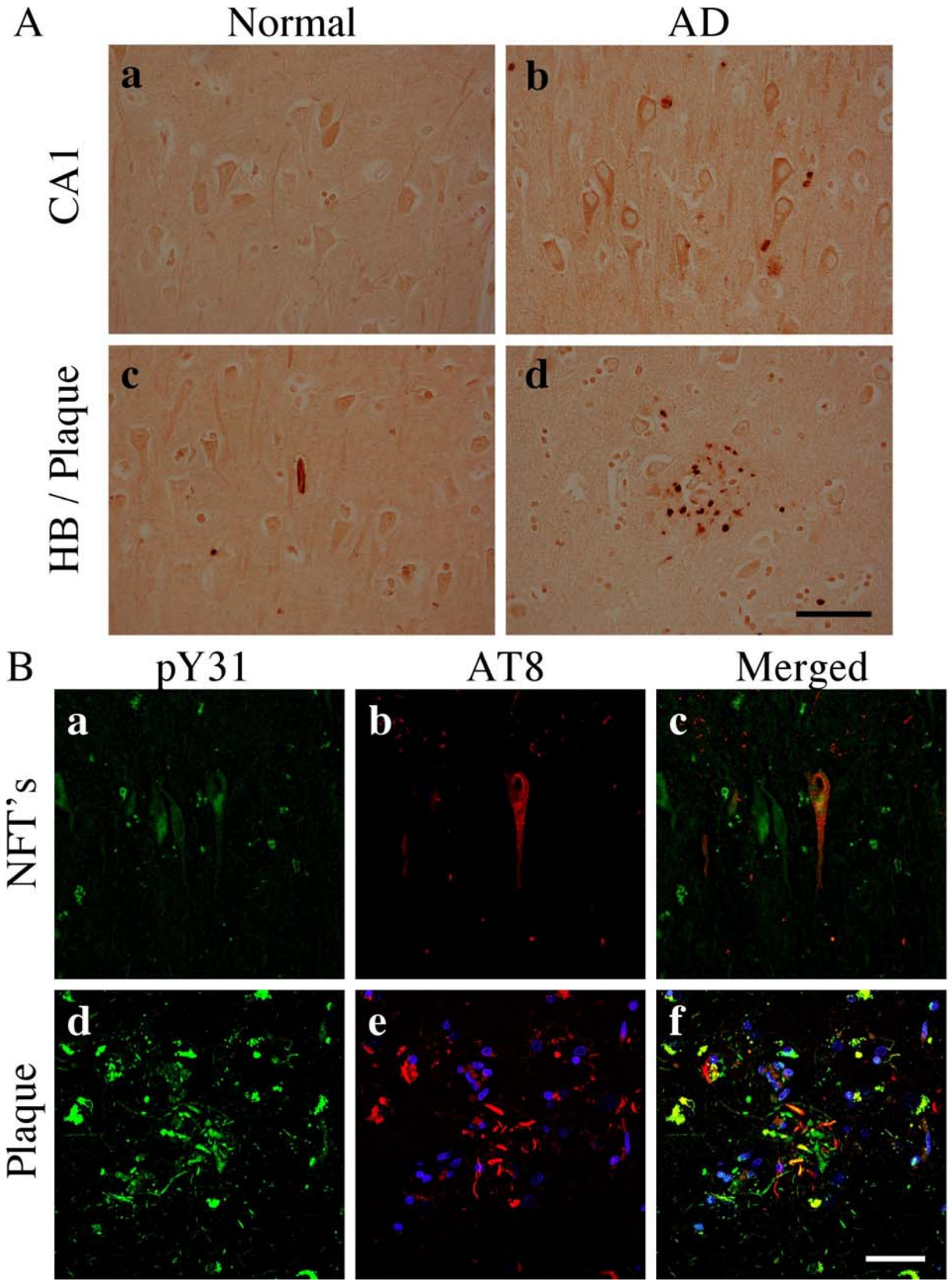
A
Normal
AD
a
b
CA1
c
d
HB / Plaque
B
pY31
AT8
Merged
a
b
c
NFT's
d
e
f
Plaque

Figure 31. Expression of phosphorylated Y31 (pY31) paxillin in human hippocampus
(A): Hippocampal sections were labeled with anti-pY31 paxillin antibody from both control and AD subjects **(a and b).** Magnification is 400X. pY31 paxillin localized to Hirano bodies **(c)** and neuritic plaques **(d). (B):** LSCM with pY31 paxillin (green), nucleus (blue) and AT8 labeled hyperphosphorylated tau (red). pY31 paxillin immunofluorescence was co-localized in the majority of AT8 positive pyramidal neurons in both NFTs and neuritic processes within plaque pathology **(a – f)**. Scale bars = A: **(a – d)** 50μm, B: **(a – f)** 50μm.

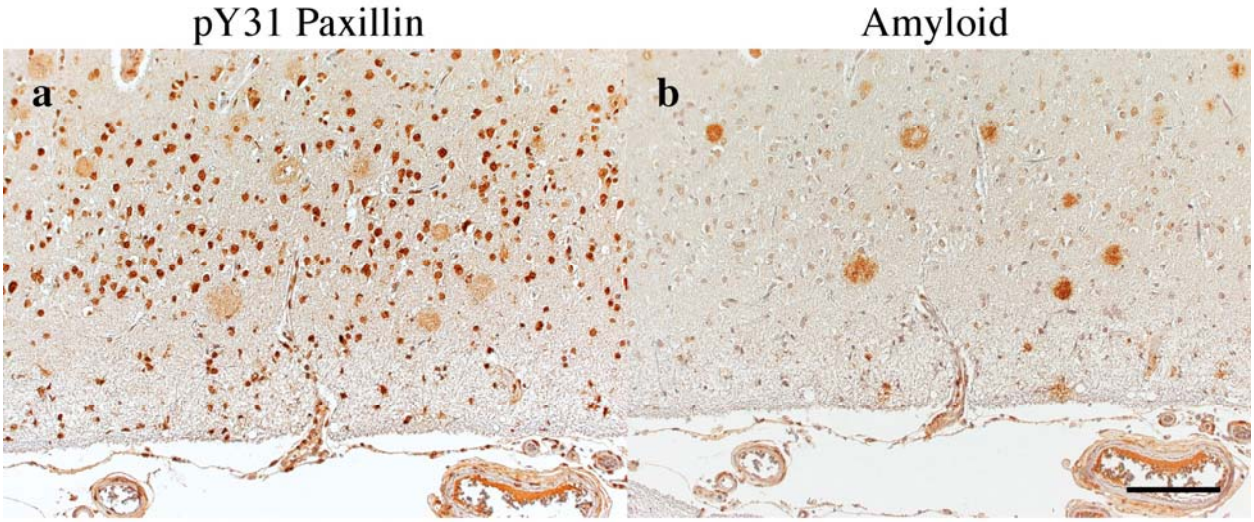

Figure 32. Expression of phosphorylated Y31 (pY31) paxillin in plaques
Tissue sections from AD hippocampus immunostained with pY31 paxillin antibody reveals protein expression in plaques as determined by serial tissue sections stained with antibodies for amyloid. Scale bar = 200μm

sections stained for pY31 and amyloid showed overlapping plaque positive staining (Fig. 32).

Phosphorylated Y118 (pY118) paxillin immunoreactivity was predominately located in the nucleus of hippocampal pyramidal neurons in control subjects (Fig. 33 A, Normal). In the CA1 hippocampal subfield of AD subjects, pY118 paxillin immunoreactivity was decreased within nuclei. However, the presence of pY118 paxillin positive granulovacular degeneration (GVD) bodies was observed in AD subjects (Fig. 33 A, AD). Both of these differences in pY118 immunostaining between control and AD subjects reached statistical significance in the CA1

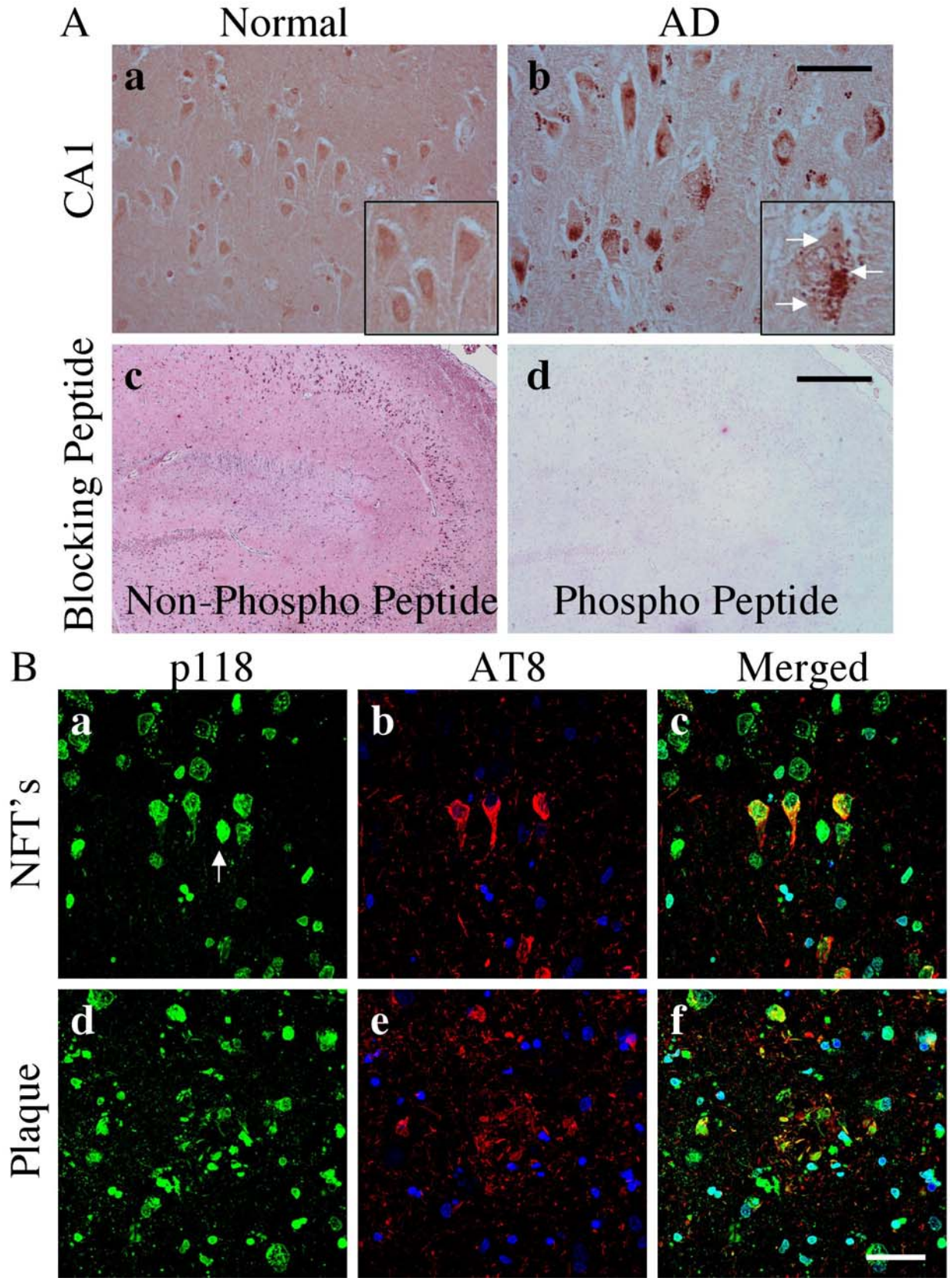
A
Normal
AD
a
b
CA1
Blocking Peptide
c
d
Non-Phospho Peptide
Phospho Peptide
B
p118
AT8
Merged
a
b
c
NFT's
d
e
f
Plaque

Figure 33. Expression of phosphorylated Y118 (pY118) paxillin in human hippocampus
(A): Hippocampal sections from control and AD subjects labeled with anti-pY118 paxillin antibody. CA1 pyramidal neurons in AD hippocampus contain elevated levels of pY118 paxillin immunoreactivity in GVD bodies. Insets are higher magnification showing pY118 paxillin immunoreactivity in CA1 pyramidal neurons. Arrows in AD inset indicate GVD bodies within a CA1 pyramidal neuron. pY118 paxillin specific peptide and non-specific peptide blocking controls were perfomed **(c and d). (B):** LSCM with pY118 paxillin (green), nucleus (blue) and AT8 labeled hyperphosphorylated tau (red). pY118 paxillin immunofluorescence was co-localized in the majority of AT8 positive pyramidal neurons in both NFTs and processes within plaque pathology **(a – f)**. Note extensive co-localization of pY118 paxillin in nuclei of neuronal and non-neuronal cells. Scale bars = A: **(a and b)** 50μm, **(c and d)** 500μm, B: **(a - f)** 50μm

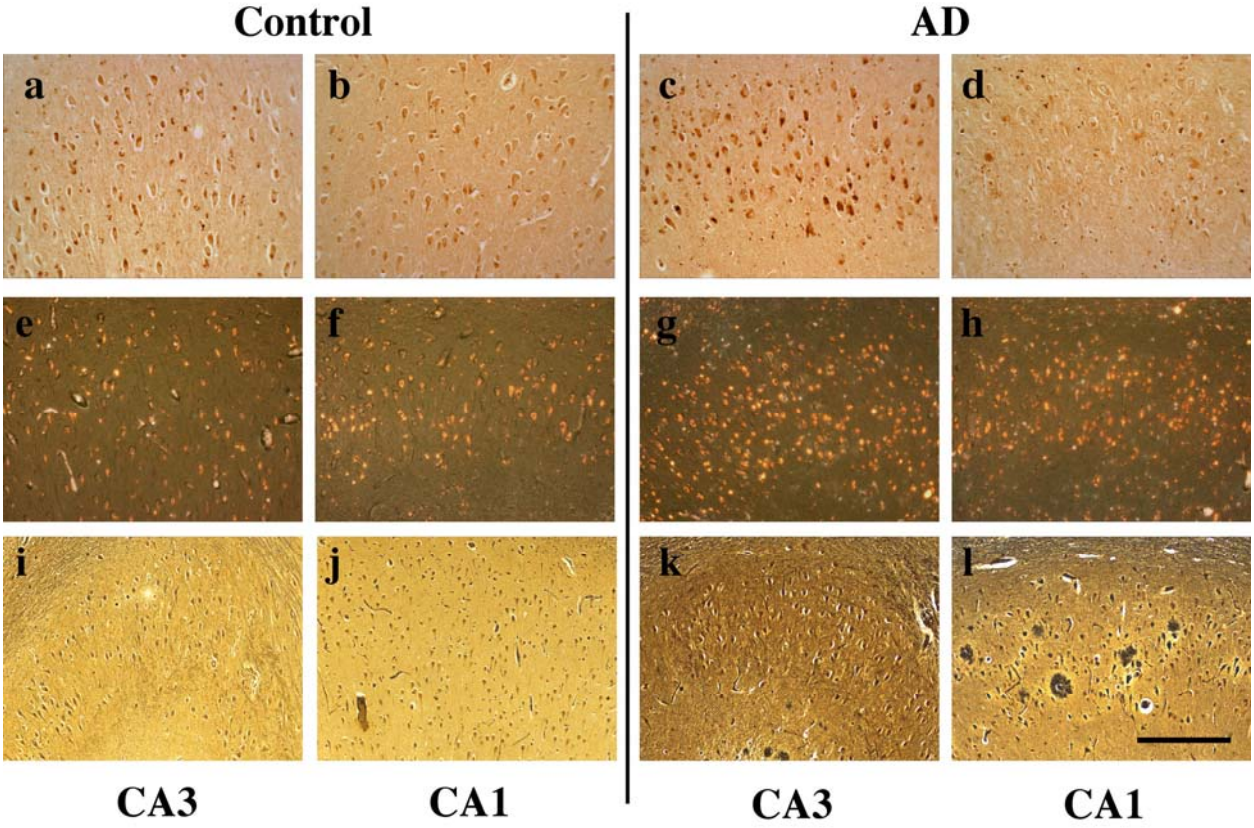

Figure 34. Internal control for lipofuscin for phosphorylated Y118 (pY118) paxillin immunoreactivity
Serial hippocampus sections were used to determine the specificity of anti-pY118 paxillin antibodies. pY118 immunoreactivity in control tissue **(a and b)** and AD tissue **(c and d)**. Autofluorescence was detected in control tissue **(e and f)** and AD tissue **(g and h)** by using a triple color (blue, green, and red) fluorescent microscope to view unstained hippocampus sections. A Bielschowsky stain in control tissue **(i and j)** and AD tissue **(k and l)** was utilized to determine the number of pyramidal neurons in the hippocampus sections. Scale bars = **(a - l)** 400μm.

subfield (Table 10, Rows 7 and 8). The specificity of the pY118 paxillin immunoreactivity was confirmed using phosphorylated and non-phosphorylated blocking peptides (Fig. 33 A, panels c andd). An internal control for lipofuscin (considered nondegradeable intracelluar garbage that some antibodies recognized nonspecifically) was developed to determine the specificity of the pY118 paxillin antibody at the light level and LSCM level. Using serial sections from control and AD subjects, a direct comparison of the IHC staining with the pY118 paxillin antibody was made with the autofluorescence profile using a triple cube for all wavelengths used in IF (Blue, Green, and Red) to determine if the level of autofluorescence was altered in AD subjects (Fig. 34). A Bielschowsky stain of the hippocampus from both control and AD subjects was also used to determine the architecture of the hippocampus and accompanying pathology. All images were aligned to determine overlap of the antibody detection signal and lipofuscin. This technique confirmed that the pY118 staining was beyond non-specific binding to lipofuscin in pyramidal neurons of the hippocampus. By LSCM, pY118 paxillin was observed in AT8 positive NFTs and plaques (Fig. 33 B). pY118 paxillin immunofluorescence was also found in GVD bodies that were negative for AT8 (Fig. 33 B, arrows in panels a – c). Abundant pY118 paxillin within nuclei of neuronal and non-neuronal cells was readily detected (Fig. 33 B, panels a – f). pY31 paxillin and pY118 paxillin recognized both internal and external epitopes in Hirano bodies (Fig. 31, panel c; Fig. 35). Hirano bodies are formed after aberrant caspase cleavage of actin filaments (fractin) that enable their crystallization which form a non-degradable protein complex. These crystalline structures are typicallyassociated with normal senescence and not specific to AD. However, it is believed that AD sublects may contain a greater number of Hirano bodies (111-114).

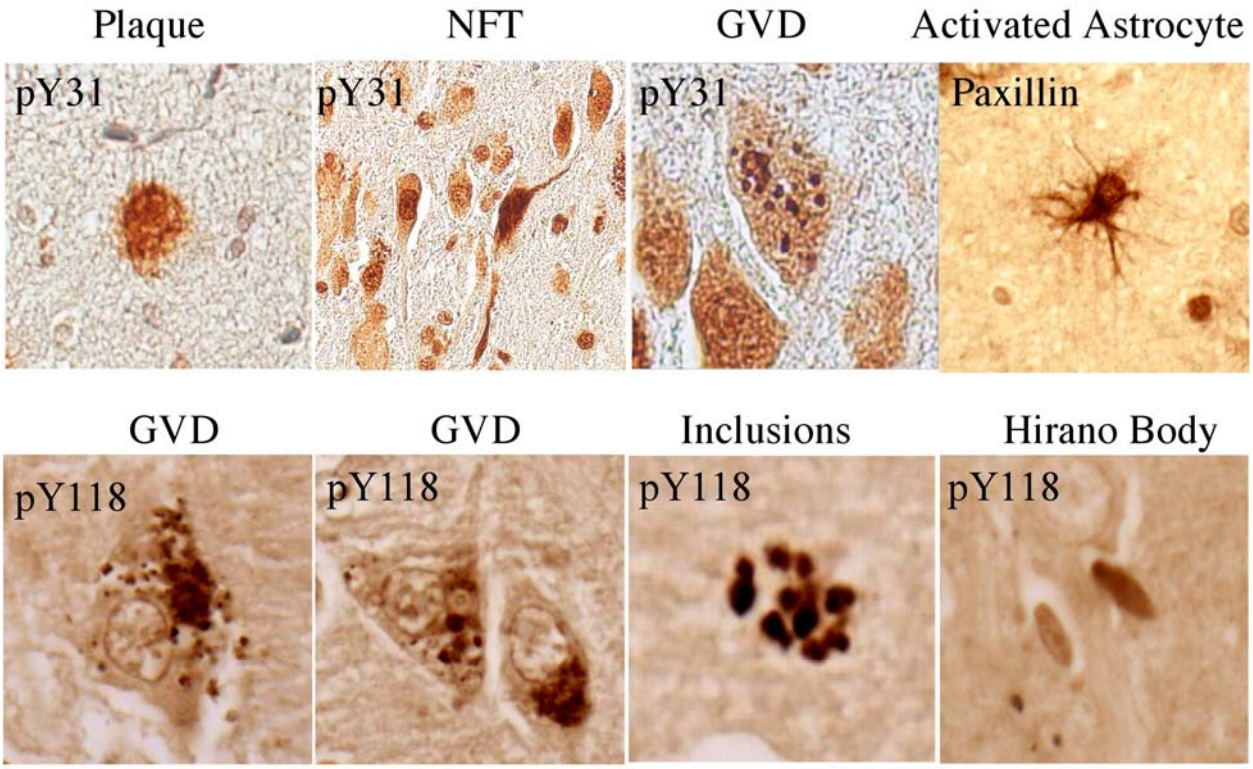

Figure 35. Pathological hallmarks in AD recognized by paxillin and activated isoforms of paxillin
Plaques = pY31, NFTs = pY31, GVDs = p118, activated astrocytes = paxillin, and Hirano bodies = pY118. Both pY31 and pY118 recognize both internal and expernal epitopes within Hirano bodies. pY31 detected a subset of GVDs while pY118 detects the majority of GVDs. pY118 detected inclusions that were not adjacent to neuronal cell bodies.

Phosphorylation of paxillin serine residues in control and AD brain were examined. Immunoblot analysis of the soluble fraction revealed a specific immunoreactive band of the appropriate molecular mass for pS126 specific antibodies (data not shown). However, my data did not reveal statistically significant differences in protein levels of pS126 in AD (data not shown). To further determine the cell types that exhibit serine phorphorylated isoforms of paxillin, both light microscopy and LSCM of control and AD tissue sections were performed. Phosphorylated S126 (pS126) paxillin immunoreactivity was detected in the soma and nucleus of neurons throughout the hippocampus of control subjects (Fig. 36 A). Within AD hippocampus,

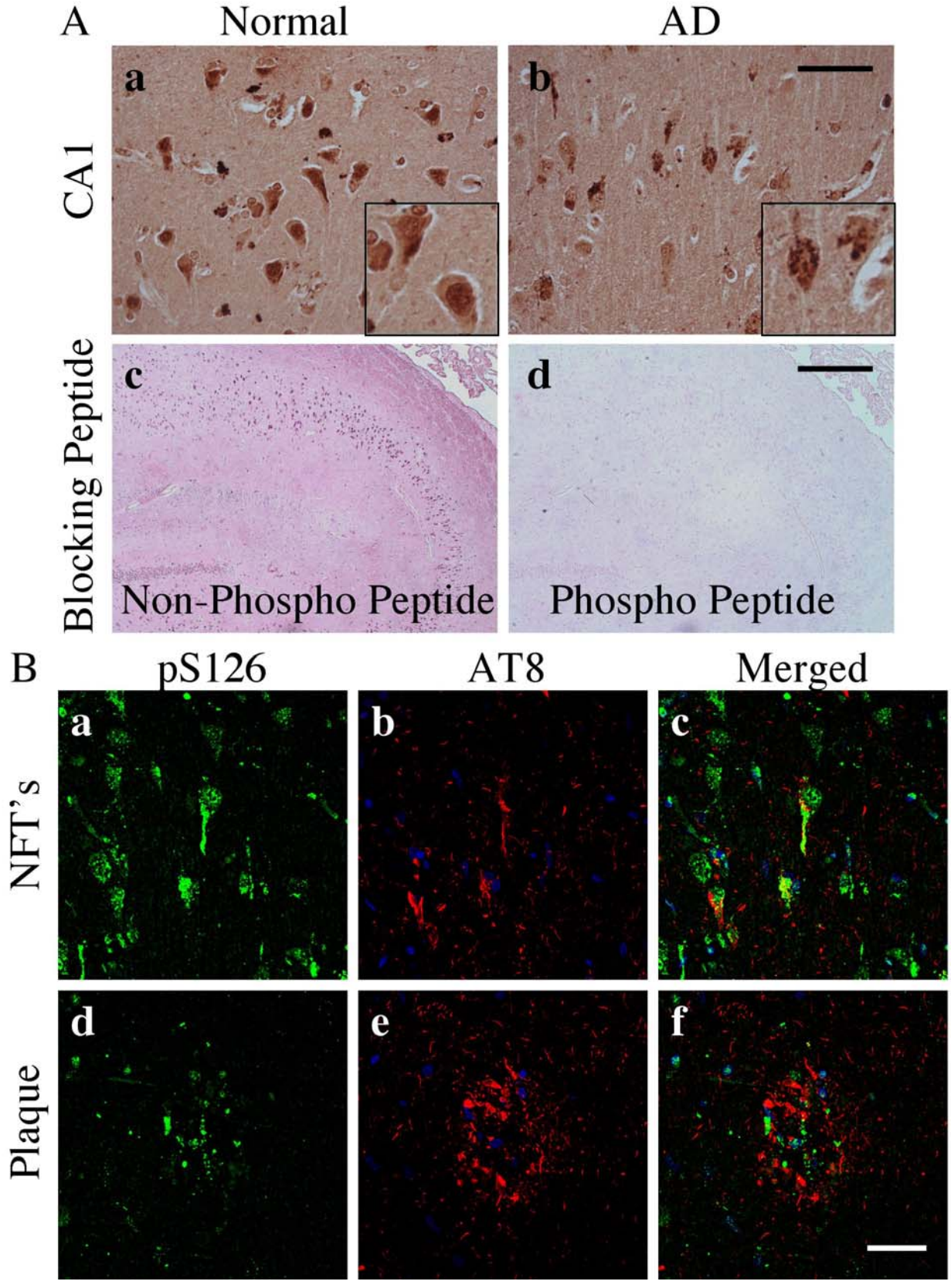
A
Normal
AD
a
b
CA1
Blocking Peptide
c
d
Non-Phospho Peptide
Phospho Peptide
B
pS126
AT8
Merged
a
b
c
NFT's
d
e
f
Plaque

Figure 36. Expression of phosphorylated S126 (pS126) paxillin in human hippocampus
(A): Hippocampal sections from control and AD subjects labeled with anti-pS126 paxillin antibody. CA1 pyramidal neurons in AD hippocampus contain elevated levels of pS126 paxillin immunoreactivity in GVD bodies and reduced nuclear pS126 paxillin compared to controls subjects. Insets are high power magnification of pS126 paxillin immunoreactivity in CA1 pyramidal neurons **(a and b)**. pS126 paxillin specific peptide and non-specific peptide blocking controls were perfomed **(c and d). (B):** LSCM with pS126 paxillin (green), nucleus (blue) and AT8 labeled hyperphosphorylated tau (red). pS126 paxillin immunofluorescence was co-localized in the majority of AT8 positive pyramidal neurons in both NFTs and processes within plaque pathology **(a – f)**. Scale bars = A: **(a and b)** 50μm, **(c and d)** 500μm, B: **(a - f)** 50μm

pS126 paxillin was significantly elevated in GVD bodies in the cytoplasm of CA1 pyramidal neurons (Fig. 36 A; Table 10, Row 9). The specificity of the pS126 paxillin antibody was confirmed using phosphorylated and non-phosphorylated blocking peptides (Fig. 36). Phosphorylated S178 (pS178) paxillin immunoreactivity was also detected in neuronal soma and nuclei throughout the hippocampus of control subjects (Fig. 37 A). In CA1 pyramidal neurons of AD subjects, significantly decreased levels of pS178 paxillin soma and nuclear and increased cytoplasmic granule staining were observed (Fig. 37 A; Table 10, Row 10). pS178 paxillin immunofluorescence was observed in neuronal processes, GVD bodies and NFTs in pyramidal neurons throughout the hippocampus (Fig. 37 B, panels a – c). pS178 paxillin in both AT8 positive and negative neuritic processes in plaques were detected (Fig. 37 B, panels d – f).

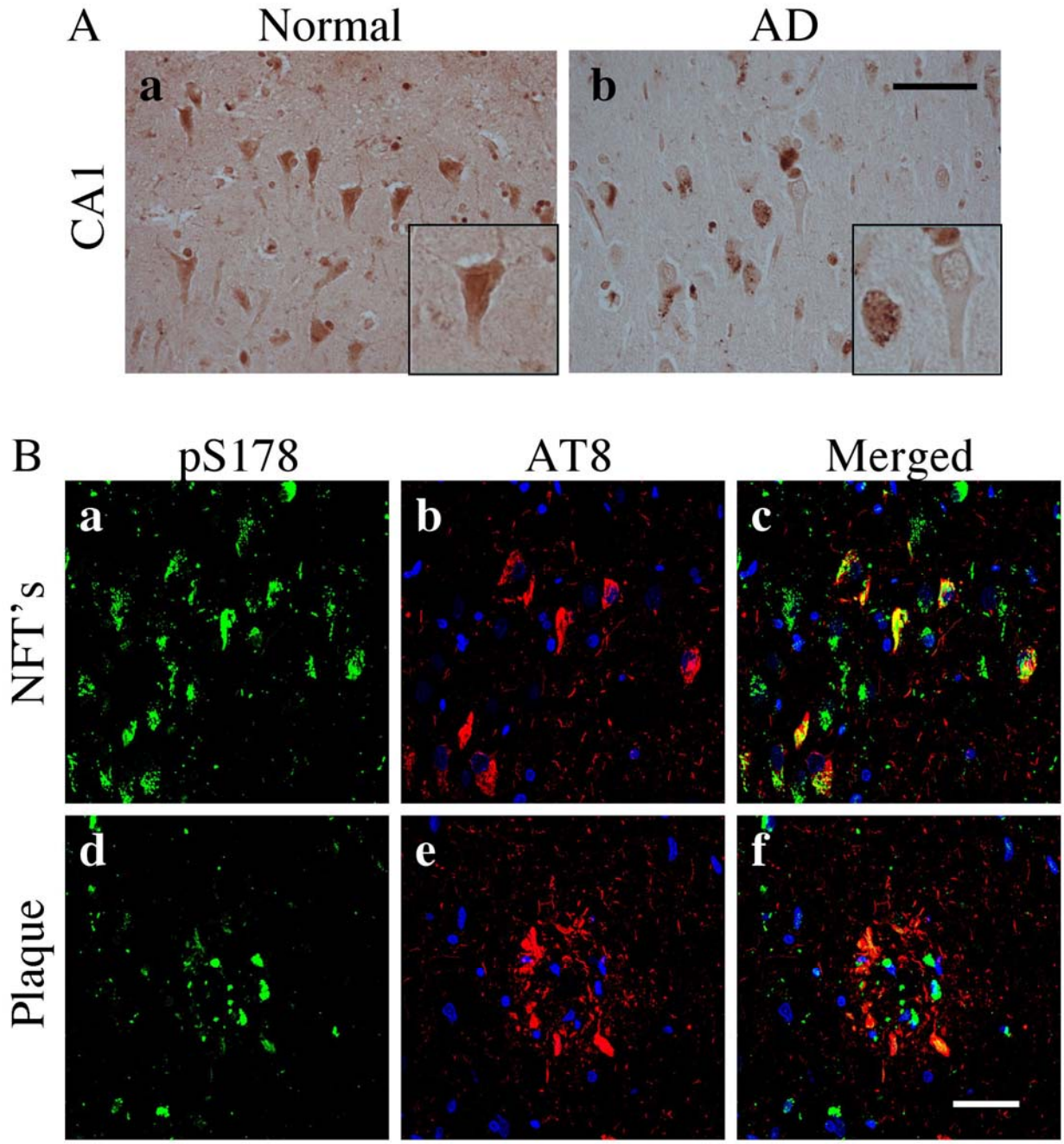

Figure 37. Expression of phosphorylated S178 (pS178) paxillin in human hippocampus
(A): Control and AD sections immunolabeled for pS178 paxillin. CA1 pyramidal neurons in AD hippocampus contain elevated levels of pS178 paxillin immunoreactivity in GVD bodies and reduced nuclear pS178 paxillin compared to controls subjects. Insets are high power magnification of pS178 paxillin immunoreactivity in CA1 pyramidal neurons **(a and b)**. **(B):** LSCM with pS178 paxillin (green), nucleus (blue) and AT8 labeled hyperphosphorylated tau (red). pS178 paxillin immunofluorescence was co-localized in the majority of AT8 positive pyramidal neurons in both NFTs and processes within plaque pathology **(a – f)**. Scale bars = A: **(a and b)** 50μm, **(a - f)** 50μm.

Table 10. Statistical Analysis

Antibody	Row #	Test Comparison	Control vs. Combined AD	Control vs. Early-Stage vs. Late-Stage AD
Hic-5		**Increased in AD**		
	1	CA1 Subfield	0.007*	0.005*
	2	Plaque Pathology	0.007*	0.003*
Paxillin		**Increased in AD**		
	3	Activated Astrocytes	0.019*	0.063
		Decreased in AD		
	4	CA1 Neurons: Nuclei	0.001*	0.007*
	5	Choroid plexus: Nuclei	0.003*	0.019*
pY31 Paxillin		**Decreased in AD**		
	6	CA1 Pyramidal Neurons	0.005*	0.014*
pY118 Paxillin		**Decreased in AD**		
	7	CA1 Subfield: Nuclei	0.001*	0.009*
		Increased in AD		
	8	GVDs in CA1 Neurons	0.001*	0.009*
pS126 Paxillin		**Increased in AD**		
	9	GVDs in CA1 Neurons	0.003*	0.008*
pS178 Paxillin		**Decreased in AD**		
	10	CA1 Subfield	0.003*	0.019*

Qualitative analysis of rank "intensity" order data comparing control vs. combined AD (early-stage and late-stage AD) subjects and control vs. early-stage AD subjects vs. late-stage AD subjects. Probability values less than 0.05 are considered significant. Control vs. combined AD cases, the Mann-Whitney statistical test was performed with the antibodies used in the case study. Two-tailed *p* values are shown. (*) = Significant differences between control and combined AD subjects. Control vs. early-stage vs. late-stage AD cases, the Kruskal-Wallis statistical test was performed with the antibodies used in the case study. Qualitative analysis of rank "intensity" order data comparing control vs. early-stage AD vs. late-stage AD subjects. For example, in row 2, hic-5 expression in CA1 neurons control subjects have lower expression compared to early-stage AD and early-stage AD subjects. Two-tailed P values are shown. (*) = Significant values indicate whether expression of proteins is different in control, early-stage AD and/or late-stage AD subjects. GVDs= granulovacuolar degenerative bodies.

4.7 COIMMUNOPRECIPITATION WITH P-TAU AND PRO-GROWTH MARKERS

While the analysis of phospho-specific paxillin expression provides an indirect assessment of distinct functional forms of paxillin (subject to activation by different signaling pathways), an independent approach was used to assess paxillin and Hic-5 functionality in AD and normal subjects. Therefore, coimmunoprecipitation assays were performed to assess whether Hic-5 and/or paxillin interacted with phosphorylated tau. Phosphorylated tau is known to interact with a number of intracellular signaling molecules and alter cellular response to various environmental cues. Coimmunprecipitation assays were performed as described in Chapter 3. As shown in Figure 38, pTau coimmunoprecipitated with Hic-5, paxillin and phosphorylated isoforms of paxillin (i.e. pY31, pY118) in AD but not in controls. Thus, Hic-5, paxillin and at least two phosphorylated isoforms of paxillin are stably associated with pTau. These immunoblots were further analyzed with known pro-growth phospho epitopes of c-Abl, SRC, and ERK1/2 proteins. Hic-5, paxillin, pY31, pY118, and c-Abl are associated with ERK1/2 and SRC in both control and AD subjects. The association of pY31 and pY118 paxillin with c-Abl may be greater in extracts from AD vs. control subjects. One possible mechanism of these interactions is that paxillin and c-Abl are involved in abbearant cell signaling during AD progression. However, additional experiments are required to confirm this observation.

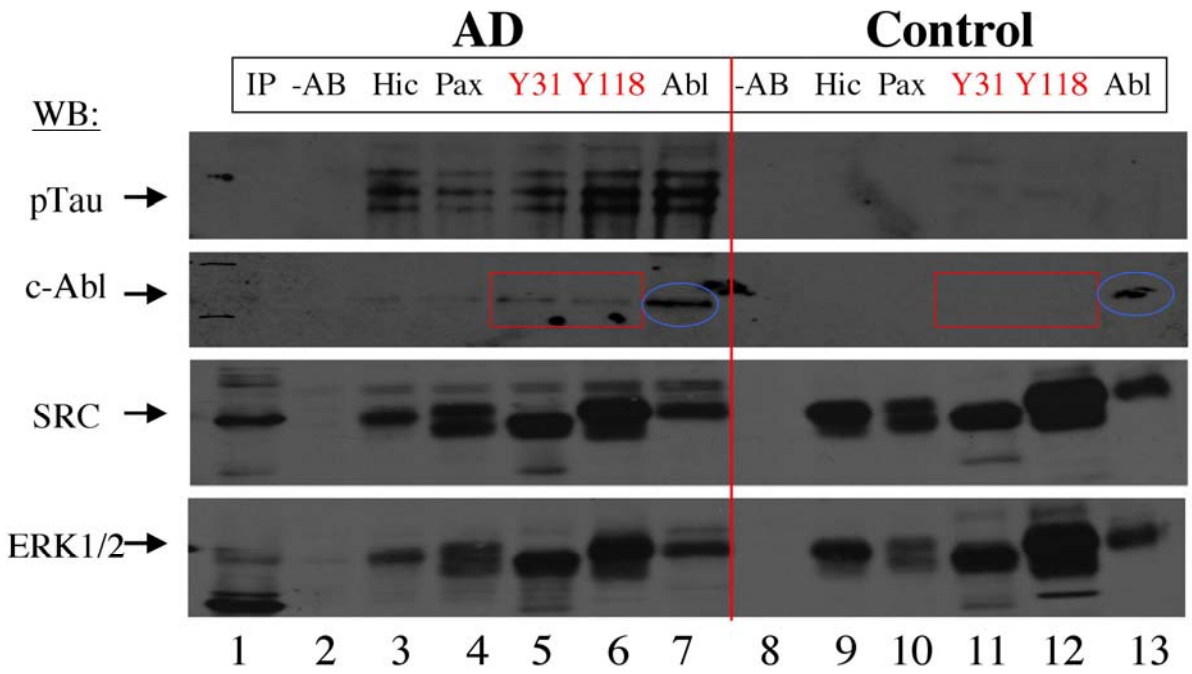

Figure 38. Coimmunoprecipitation of Hic-5, paxillin, activated paxillin isoforms, and c-Abl with pTau

Fresh frozen hippocampus from one neuropathologically confirmed AD (lanes 1-5) and one non-neurologic disease control (lanes 6-10) cases were homogenized as described in Methods to generate total homogenate. Equal amounts of protein from each total homogenate were immunoprecipitated with specific antibodies (lanes 2 and 8 = no antibody control, lanes 3 & 9 = Hic-5, lanes 4 & 10 = paxillin, lanes 5 & 11 = pY31 paxillin, lanes 6 & 12= pY118 paxillin, and lanes 7 & 13). Equal amounts of bound complexes from each antibody were loaded in gel lanes and immunolabeled with pTau (AT8), c-Abl, SRC, ERK1/2. Red boxes indicate that c-Abl associated with pY31 and pY118 paxillin in AD and not in control subjects while the blue circles indicates c-Abl antibodies used in the immunoprecipitation recognized itself by immunolabeling.

5.0 DISCUSSION

The participation of focal adhesion proteins in the pathogenesis of Alzheimer's disease (AD) has been postulated based upon *in vitro* interactions of integrins with β-amyloid *in vitro* (144, 156-159). Integrin activation by ß-amyloid could trigger downstream signaling events via focal adhesion proteins that differentially affect neuronal cell function and survival. Overall, the WB analysis in human hippocampus only observed a significant decrease in early-stage AD for Hic-5 and did not demonstrate changes in AD compared to control subjects in either TX-100 soluble or insoluble fractions for paxillin or activated isoforms of paxillin. To gain better understanding of the nature of these alterations, IHC and LSCM was used to assess the expression and subcellular distribution of Hic-5, paxillin and phosphorylated isoforms of paxillin in the hippocampus of control, early-stage AD and late-stage AD. Distinct patterns of expression for Hic-5 and paxillin in the hippocampus were observed. Both Hic-5 and paxillin exhibit altered immunostaining within the CA1 subfield of AD hippocampus when compared to control hippocampus.

Hic-5 was predominately expressed in neurons and localized to NFTs. The increased expression of Hic-5 appears to be a primary cell signaling molecule and levels change early during AD progression. Both oxidative stress and TGFβ are known regulators of the immune response and been shown to regulate Hic-5 expression and both have been shown to be upregulated during AD progression. However, Hic-5 expression levels in AD may be due to decreased degradation. Many ofproteosomal degradation pathway have also shown to be

downregulated during AD progression. Paxillin was detected in reactive astrocytes and CA1 pyramidal neurons while phosphorylated isoforms of paxillin were observed in pyramidal neurons and NFTs throughout the hippocampus. Hic-5 and paxillin was detected in compexes immunoprecipitated with phosphorylated tau and colocalized of phosphorylated paxillin in both GVD bodies and Hirano Bodies in AD hippocampus were observed.

These results provide the first characterization of Hic-5 and paxillin expression and distribution in the human brain with increased levels in AD brain, as shown by immunoblot. Hic-5 was expressed predominantly in pyramidal neurons of human hippocampus. To date, the only known function of Hic-5 in neurons is its regulation of surface levels of DAT in rat midbrain neuronal cultures and inhibition of dopamine uptake (270). Within the midbrain a direct interaction between Hic-5 and DAT may be responsible for this effect. My observation that Hic-5 protein levels are significantly elevated within CA1 pyramidal neurons in AD subjects suggest that it may function similarly in sequestering cell surface receptors or transporters away from the plasma membrane to alter function and intracellular signaling. A recent study analyzed the expression and localization of dopamine receptor (DR1-5) subtypes in control vs. AD brains and further suggests that the dopaminergic system is altered in AD (276). It would be interesting to determine whether Hic-5 plays any role in regulating these dopamine receptor subtypes or other neuronal cell surface receptors during AD.

Hic-5 was predominantly located within the cell body of pyramidal neurons and excluded from the nucleus in most cells in both control and AD hippocampus. Hic-5 in the nucleus of a subset of CA1 pyramidal neurons and non-neuronal cells in AD subjects, and colocalization of Hic-5 with pTau in NFTs were detected. Hic-5 was also observed in the core of many amyloid plaques. Future studies are required to further determine the potential role of oxidative stress in

modulating Hic-5 *in vivo* distribution in the brain. However, these results indicate that the subcellular distribution of the focal adhesion protein Hic-5 is altered during AD.

Paxillin is predominantly expressed in activated glia throughout the hippocampus and elevated in AD subjects. LSCM of paxillin and GFAP confirmed that paxillin is present in many reactive astrocytes throughout all regions of the hippocampus. Prior studies have not detected paxillin in astrocytes of human brain. However, in rodent models of brain trauma increased paxillin protein levels were observed only in reactive glia of the white matter (277). These authors suggested that initial glial reactions to trauma generate new "focal contacts" requiring GFAP and paxillin (277). It is possible that colocalization of paxillin in GFAP positive astrocytes in AD brain reflects a generation of new focal adhesions required for astrocytic motility and activation during AD. Interestingly, in control subjects paxillin was detected in focal granules in the nucleus of both CA1 pyramidal neurons and cells of the choroid plexus whereas paxillin immunoreactivity in the nucleus was significantly decreased in AD subjects. While alterations in CA1 pyramidal neurons have been extensively observed in various neurodegenerative disorders and trauma, only more recent studies have observed alterations in the structure and function of the choroid plexus in AD (278-282). The choroid plexus is known undergo morphological alterations in late-stage AD (279, 280). It has also been postulated that the choroid plexus is responsible for removing Aβ from the brain cerebrospinal fluid (283). Changes in the localization of paxillin out of focal nuclear granules and the nucleus in both CA1 neurons and choroids plexus cells may be reflecting key regulatory signaling pathways in AD.

Specific phosphorylated isoforms of paxillin have been shown to reflect the activation of distinct signaling pathways. Paxillin is phosphorylated on tyrosine residues Y31 and Y118 sites upon the initial activation of ECM-integrin signaling and the formation of intracellular focal

adhesion sites. In cultured neurons, paxillin is also rapidly phosphorylated on tyrosine residues in the presence of fibrillar β-amyloid and located to dystrophic neurites surrounding amyloid plaques in AD brain tissue (158). Phosphorylation of paxillin on serine residues S126 and S178 is regulated by JNK signaling pathways (145-147, 234). By immunoblot, no changes in the levels of pY31, pY118, pS126, or pS178 paxillin in AD brain were detected. Though immunoblot analysis of the soluble fraction did reveal a band of the appropriate molecular mass for pS178 in the majority of control subjects, two additional bands were observed in the majority of AD subjects (data not shown). Additional biochemical analysis is necessary for the presence of pS178 in these additional larger molecular weight bands to determine significant differences in levels of this protein and whether homodimers/trimers are present and elevated in AD brains by WB analysis. Analysis of the presence and distribution of each phosphorylated isoform of paxillin in control and AD hippocampus occurred. In control hippocampus, both pY31 and pY118 are predominantly observed in the cellular processes and soma of pyramidal neurons. In early-stage and late-stage AD, phosphorylated pY31 and pY118 levels are significantly decreased in the CA1 subfield. In addition, pY118 was detected in GVD bodies in the cell soma of pyramidal neurons in AD while GVD bodies were devoid of pY31 staining. The differences in staining of these two phosphorylated paxillin isoforms are perhaps reflective of the activation of distinct signaling pathways in AD. In control subjects, all four anti-phospho paxillin antibodies used in this study labeled well-defined nuclei in CA1 pyramidal neurons whereas the nuclear localization was reduced in AD subjects. Both pS126 and pS178 were present in GVD bodies and NFTs in AD hippocampus, with highest levels in the CA1 subfield. Biochemical data supporting direct interactions of pS126 and pS178 paxillin with tau awaits future studies. These results suggest that altered paxillin phosphorylation occurs during AD and that paxillin protein is

redistributed to intracellular protein aggregates and NFTs. The presence of phosphorylated paxillin in both Hirano bodies and GVD bodies is an exciting observation. Future studies are necessary to determine the role of paxillin in the generation of these pathologic features in AD.

The localization of phosphorylated paxillin within nuclei is a novel finding that warrants further investigation to determine its role during AD. Hic-5 nucleocytoplasmic shuttling is regulated by reactive oxygen species (ROS) but no evidence for ROS regulation of paxillin shuttling has been previously shown. My *in vivo* results demonstrate specific phosphorylated isoforms of paxillin within nuclei, suggesting specific signaling cascades and phosphorylation events may regulate paxillin shuttling. Interestingly, a decreased total paxillin in the nucleus of CA1 pyramidal neurons and in cells of the choroid plexus during AD was observed. The role of paxillin in the nucleus is poorly understood, although one can argue that paxillin can function as a coactivator for steroid hormone receptors (151). Another role of nuclear paxillin is to direct transport of mRNA out of the nucleus to sites of adhesion complexes involved in cell migration via interaction with poly(A)-binding protein (153). It is possible that phosphorylated paxillin may also regulate gene expression or mRNA trafficking in AD hippocampus.

When comparing the immunostaining pattern of non-phosphorylated to activated paxillin in the human hippocampus, a clear distinction can be made. Paxillin was predominantly expressed in glial cells while phosphorylated and activated paxillin was predominantly detected in neurons. The basis for this difference may reflect the differential state of paxillin phosphorylation in neurons and glia. Prior *in vitro* models demonstrated that activation of astrocytes generated a loss of paxillin phosphorylation on tyrosine residues (284). Phosphorylated isoforms of paxillin in the nuclei of non-neuronal cells were observed, suggesting that in glia the location of phosphorylated paxillin is predominately in the nucleus.

The lack of paxillin immunoreactivity using an antibody to the non-phosphorylated epitope in Hirano bodies and GVD bodies may reflect the inability of this paxillin antibody to recognize its epitope upon paxillin activation or in protein aggregates.

Surprisingly, many of these antibodies for phospho-paxillin localized to five pathological landmarks in AD including neuritic plaques, neurofibrilliary tangles, dystrophic neurites, Hirano bodies and GVD bodies. However, no phospho-paxillin antibody used in this study was found in morphologically appearing activated astrocytes. The lack of total paxillin immunoreactivity in Hirano bodies and GVD bodies may indicate aberrant signaling pathways specifically utilizing phospho-paxillin isoforms. GVD bodies are a hallmark of AD pathology consisting of single membrane vesicles that are formed from lysosomal autophagy of cytoplasmic substances containing cytoskeleton proteins including neurofilament, tau and tubulin. Phospho-paxillin isoforms found to stain GVD bodies of pyramidal neurons ranged from only a few to fifty or more granular protein complexes. The difference in cellular utilization of total paxillin vs. phospho-paxillin isoforms in control vs. AD brain reflects the activation of specific endpoints for distinct signaling pathways. Both GVD bodies and Hirano bodies occur in aging brains and may reflect a survival pathway that neurons utilize during chronic neurotoxic insults to delay cell death. Tyrosine kinases may therefore be key mediators in these hallmarks of AD as well and as their known roles in formation of plaques and tangles. The mechanisms allowing these hallmarks to form may also be integral in the pathogenesis of AD. *In vitro* studies are now able to recreate these hallmarks and their exact role in neuronal cell death will be examined.

6.0 CONCLUSION

These results implicate both Hic-5 and paxillin signaling pathways in the pathobiology of AD. These important scaffolding proteins that link the extracellular matrix to various intracellular signaling pathways are altered in specific cell types during AD and contained within neuropathologic hallmarks of the disease. The early alteration of expression and function of focal adhesion signaling pathway related proteins in AD brains supports the hypothesis that integrin/focal adhesion signal pathway is a primary participant in neuronal cell dysfunction in AD and not due to a secondary event. Given the data relating focal adhesion activation by Aβ and neuronal cell death pathways, attention to focal adhesion proteins, and downstream pathways warrant further investigation in AD. Continued studies of these and other focal adhesion proteins are necessary to evaluate their roles in AD pathogenesis and as potential therapeutic targets for AD and other neurodegenerative diseases.

7.0 FUTURE DIRECTION

The future directions of this project should include detailed investigation into the mechanism of Hic-5 and paxillin function at both genomic and nongenomic levels to reveal how their functions are affected in response to changes in the redox state that impact neuronal cell survival. Hic-5 and paxillin may be therapeutic targets for human diseases associated with oxidative stress. My thesis data implicates both hic-5 and paxillin signaling pathways within the pathobiology of AD. Hic-5 and phosphorylated isoforms of paxillin colocalize with NFTs, while paxillin is predominantly found in reactive astrocytes in the hippocampus of AD brains. Thus, important scaffolding proteins that link various intracellular signaling pathways to the ECM are modified and exhibit altered subcellular distribution during AD. Specifically, these results provide novel insight regarding the response of signaling molecules that impact both cytoplasmic and nuclear targets of protein phosphorylation cascades altered in AD hippocampus. The number of human cases studied and hypotheses generated during this thesis adds to existing *in vitro* data linking focal adhesion proteins in the pathogenesis of AD. The function of these focal adhesion proteins and interacting molecules has been extensively studied in other cellular models and the incorporation of data from those studies into neuronal models could uncover key alterations in AD. Further analysis of these and other focal adhesion proteins in AD pathogenesis is currently underway and may provide novel therapeutic targets for AD and other neurodegenerative diseases.

7.1 FUNCTIONAL STUDIES OF HIC-5 AND PAXILLIN IN NEURONS

Hic-5 and paxillin expression and subcellular localization patterns will be addressed in models of neurodegenerative disease associated with chronic oxidative stress, such as AD and PD or acute oxidative stress including ischemia. Paxillin's role in Aß-induced neuronal toxicity and data shown above in AD tissue point to this model, while Hic-5's interactions with DAT and possible involvement in PD and dopamine toxicity point to the relevance of this model. The neurotoxins glutamate and Aß may be physiologically more relevant than H_2O_2 and will be used due to their direct association with oxidative stress and disease. Amyloid plaques and NFT formation are the major hallmarks of AD and their generation may be influenced by ROS. While Hic-5 and paxillin share many interacting partners, this may have been predicted because of the high degree of relatedness between their LIM domains. This also suggests these proteins may act competitively in many signal transduction pathways. The potential interactions between Hic-5 and paxillin have not been studied in any neuronal system. The development of an *in vitro* model to determine the impact of oxidative stress on Hic-5 and paxillin will be used to explore potential natural paxillin antagonistic moieties to ultimately disrupt paxillin's role in Aβ-induced neuronal toxicity.

H_2O_2 leads to nuclear accumulation of Hic-5 in fibroblasts and osteoblasts. The generation of oxidative stress with H_2O_2 and neurotoxins has been established in neuronal cell lines (HT-22: mouse hippocampus, SH-SY5Y: human neuroblastoma, and N27: human DA cells). Thus, Hic-5 and paxillin expression and subcellular localization patterns will be

determined following oxidative stress generated in these neuronal cell lines by neurotoxins. These cells will be treated with varying amounts of H_2O_2 (0.1 to 1mM), glutamate (5 to 10 mM), and serum (1 to 10 %) to standardize a death curve for oxidative stress necessary to validate and reproduce findings between toxins and neuronal cells used in the study. Flow cytometry using antibodies to Annexin that identify this protein on the cell surface as an early marker for apoptosis mediated cell death could be used to aid in the standardization after toxic treatments. Conditions will then be chosen for neuronal cells resulting in approximately 25% cell death after ~8 hours treatment of oxidative stress by using multiple methods for cell counting. Changes in Hic-5 and paxillin expression and subcellular localization will be examined using WB, IHC, and IF analysis. Previous results from our lab determined a key regulatory event involved in apoptosis found using these conditions (173). To assay for changes in the expression of Hic-5 and paxillin, WB analysis will be performed using extracts from cells treated for different time points with varying doses of H_2O_2. Hic-5 and paxillin localization in oxidatively stressed cells will also be assessed by LSCM. GFP-Hic-5 and GFP-paxillin constructs will be used to examine H_2O_2 effects on Hic-5 and paxillin localization. Both glutamate and Aβ fibrils will be used to further address the direct impact of oxidative stress on Hic-5 and paxillin expression and subcellular localization in neuronal cells.

Hic-5 and paxillin function at the genomic and nongenomic levels in oxidatively stressed neurons and may impact neuronal cell survival. Neuronal cells will be transfected with Hic-5 and paxillin deletion mutant constructs based on proposed experimental methods to determine natuaral antagonistic moieties and exposed to H_2O_2, glutamate or Aß to identify their impact in neuronal cell responses to oxidative stress. Nongenomic functions of Hic-5 and paxillin mutant peptides will be addressed by determining the degree of paxillin activation/phosphorylation and

formation of dystrophic neurites in Aß-induced neuronal toxicity. Numerous phosphorylation sites within paxillin have been determined and mapped by mass spectrometry (135). Other post-translational modifications have been observed to regulate paxillin including O-linked N-acetylglucosamine (GlcNAc) moiety on Ser74 and ubiquination in the N-terminous. Each modification may regulate paxillin's role in neuronal cell death. The functional effects of multiple post-translational modifications on paxillin remain unknown and determining how paxillin is regulated by post-translational modifications will help our understanding in paxillin's role in neuronal cell death. To identify post-translational modifications implicated in Hic-5 and paxillin function in oxidatively stressed neurons, WB analysis, LSCM, and mass spectrometry will be used to gain insight into cell signaling and neuronal cell death. To identify protein-protein interactions for Hic-5 and paxillin in oxidatively stressed neurons, WB analysis, IP assays, and LSCM will be used. To assay changes in protein-DNA interactions for Hic-5 and paxillin in oxidatively stressed neurons, RT-PCR, chromatin IP assays (ChIPs), and EMSAs on putative Hic-5 and paxillin target genes will be performed. Gene transcripts regulated by Hic-5, paxillin, and antioxidant response elements will be targeted including c-fos.

7.2 EXPRESSION AND DISTRIBUTION IN OTHER NEURODEGENERATIVE DISEASES

Results presented here provide the first characterization of hic-5 and paxillin expression and distribution in the human brain with increased levels in AD brain. Hic-5 was expressed predominantly in pyramidal neurons of human hippocampus. To date, the only known function of hic-5 in neurons is its regulation of surface levels of DAT in rat midbrain neuronal cultures

and inhibition of dopamine uptake (270). Within the midbrain a direct interaction between hic-5 and DAT may be responsible for this effect. The observation that hic-5 protein levels are significantly elevated within CA1 pyramidal neurons in AD subjects suggests that Hic-5 may function similarly in sequestering cell surface receptors or transporters away from the plasma membrane to alter function and intracellular signaling. A recent study analyzed the expression and localization of dopamine receptor (DR1-5) subtypes in control vs. AD brains and further suggests that the dopaminergic system is altered in AD (276). It would be useful to determine whether hic-5 plays any role in regulating these dopamine receptor subtypes or other neuronal cell surface receptors during AD and PD. Also, Hic-5 localization cells within the subiculum that appear to be pTau negative indicates that Hic-5 may have role in FTD, FTD-ALS, and pure tauopathies. Paxillin expression in activated astrocytes suggests that paxillin may be regulated by cytokines associated with AD or other neurodegenerative disease with elevate immune responses. How cytokines regulate paxillin expression in these cells may help determine how paxillin regulates neuronal cell death.

7.3 HIGH-THROUGHPUT DRUG SCREEN

The generation of a high-throughput drug screen could be developed to determine the role each focal adhesion protein has in the formation of the focal adhesion-unit. A cell free *in vitro* assay using either full length or mutated truncated functional domains of these proteins could be used to determine colocalization (assembly and disassembly of focal adhesions). The proteins generated will be tagged in such a manner that each express only a portion of the amino acids required for visualization of the fluorescent markers used and can then determine colocalization

with proteins generated expressing the missing amino acids. Colocalization of proteins can be performed by photo bleaching and recovery of fluorescence of the desired complexes. Once this assay has been established, numerous drugs could then be tested to determine how they regulate focal adhesion turnover properties.

7.4 TRANSGENIC ANIMAL STUDIES

Results acquired from *in vitro* models previously proposed will then be used to generate transgenic animals expressing genes in brain found to disrupt Aβ toxic affects of paxillin. The creation of transgenic animal models provides a powerful approach to study the effects of introduced specific genes. To confirm proposed *in vitro* results, animals expressing potential paxillin antagonistic peptides will then be mated with animals models for neurodegeneration to validate *in vitro* data in an effort to slow, stop, or reverse neuronal cell death. Loss of memory is ultimately linked to neuronal cell death and cell losses are pivital to numerous neurodegenerative disorders including AD. Transgenic animal models generated from in vitro results including Hic-5 and paxillin mutants will need to be characterized with known cognitive and behavioral assessments to determine the relevance to disrupting paxillin's role in neuronal cell death. Current FDA approved therapeutic drugs for AD will also be used in an effort to determine if they have an ability to disrupt paxillin's role in neuronal death. As mentioned in the Introduction, during advanced stages of AD subjects are prescribed a combined dosage of multiple drug targets to slow AD progression. Therefore, the combined use of multiple AD drugs will be used to optimize the disruption of paxillin's role in neuronal death based on severity of pathogical observations.

7.5 THERAPEUTIC OPPORTUNITIES

Discovery of alterations in focal adhesion protein expression and subcellular location implicated in AD pathogenesis may provide novel therapeutic targets for AD and other neurodegenerative diseases. My results determined altered expression and subcellular localization of Hic-5 and paxillin in AD. Combined with results implicating paxillin LIM domains mediating Aβ toxic effects in neurons and results present in this dissertation may lead to the design of drugs specifically targeting focal adhesion protein expression and function. At this time, focal adhesion turnover rates require a delicate balance of stability to maintain connections and plasticity to allow neuronal processes the ability to migrate and make functional new connections in the presence of ongoing cell death. The timing of which of focal adhesion formation and disassembly may be the key to maintaing learning and memory as one ages.

BIBLIOGRAPHY

1. Alzheimer A, Stelzmann RA, Schnitzlein HN, et al. An English translation of Alzheimer's 1907 paper, "Uber eine eigenartige Erkankung der Hirnrinde". Clin Anat 1995;8:429-31
2. Pomponi M.Marta M. "On the suggestion of Dr. Alzheimer I examined the following four cases." Dedicated to Gaetano Perusini. Aging (Milano) 1993;5:135-9
3. Minino AM, Heron MP, Murphy SL, et al. Deaths: final data for 2004. Natl Vital Stat Rep 2007;55:1-119
4. Kukull WA.Bowen JD. Dementia epidemiology. Med Clin North Am 2002;86:573-90
5. Plassman BL, Langa KM, Fisher GG, et al. Prevalence of dementia in the United States: the aging, demographics, and memory study. Neuroepidemiology 2007;29:125-32
6. Zhang MY, Katzman R, Salmon D, et al. The prevalence of dementia and Alzheimer's disease in Shanghai, China: impact of age, gender, and education. Ann Neurol 1990;27:428-37
7. Kukull WA, Higdon R, Bowen JD, et al. Dementia and Alzheimer disease incidence: a prospective cohort study. Arch Neurol 2002;59:1737-46
8. Evans DA, Hebert LE, Beckett LA, et al. Education and other measures of socioeconomic status and risk of incident Alzheimer disease in a defined population of older persons. Arch Neurol 1997;54:1399-405
9. Stern Y, Gurland B, Tatemichi TK, et al. Influence of education and occupation on the incidence of Alzheimer's disease. Jama 1994;271:1004-10
10. Gatz M, Reynolds CA, Fratiglioni L, et al. Role of genes and environments for explaining Alzheimer disease. Arch Gen Psychiatry 2006;63:168-74
11. Andel R, Crowe M, Pedersen NL, et al. Complexity of work and risk of Alzheimer's disease: a population-based study of Swedish twins. J Gerontol B Psychol Sci Soc Sci 2005;60:P251-8
12. Masters CL, Gajdusek DC.Gibbs CJ, Jr. The familial occurrence of Creutzfeldt-Jakob disease and Alzheimer's disease. Brain 1981;104:535-58
13. Karlinsky H, Vaula G, Haines JL, et al. Molecular and prospective phenotypic characterization of a pedigree with familial Alzheimer's disease and a missense mutation in codon 717 of the beta-amyloid precursor protein gene. Neurology 1992;42:1445-53
14. Sherrington R, Rogaev EI, Liang Y, et al. Cloning of a gene bearing missense mutations in early-onset familial Alzheimer's disease. Nature 1995;375:754-60
15. Goate A, Chartier-Harlin MC, Mullan M, et al. Segregation of a missense mutation in the amyloid precursor protein gene with familial Alzheimer's disease. Nature 1991;349:704-6
16. Levy-Lahad E, Wijsman EM, Nemens E, et al. A familial Alzheimer's disease locus on chromosome 1. Science 1995;269:970-3

17. Hyman BT, Gomez-Isla T, West H, et al. Clinical and neuropathological correlates of apolipoprotein E genotype in Alzheimer's disease. Window on molecular epidemiology. Ann N Y Acad Sci 1996;777:158-65
18. Gatz M, Fratiglioni L, Johansson B, et al. Complete ascertainment of dementia in the Swedish Twin Registry: the HARMONY study. Neurobiol Aging 2005;26:439-47
19. Watson GS, Peskind ER, Asthana S, et al. Insulin increases CSF Abeta42 levels in normal older adults. Neurology 2003;60:1899-903
20. Evans DA, Funkenstein HH, Albert MS, et al. Prevalence of Alzheimer's disease in a community population of older persons. Higher than previously reported. Jama 1989;262:2551-6
21. Citron M, Diehl TS, Capell A, et al. Inhibition of amyloid beta-protein production in neural cells by the serine protease inhibitor AEBSF. Neuron 1996;17:171-9
22. Qiu WQ, Walsh DM, Ye Z, et al. Insulin-degrading enzyme regulates extracellular levels of amyloid beta-protein by degradation. J Biol Chem 1998;273:32730-8
23. Miller BC, Eckman EA, Sambamurti K, et al. Amyloid-beta peptide levels in brain are inversely correlated with insulysin activity levels in vivo. Proc Natl Acad Sci U S A 2003;100:6221-6
24. Farris W, Mansourian S, Chang Y, et al. Insulin-degrading enzyme regulates the levels of insulin, amyloid beta-protein, and the beta-amyloid precursor protein intracellular domain in vivo. Proc Natl Acad Sci U S A 2003;100:4162-7
25. Bertram L, Blacker D, Mullin K, et al. Evidence for genetic linkage of Alzheimer's disease to chromosome 10q. Science 2000;290:2302-3
26. Craft S. Insulin resistance syndrome and Alzheimer's disease: age- and obesity-related effects on memory, amyloid, and inflammation. Neurobiol Aging 2005;26 Suppl 1:65-9
27. Fewlass DC, Noboa K, Pi-Sunyer FX, et al. Obesity-related leptin regulates Alzheimer's Abeta. Faseb J 2004;18:1870-8
28. Sorrentino MJ. Implications of the metabolic syndrome: the new epidemic. Am J Cardiol 2005;96:3E-7E
29. Vilalta-Franch J, Lopez-Pousa S, Garre-Olmo J, et al. [Metabolic syndrome in Alzheimer's disease: clinical and developmental influences]. Rev Neurol 2008;46:13-7
30. Launer LJ. Demonstrating the case that AD is a vascular disease: epidemiologic evidence. Ageing Res Rev 2002;1:61-77
31. Volpato S, Zuliani G, Guralnik JM, et al. The inverse association between age and cholesterol level among older patients: the role of poor health status. Gerontology 2001;47:36-45
32. Reitz C, Tang MX, Manly J, et al. Hypertension and the risk of mild cognitive impairment. Arch Neurol 2007;64:1734-40
33. Khachaturian AS, Zandi PP, Lyketsos CG, et al. Antihypertensive medication use and incident Alzheimer disease: the Cache County Study. Arch Neurol 2006;63:686-92
34. Morrison RA, McGrath A, Davidson G, et al. Low blood pressure in Down's syndrome, A link with Alzheimer's disease? Hypertension 1996;28:569-75
35. Havlik RJ, Foley DJ, Sayer B, et al. Variability in midlife systolic blood pressure is related to late-life brain white matter lesions: the Honolulu-Asia Aging study. Stroke 2002;33:26-30
36. Tyas SL, White LR, Petrovitch H, et al. Mid-life smoking and late-life dementia: the Honolulu-Asia Aging Study. Neurobiol Aging 2003;24:589-96

37. Koch S, Donarski N, Goetze K, et al. Characterization of four lipoprotein classes in human cerebrospinal fluid. J Lipid Res 2001;42:1143-51
38. Ashford JW. APOE genotype effects on Alzheimer's disease onset and epidemiology. J Mol Neurosci 2004;23:157-65
39. Gomez-Isla T, West HL, Rebeck GW, et al. Clinical and pathological correlates of apolipoprotein E epsilon 4 in Alzheimer's disease. Ann Neurol 1996;39:62-70
40. American Psychiatric Association..American Psychiatric Association. Task Force on DSM-IV. Diagnostic and statistical manual of mental disorders : DSM-IV-TR. In: Washington, DC: American Psychiatric Association, 2000
41. Reisberg B. Alzheimer's disease. Stages of cognitive decline. Am J Nurs 1984;84:225-8
42. Petersen RC, Smith GE, Waring SC, et al. Mild cognitive impairment: clinical characterization and outcome. Arch Neurol 1999;56:303-8
43. DeCarli C. Mild cognitive impairment: prevalence, prognosis, aetiology, and treatment. Lancet Neurol 2003;2:15-21
44. Gauthier S, Reisberg B, Zaudig M, et al. Mild cognitive impairment. Lancet 2006;367:1262-70
45. Grundman M, Petersen RC, Ferris SH, et al. Mild cognitive impairment can be distinguished from Alzheimer disease and normal aging for clinical trials. Arch Neurol 2004;61:59-66
46. Folstein MF, Folstein SE.McHugh PR. "Mini-mental state". A practical method for grading the cognitive state of patients for the clinician. J Psychiatr Res 1975;12:189-98
47. Lin KN, Wang PN, Liu CY, et al. Cutoff scores of the cognitive abilities screening instrument, Chinese version in screening of dementia. Dement Geriatr Cogn Disord 2002;14:176-82
48. Powlishta KK, Von Dras DD, Stanford A, et al. The clock drawing test is a poor screen for very mild dementia. Neurology 2002;59:898-903
49. Sager MA, Hermann BP, La Rue A, et al. Screening for dementia in community-based memory clinics. Wmj 2006;105:25-9
50. Teng EL.Chui HC. The Modified Mini-Mental State (3MS) examination. J Clin Psychiatry 1987;48:314-8
51. Gelb DJ. Measurement of progression in Alzheimer's disease: a clinician's perspective. Stat Med 2000;19:1393-400
52. Goldstein LE, Muffat JA, Cherny RA, et al. Cytosolic beta-amyloid deposition and supranuclear cataracts in lenses from people with Alzheimer's disease. Lancet 2003;361:1258-65
53. Klunk WE, Engler H, Nordberg A, et al. Imaging brain amyloid in Alzheimer's disease with Pittsburgh Compound-B. Ann Neurol 2004;55:306-19
54. Logothetis NK, Pauls J, Augath M, et al. Neurophysiological investigation of the basis of the fMRI signal. Nature 2001;412:150-7
55. Ogawa S, Lee TM, Nayak AS, et al. Oxygenation-sensitive contrast in magnetic resonance image of rodent brain at high magnetic fields. Magn Reson Med 1990;14:68-78
56. Price JC, Klunk WE, Lopresti BJ, et al. Kinetic modeling of amyloid binding in humans using PET imaging and Pittsburgh Compound-B. J Cereb Blood Flow Metab 2005;25:1528-47

57. American Biogenetic Sciences I. ABS Issued U.S. Patent for Method of Diagnosing A;zheimer's Disease. Doctor's Guide: Electronic Version 1996;
58. Goldknopf IL. Blood-based proteomics for personalized medicine: examples from neurodegenerative disease. Expert Rev Proteomics 2008;5:1-8
59. Sheta EA, Appel SH.Goldknopf IL. 2D gel blood serum biomarkers reveal differential clinical proteomics of the neurodegenerative diseases. Expert Rev Proteomics 2006;3:45-62
60. Herukka SK, Hallikainen M, Soininen H, et al. CSF Abeta42 and tau or phosphorylated tau and prediction of progressive mild cognitive impairment. Neurology 2005;64:1294-7
61. Itoh N, Arai H, Urakami K, et al. Large-scale, multicenter study of cerebrospinal fluid tau protein phosphorylated at serine 199 for the antemortem diagnosis of Alzheimer's disease. Ann Neurol 2001;50:150-6
62. Sunderland T, Linker G, Mirza N, et al. Decreased beta-amyloid1-42 and increased tau levels in cerebrospinal fluid of patients with Alzheimer disease. Jama 2003;289:2094-103
63. Iqbal K, Flory M, Khatoon S, et al. Subgroups of Alzheimer's disease based on cerebrospinal fluid molecular markers. Ann Neurol 2005;58:748-57
64. Hamilton RL. Lewy bodies in Alzheimer's disease: a neuropathological review of 145 cases using alpha-synuclein immunohistochemistry. Brain Pathol 2000;10:378-84
65. Khachaturian ZS. Diagnosis of Alzheimer's disease. Arch Neurol 1985;42:1097-105
66. Mirra SS, Heyman A, McKeel D, et al. The Consortium to Establish a Registry for Alzheimer's Disease (CERAD). Part II. Standardization of the neuropathologic assessment of Alzheimer's disease. Neurology 1991;41:479-86
67. Braak H.Braak E. Neuropathological stageing of Alzheimer-related changes. Acta Neuropathol (Berl) 1991;82:239-59
68. Consensus recommendations for the postmortem diagnosis of Alzheimer's disease. The National Institute on Aging, and Reagan Institute Working Group on Diagnostic Criteria for the Neuropathological Assessment of Alzheimer's Disease. Neurobiol Aging 1997;18:S1-2
69. Terry RD.Davies P. Dementia of the Alzheimer type. Annu Rev Neurosci 1980;3:77-95
70. Selkoe DJ. The molecular pathology of Alzheimer's disease. Neuron 1991;6:487-98
71. Wasco W, Brook JD.Tanzi RE. The amyloid precursor-like protein (APLP) gene maps to the long arm of human chromosome 19. Genomics 1993;15:237-9
72. Heber S, Herms J, Gajic V, et al. Mice with combined gene knock-outs reveal essential and partially redundant functions of amyloid precursor protein family members. J Neurosci 2000;20:7951-63
73. von Koch CS, Zheng H, Chen H, et al. Generation of APLP2 KO mice and early postnatal lethality in APLP2/APP double KO mice. Neurobiol Aging 1997;18:661-9
74. Cao X.Sudhof TC. A transcriptionally [correction of transcriptively] active complex of APP with Fe65 and histone acetyltransferase Tip60. Science 2001;293:115-20
75. Kamal A, Stokin GB, Yang Z, et al. Axonal transport of amyloid precursor protein is mediated by direct binding to the kinesin light chain subunit of kinesin-I. Neuron 2000;28:449-59
76. Ohsawa I, Takamura C, Morimoto T, et al. Amino-terminal region of secreted form of amyloid precursor protein stimulates proliferation of neural stem cells. Eur J Neurosci 1999;11:1907-13

77. Perez RG, Zheng H, Van der Ploeg LH, et al. The beta-amyloid precursor protein of Alzheimer's disease enhances neuron viability and modulates neuronal polarity. J Neurosci 1997;17:9407-14
78. Schubert W, Prior R, Weidemann A, et al. Localization of Alzheimer beta A4 amyloid precursor protein at central and peripheral synaptic sites. Brain Res 1991;563:184-94
79. Yamazaki T, Koo EH.Selkoe DJ. Cell surface amyloid beta-protein precursor colocalizes with beta 1 integrins at substrate contact sites in neural cells. J Neurosci 1997;17:1004-10
80. Zheng H, Jiang M, Trumbauer ME, et al. beta-Amyloid precursor protein-deficient mice show reactive gliosis and decreased locomotor activity. Cell 1995;81:525-31
81. De Strooper B.Annaert W. Proteolytic processing and cell biological functions of the amyloid precursor protein. J Cell Sci 2000;113 (Pt 11):1857-70
82. De Strooper B, Umans L, Van Leuven F, et al. Study of the synthesis and secretion of normal and artificial mutants of murine amyloid precursor protein (APP): cleavage of APP occurs in a late compartment of the default secretion pathway. J Cell Biol 1993;121:295-304
83. Harper JD.Lansbury PT, Jr. Models of amyloid seeding in Alzheimer's disease and scrapie: mechanistic truths and physiological consequences of the time-dependent solubility of amyloid proteins. Annu Rev Biochem 1997;66:385-407
84. Shaw LM, Korecka M, Clark CM, et al. Biomarkers of neurodegeneration for diagnosis and monitoring therapeutics. Nat Rev Drug Discov 2007;6:295-303
85. Nunan J.Small DH. Regulation of APP cleavage by alpha-, beta- and gamma-secretases. FEBS Lett 2000;483:6-10
86. Kovacs DM, Fausett HJ, Page KJ, et al. Alzheimer-associated presenilins 1 and 2: neuronal expression in brain and localization to intracellular membranes in mammalian cells. Nat Med 1996;2:224-9
87. Loetscher H, Deuschle U, Brockhaus M, et al. Presenilins are processed by caspase-type proteases. J Biol Chem 1997;272:20655-9
88. Selkoe DJ. Amyloid beta-protein and the genetics of Alzheimer's disease. J Biol Chem 1996;271:18295-8
89. Spires-Jones TL, de Calignon A, Matsui T, et al. In vivo imaging reveals dissociation between caspase activation and acute neuronal death in tangle-bearing neurons. J Neurosci 2008;28:862-7
90. Jacobs PA, Baikie AG, Court Brown WM, et al. The somatic chromosomes in mongolism. Lancet 1959;1:710
91. Lejeune J, Turpin R.Gautier M. [Mongolism; a chromosomal disease (trisomy).]. Bull Acad Natl Med 1959;143:256-65
92. Heston LL. Alzheimer's Disease, Trisomy 21, and Myeloproliferative Disorders: Associations Suggesting a Genetic Diathesis. Science 1977;196:322-323
93. Barghorn S, Nimmrich V, Striebinger A, et al. Globular amyloid beta-peptide oligomer - a homogenous and stable neuropathological protein in Alzheimer's disease. J Neurochem 2005;95:834-47
94. Weingarten MD, Lockwood AH, Hwo SY, et al. A protein factor essential for microtubule assembly. Proc Natl Acad Sci U S A 1975;72:1858-62
95. Alonso AD, Zaidi T, Novak M, et al. Interaction of tau isoforms with Alzheimer's disease abnormally hyperphosphorylated tau and in vitro phosphorylation into the disease-like protein. J Biol Chem 2001;276:37967-73

96. Morishima-Kawashima M, Hasegawa M, Takio K, et al. Proline-directed and non-proline-directed phosphorylation of PHF-tau. J Biol Chem 1995;270:823-9
97. Morishima-Kawashima M, Hasegawa M, Takio K, et al. Hyperphosphorylation of tau in PHF. Neurobiol Aging 1995;16:365-71; discussion 371-80
98. Alonso A, Zaidi T, Novak M, et al. Hyperphosphorylation induces self-assembly of tau into tangles of paired helical filaments/straight filaments. Proc Natl Acad Sci U S A 2001;98:6923-8
99. Goedert M, Satumtira S, Jakes R, et al. Reduced binding of protein phosphatase 2A to tau protein with frontotemporal dementia and parkinsonism linked to chromosome 17 mutations. J Neurochem 2000;75:2155-62
100. Goedert M.Spillantini MG. Tau mutations in frontotemporal dementia FTDP-17 and their relevance for Alzheimer's disease. Biochim Biophys Acta 2000;1502:110-21
101. Ball MJ.Lo P. Granulovacuolar degeneration in the ageing brain and in dementia. J Neuropathol Exp Neurol 1977;36:474-87
102. Simchowicz T. Histopathologische Studien uber die senile Demenz. . In: Jenna, Germany: Fischer, 1911
103. Okamoto K, Hirai S, Iizuka T, et al. Reexamination of granulovacuolar degeneration. Acta Neuropathol 1991;82:340-5
104. Love S, Saitoh T, Quijada S, et al. Alz-50, ubiquitin and tau immunoreactivity of neurofibrillary tangles, Pick bodies and Lewy bodies. J Neuropathol Exp Neurol 1988;47:393-405
105. Price DL, Altschuler RJ, Struble RG, et al. Sequestration of tubulin in neurons in Alzheimer's disease. Brain Res 1986;385:305-10
106. Leroy K, Boutajangout A, Authelet M, et al. The active form of glycogen synthase kinase-3beta is associated with granulovacuolar degeneration in neurons in Alzheimer's disease. Acta Neuropathol 2002;103:91-9
107. Ghanevati M.Miller CA. Phospho-beta-catenin accumulation in Alzheimer's disease and in aggresomes attributable to proteasome dysfunction. J Mol Neurosci 2005;25:79-94
108. Kahn J, Anderton BH, Probst A, et al. Immunohistological study of granulovacuolar degeneration using monoclonal antibodies to neurofilaments. J Neurol Neurosurg Psychiatry 1985;48:924-6
109. Kannanayakal TJ, Tao H, Vandre DD, et al. Casein kinase-1 isoforms differentially associate with neurofibrillary and granulovacuolar degeneration lesions. Acta Neuropathol 2006;111:413-21
110. Su JH, Kesslak JP, Head E, et al. Caspase-cleaved amyloid precursor protein and activated caspase-3 are co-localized in the granules of granulovacuolar degeneration in Alzheimer's disease and Down's syndrome brain. Acta Neuropathol 2002;104:1-6
111. Hirano A, Dembitzer HM, Kurland LT, et al. The fine structure of some intraganglionic alterations. Neurofibrillary tangles, granulovacuolar bodies and "rod-like" structures as seen in Guam amyotrophic lateral sclerosis and parkinsonism-dementia complex. J Neuropathol Exp Neurol 1968;27:167-82
112. Hirano A, Malamud N.Ku Rland LT. Parkinsonism-dementia complex, an endemic disease on the island of Guam. II. Pathological features. Brain 1961;84:662-79
113. Goldman JE. The association of actin with Hirano bodies. J Neuropathol Exp Neurol 1983;42:146-52

114. Hirano A. Hirano bodies and related neuronal inclusions. Neuropathol Appl Neurobiol 1994;20:3-11
115. Rossiter JP, Anderson LL, Yang F, et al. Caspase-cleaved actin (fractin) immunolabelling of Hirano bodies. Neuropathol Appl Neurobiol 2000;26:342-6
116. Jordan-Sciutto K, Dragich J, Walcott D, et al. The presence of FAC1 protein in Hirano bodies. Neuropathol Appl Neurobiol 1998;24:359-66
117. Davis RC, Furukawa R.Fechheimer M. A cell culture model for investigation of Hirano bodies. Acta Neuropathol 2008;115:205-17
118. Gilmore AP. Anoikis. Cell Death Differ 2005;12 Suppl 2:1473-7
119. Howe A, Aplin AE, Alahari SK, et al. Integrin signaling and cell growth control. Curr Opin Cell Biol 1998;10:220-31
120. Reddig PJ.Juliano RL. Clinging to life: cell to matrix adhesion and cell survival. Cancer Metastasis Rev 2005;24:425-39
121. Cordes N.Meineke V. Integrin signalling and the cellular response to ionizing radiation. J Mol Histol 2004;35:327-37
122. Giancotti FG.Ruoslahti E. Integrin signaling. Science 1999;285:1028-32
123. Verdier Y, Zarandi M.Penke B. Amyloid beta-peptide interactions with neuronal and glial cell plasma membrane: binding sites and implications for Alzheimer's disease. J Pept Sci 2004;10:229-48
124. Kontaxis. LIM Domain Proteins. In: Chichester: John Wilely & Sons, 2004
125. Wehrle-Haller B.Imhof B. The inner lives of focal adhesions. Trends Cell Biol 2002;12:382-9
126. Aplin AE. Cell adhesion molecule regulation of nucleocytoplasmic trafficking. FEBS Lett 2003;534:11-4
127. Cary LA.Guan JL. Focal adhesion kinase in integrin-mediated signaling. Front Biosci 1999;4:D102-13
128. Guan JL. Focal adhesion kinase in integrin signaling. Matrix Biol 1997;16:195-200
129. Kornberg L, Earp HS, Parsons JT, et al. Cell adhesion or integrin clustering increases phosphorylation of a focal adhesion-associated tyrosine kinase. J Biol Chem 1992;267:23439-42
130. Brown MC.Turner CE. Paxillin: adapting to change. Physiol Rev 2004;84:1315-39
131. Kadrmas JL.Beckerle MC. The LIM domain: from the cytoskeleton to the nucleus. Nat Rev Mol Cell Biol 2004;5:920-31
132. Nishiya N, Tachibana K, Shibanuma M, et al. Hic-5-reduced cell spreading on fibronectin: competitive effects between paxillin and Hic-5 through interaction with focal adhesion kinase. Mol Cell Biol 2001;21:5332-45
133. Shibanuma M, Kim-Kaneyama JR, Ishino K, et al. Hic-5 communicates between focal adhesions and the nucleus through oxidant-sensitive nuclear export signal. Mol Biol Cell 2003;14:1158-71
134. Schroeder MJ, Webb DJ, Shabanowitz J, et al. Methods for the detection of paxillin post-translational modifications and interacting proteins by mass spectrometry. J Proteome Res 2005;4:1832-41
135. Webb DJ, Schroeder MJ, Brame CJ, et al. Paxillin phosphorylation sites mapped by mass spectrometry. J Cell Sci 2005;118:4925-9

136. Shibanuma M, Mochizuki E, Maniwa R, et al. Induction of senescence-like phenotypes by forced expression of hic-5, which encodes a novel LIM motif protein, in immortalized human fibroblasts. Mol Cell Biol 1997;17:1224-35
137. Thomas SM, Hagel M.Turner CE. Characterization of a focal adhesion protein, Hic-5, that shares extensive homology with paxillin. J Cell Sci 1999;112 (Pt 2):181-90
138. Gao Z.Schwartz LM. Identification and analysis of Hic-5/ARA55 isoforms: Implications for integrin signaling and steroid hormone action. FEBS Lett 2005;579:5651-7
139. Gao ZL, Deblis R, Glenn H, et al. Differential roles of HIC-5 isoforms in the regulation of cell death and myotube formation during myogenesis. Exp Cell Res 2007;
140. de Curtis I.Malanchini B. Integrin-mediated tyrosine phosphorylation and redistribution of paxillin during neuronal adhesion. Exp Cell Res 1997;230:233-43
141. Leventhal PS.Feldman EL. Tyrosine phosphorylation and enhanced expression of paxillin during neuronal differentiation in vitro. J Biol Chem 1996;271:5957-60
142. Schaller MD.Parsons JT. pp125FAK-dependent tyrosine phosphorylation of paxillin creates a high-affinity binding site for Crk. Mol Cell Biol 1995;15:2635-45
143. Turner CE, Schaller MD.Parsons JT. Tyrosine phosphorylation of the focal adhesion kinase pp125FAK during development: relation to paxillin. J Cell Sci 1993;105 (Pt 3):637-45
144. Zhang C, Lambert MP, Bunch C, et al. Focal adhesion kinase expressed by nerve cell lines shows increased tyrosine phosphorylation in response to Alzheimer's A beta peptide. J Biol Chem 1994;269:25247-50
145. Huang C, Borchers CH, Schaller MD, et al. Phosphorylation of paxillin by p38MAPK is involved in the neurite extension of PC-12 cells. J Cell Biol 2004;164:593-602
146. Huang C, Jacobson K.Schaller MD. A role for JNK-paxillin signaling in cell migration. Cell Cycle 2004;3:4-6
147. Huang C, Rajfur Z, Borchers C, et al. JNK phosphorylates paxillin and regulates cell migration. Nature 2003;424:219-23
148. Ghogomu SM, van Venrooy S, Ritthaler M, et al. HIC-5 is a novel repressor of lymphoid enhancer factor/T-cell factor-driven transcription. J Biol Chem 2006;281:1755-64
149. Guerrero-Santoro J, Yang L, Stallcup MR, et al. Distinct LIM domains of Hic-5/ARA55 are required for nuclear matrix targeting and glucocorticoid receptor binding and coactivation. J Cell Biochem 2004;92:810-9
150. Heitzer MD.DeFranco DB. Mechanism of action of Hic-5/androgen receptor activator 55, a LIM domain-containing nuclear receptor coactivator. Mol Endocrinol 2006;20:56-64
151. Kasai M, Guerrero-Santoro J, Friedman R, et al. The Group 3 LIM domain protein paxillin potentiates androgen receptor transactivation in prostate cancer cell lines. Cancer Res 2003;63:4927-35
152. Shibanuma M, Kim-Kaneyama JR, Sato S, et al. A LIM protein, Hic-5, functions as a potential coactivator for Sp1. J Cell Biochem 2004;91:633-45
153. Woods AJ, Roberts MS, Choudhary J, et al. Paxillin associates with poly(A)-binding protein 1 at the dense endoplasmic reticulum and the leading edge of migrating cells. J Biol Chem 2002;277:6428-37
154. Yang L, Guerrero J, Hong H, et al. Interaction of the tau2 transcriptional activation domain of glucocorticoid receptor with a novel steroid receptor coactivator, Hic-5, which localizes to both focal adhesions and the nuclear matrix. Mol Biol Cell 2000;11:2007-18

155. Sonoda Y, Watanabe S, Matsumoto Y, et al. FAK is the upstream signal protein of the phosphatidylinositol 3-kinase-Akt survival pathway in hydrogen peroxide-induced apoptosis of a human glioblastoma cell line. J Biol Chem 1999;274:10566-70
156. Williamson R, Scales T, Clark BR, et al. Rapid tyrosine phosphorylation of neuronal proteins including tau and focal adhesion kinase in response to amyloid-beta peptide exposure: involvement of Src family protein kinases. J Neurosci 2002;22:10-20
157. Berg MM, Krafft GA.Klein WL. Rapid impact of beta-amyloid on paxillin in a neural cell line. J Neurosci Res 1997;50:979-89
158. Grace EA.Busciglio J. Aberrant activation of focal adhesion proteins mediates fibrillar amyloid beta-induced neuronal dystrophy. J Neurosci 2003;23:493-502
159. Caltagarone J, Jing Z.Bowser R. Focal adhesions regulate Abeta signaling and cell death in Alzheimer's disease. Biochim Biophys Acta 2007;1772:438-45
160. Jin K, Peel AL, Mao XO, et al. Increased hippocampal neurogenesis in Alzheimer's disease. Proc Natl Acad Sci U S A 2004;101:343-7
161. Schwartz MA.Assoian RK. Integrins and cell proliferation: regulation of cyclin-dependent kinases via cytoplasmic signaling pathways. J Cell Sci 2001;114:2553-60
162. Zamir E.Geiger B. Molecular complexity and dynamics of cell-matrix adhesions. J Cell Sci 2001;114:3583-90
163. Smith DS, Leone G, DeGregori J, et al. Induction of DNA replication in adult rat neurons by deregulation of the retinoblastoma/E2F G1 cell cycle pathway. Cell Growth Differ 2000;11:625-33
164. Lambert MP, Stevens G, Sabo S, et al. Beta/A4-evoked degeneration of differentiated SH-SY5Y human neuroblastoma cells. J Neurosci Res 1994;39:377-85
165. Zhao JH, Reiske H.Guan JL. Regulation of the cell cycle by focal adhesion kinase. J Cell Biol 1998;143:1997-2008
166. Zhao J, Pestell R.Guan JL. Transcriptional activation of cyclin D1 promoter by FAK contributes to cell cycle progression. Mol Biol Cell 2001;12:4066-77
167. Kasahara T, Koguchi E, Funakoshi M, et al. Antiapoptotic action of focal adhesion kinase (FAK) against ionizing radiation. Antioxid Redox Signal 2002;4:491-9
168. Calalb MB, Polte TR.Hanks SK. Tyrosine phosphorylation of focal adhesion kinase at sites in the catalytic domain regulates kinase activity: a role for Src family kinases. Mol Cell Biol 1995;15:954-63
169. Golubovskaya V, Kaur A.Cance W. Cloning and characterization of the promoter region of human focal adhesion kinase gene: nuclear factor kappa B and p53 binding sites. Biochim Biophys Acta 2004;1678:111-25
170. Golubovskaya VM, Finch R.Cance WG. Direct interaction of the N-terminal domain of focal adhesion kinase with the N-terminal transactivation domain of p53. J Biol Chem 2005;280:25008-21
171. Ivankovic-Dikic I, Gronroos E, Blaukat A, et al. Pyk2 and FAK regulate neurite outgrowth induced by growth factors and integrins. Nat Cell Biol 2000;2:574-81
172. Bowser R.Smith MA. Cell cycle proteins in Alzheimer's disease: plenty of wheels but no cycle. J Alzheimers Dis 2002;4:249-54
173. Yu X, Caltagarone J, Smith MA, et al. DNA damage induces cdk2 protein levels and histone H2B phosphorylation in SH-SY5Y neuroblastoma cells. J Alzheimers Dis 2005;8:7-21

174. Ogawa O, Lee HG, Zhu X, et al. Increased p27, an essential component of cell cycle control, in Alzheimer's disease. Aging Cell 2003;2:105-10
175. Busser J, Geldmacher DS.Herrup K. Ectopic cell cycle proteins predict the sites of neuronal cell death in Alzheimer's disease brain. J Neurosci 1998;18:2801-7
176. Jordan-Sciutto KL, Malaiyandi LM.Bowser R. Altered distribution of cell cycle transcriptional regulators during Alzheimer disease. J Neuropathol Exp Neurol 2002;61:358-67
177. Jordan-Sciutto K, Rhodes J.Bowser R. Altered subcellular distribution of transcriptional regulators in response to Abeta peptide and during Alzheimer's disease. Mech Ageing Dev 2001;123:11-20
178. Hoozemans JJ, Stieler J, van Haastert ES, et al. The unfolded protein response affects neuronal cell cycle protein expression: implications for Alzheimer's disease pathogenesis. Exp Gerontol 2006;41:380-6
179. Arendt T, Holzer M, Grossmann A, et al. Increased expression and subcellular translocation of the mitogen activated protein kinase kinase and mitogen-activated protein kinase in Alzheimer's disease. Neuroscience 1995;68:5-18
180. Haddad JJ. Mitogen-activated protein kinases and the evolution of Alzheimer's: a revolutionary neurogenetic axis for therapeutic intervention? Prog Neurobiol 2004;73:359-77
181. Webster B, Hansen L, Adame A, et al. Astroglial activation of extracellular-regulated kinase in early stages of Alzheimer disease. J Neuropathol Exp Neurol 2006;65:142-51
182. Zalewska T, Makarewicz D, Janik B, et al. Neonatal cerebral hypoxia-ischemia: involvement of FAK-dependent pathway. Int J Dev Neurosci 2005;23:657-62
183. Schlaepfer DD.Hunter T. Focal adhesion kinase overexpression enhances ras-dependent integrin signaling to ERK2/mitogen-activated protein kinase through interactions with and activation of c-Src. J Biol Chem 1997;272:13189-95
184. Kacimi R.Gerdes AM. Alterations in G protein and MAP kinase signaling pathways during cardiac remodeling in hypertension and heart failure. Hypertension 2003;41:968-77
185. Yamamoto D, Sonoda Y, Hasegawa M, et al. FAK overexpression upregulates cyclin D3 and enhances cell proliferation via the PKC and PI3-kinase-Akt pathways. Cell Signal 2003;15:575-83
186. Koyama Y, Yoshioka Y, Shinde M, et al. Focal adhesion kinase mediates endothelin-induced cyclin D3 expression in rat cultured astrocytes. J Neurochem 2004;90:904-12
187. Reiske HR, Zhao J, Han DC, et al. Analysis of FAK-associated signaling pathways in the regulation of cell cycle progression. FEBS Lett 2000;486:275-80
188. Russo C, Dolcini V, Salis S, et al. Signal transduction through tyrosine-phosphorylated carboxy-terminal fragments of APP via an enhanced interaction with Shc/Grb2 adaptor proteins in reactive astrocytes of Alzheimer's disease brain. Ann N Y Acad Sci 2002;973:323-33
189. Russo C, Venezia V, Repetto E, et al. The amyloid precursor protein and its network of interacting proteins: physiological and pathological implications. Brain Res Brain Res Rev 2005;48:257-64
190. Cheng M, Sexl V, Sherr CJ, et al. Assembly of cyclin D-dependent kinase and titration of p27Kip1 regulated by mitogen-activated protein kinase kinase (MEK1). Proc Natl Acad Sci U S A 1998;95:1091-6

191. Walker JL.Assoian RK. Integrin-dependent signal transduction regulating cyclin D1 expression and G1 phase cell cycle progression. Cancer Metastasis Rev 2005;24:383-93
192. Zhao J, Bian ZC, Yee K, et al. Identification of transcription factor KLF8 as a downstream target of focal adhesion kinase in its regulation of cyclin D1 and cell cycle progression. Mol Cell 2003;11:1503-15
193. Suske G, Bruford E.Philipsen S. Mammalian SP/KLF transcription factors: bring in the family. Genomics 2005;85:551-6
194. Wang X.Zhao J. KLF8 transcription factor participates in oncogenic transformation. Oncogene 2006;
195. Chen Y, Wang SM, Wu JC, et al. Effects of PPARgamma agonists on cell survival and focal adhesions in a Chinese thyroid carcinoma cell line. J Cell Biochem 2006;98:1021-35
196. Micsenyi A, Tan X, Sneddon T, et al. Beta-catenin is temporally regulated during normal liver development. Gastroenterology 2004;126:1134-46
197. Fuentealba RA, Farias G, Scheu J, et al. Signal transduction during amyloid-beta-peptide neurotoxicity: role in Alzheimer disease. Brain Res Brain Res Rev 2004;47:275-89
198. Essers MA, de Vries-Smits LM, Barker N, et al. Functional interaction between beta-catenin and FOXO in oxidative stress signaling. Science 2005;308:1181-4
199. Alvarez AR, Godoy JA, Mullendorff K, et al. Wnt-3a overcomes beta-amyloid toxicity in rat hippocampal neurons. Exp Cell Res 2004;297:186-96
200. Garrido JL, Godoy JA, Alvarez A, et al. Protein kinase C inhibits amyloid beta peptide neurotoxicity by acting on members of the Wnt pathway. Faseb J 2002;16:1982-4
201. Greer EL.Brunet A. FOXO transcription factors at the interface between longevity and tumor suppression. Oncogene 2005;24:7410-25
202. Hosaka T, Biggs WH, 3rd, Tieu D, et al. Disruption of forkhead transcription factor (FOXO) family members in mice reveals their functional diversification. Proc Natl Acad Sci U S A 2004;101:2975-80
203. Strachan GD, Morgan KL, Otis LL, et al. Fetal Alz-50 clone 1 interacts with the human orthologue of the Kelch-like Ech-associated protein. Biochemistry 2004;43:12113-22
204. Velichkova M.Hasson T. Keap1 in adhesion complexes. Cell Motil Cytoskeleton 2003;56:109-19
205. Velichkova M.Hasson T. Keap1 regulates the oxidation-sensitive shuttling of Nrf2 into and out of the nucleus via a Crm1-dependent nuclear export mechanism. Mol Cell Biol 2005;25:4501-13
206. Lee JM, Li J, Johnson DA, et al. Nrf2, a multi-organ protector? Faseb J 2005;19:1061-6
207. Jordan-Sciutto KL, Dragich JM, Rhodes JL, et al. Fetal Alz-50 clone 1, a novel zinc finger protein, binds a specific DNA sequence and acts as a transcriptional regulator. J Biol Chem 1999;274:35262-8
208. Barak O, Lazzaro MA, Lane WS, et al. Isolation of human NURF: a regulator of Engrailed gene expression. Embo J 2003;22:6089-100
209. Kuan CY, Schloemer AJ, Lu A, et al. Hypoxia-ischemia induces DNA synthesis without cell proliferation in dying neurons in adult rodent brain. J Neurosci 2004;24:10763-72
210. Herrup K, Neve R, Ackerman SL, et al. Divide and die: cell cycle events as triggers of nerve cell death. J Neurosci 2004;24:9232-9
211. Yang Y, Geldmacher DS.Herrup K. DNA replication precedes neuronal cell death in Alzheimer's disease. J Neurosci 2001;21:2661-8

212. Herrup K.Busser JC. The induction of multiple cell cycle events precedes target-related neuronal death. Development 1995;121:2385-95
213. Whitehouse PJ, Price DL, Clark AW, et al. Alzheimer disease: evidence for selective loss of cholinergic neurons in the nucleus basalis. Ann Neurol 1981;10:122-6
214. Davies P.Maloney AJ. Selective loss of central cholinergic neurons in Alzheimer's disease. Lancet 1976;2:1403
215. Muller WE, Mutschler E.Riederer P. Noncompetitive NMDA receptor antagonists with fast open-channel blocking kinetics and strong voltage-dependency as potential therapeutic agents for Alzheimer's dementia. Pharmacopsychiatry 1995;28:113-24
216. Tariot PN, Solomon PR, Morris JC, et al. A 5-month, randomized, placebo-controlled trial of galantamine in AD. The Galantamine USA-10 Study Group. Neurology 2000;54:2269-76
217. DeLaGarza VW. Pharmacologic treatment of Alzheimer's disease: an update. Am Fam Physician 2003;68:1365-72
218. Cummings JL, Frank JC, Cherry D, et al. Guidelines for managing Alzheimer's disease: Part II. Treatment. Am Fam Physician 2002;65:2525-34
219. Geib SJ, Tuckmantel W.Kozikowski AP. Huperzine A--a potent acetylcholinesterase inhibitor of use in the treatment of Alzheimer's disease. Acta Crystallogr C 1991;47 (Pt 4):824-7
220. Lim GP, Chu T, Yang F, et al. The curry spice curcumin reduces oxidative damage and amyloid pathology in an Alzheimer transgenic mouse. J Neurosci 2001;21:8370-7
221. Joseph JA, Fisher DR.Carey AN. Fruit extracts antagonize Abeta- or DA-induced deficits in Ca2+ flux in M1-transfected COS-7 cells. J Alzheimers Dis 2004;6:403-11; discussion 443-9
222. Lim WS, Gammack JK, Van Niekerk J, et al. Omega 3 fatty acid for the prevention of dementia. Cochrane Database Syst Rev 2006;CD005379
223. in t' Veld BA, Ruitenberg A, Hofman A, et al. Nonsteroidal antiinflammatory drugs and the risk of Alzheimer's disease. N Engl J Med 2001;345:1515-21
224. Zandi PP, Anthony JC, Khachaturian AS, et al. Reduced risk of Alzheimer disease in users of antioxidant vitamin supplements: the Cache County Study. Arch Neurol 2004;61:82-8
225. Kruman, II, Kumaravel TS, Lohani A, et al. Folic acid deficiency and homocysteine impair DNA repair in hippocampal neurons and sensitize them to amyloid toxicity in experimental models of Alzheimer's disease. J Neurosci 2002;22:1752-62
226. Rockwood K. Epidemiological and clinical trials evidence about a preventive role for statins in Alzheimer's disease. Acta Neurol Scand Suppl 2006;185:71-7
227. Lyketsos CG, Colenda CC, Beck C, et al. Position statement of the American Association for Geriatric Psychiatry regarding principles of care for patients with dementia resulting from Alzheimer disease. Am J Geriatr Psychiatry 2006;14:561-72
228. Michelsen JW, Schmeichel KL, Beckerle MC, et al. The LIM motif defines a specific zinc-binding protein domain. Proc Natl Acad Sci U S A 1993;90:4404-8
229. Schmeichel KL.Beckerle MC. The LIM domain is a modular protein-binding interface. Cell 1994;79:211-9
230. Schmeichel KL.Beckerle MC. Molecular dissection of a LIM domain. Mol Biol Cell 1997;8:219-30

231. Sanchez-Garcia I.Rabbitts TH. The LIM domain: a new structural motif found in zinc-finger-like proteins. Trends Genet 1994;10:315-20
232. Way JC.Chalfie M. mec-3, a homeobox-containing gene that specifies differentiation of the touch receptor neurons in C. elegans. Cell 1988;54:5-16
233. Karlsson O, Thor S, Norberg T, et al. Insulin gene enhancer binding protein Isl-1 is a member of a novel class of proteins containing both a homeo- and a Cys-His domain. Nature 1990;344:879-82
234. Abou Zeid N, Valles AM.Boyer B. Serine phosphorylation regulates paxillin turnover during cell migration. Cell Commun Signal 2006;4:8
235. Perez-Alvarado GC, Miles C, Michelsen JW, et al. Structure of the carboxy-terminal LIM domain from the cysteine rich protein CRP. Nat Struct Biol 1994;1:388-98
236. Li PM, Reichert J, Freyd G, et al. The LIM region of a presumptive Caenorhabditis elegans transcription factor is an iron-sulfur- and zinc-containing metallodomain. Proc Natl Acad Sci U S A 1991;88:9210-3
237. Zhang J, Zhang LX, Meltzer PS, et al. Molecular cloning of human Hic-5, a potential regulator involved in signal transduction and cellular senescence. Mol Carcinog 2000;27:177-83
238. Salgia R, Li JL, Lo SH, et al. Molecular cloning of human paxillin, a focal adhesion protein phosphorylated by P210BCR/ABL. J Biol Chem 1995;270:5039-47
239. Glenney JR, Jr..Zokas L. Novel tyrosine kinase substrates from Rous sarcoma virus-transformed cells are present in the membrane skeleton. J Cell Biol 1989;108:2401-8
240. Turner CE, Glenney JR, Jr..Burridge K. Paxillin: a new vinculin-binding protein present in focal adhesions. J Cell Biol 1990;111:1059-68
241. Mackin NA, Sousou TJ.Erdman SE. The PXL1 gene of Saccharomyces cerevisiae encodes a paxillin-like protein functioning in polarized cell growth. Mol Biol Cell 2004;15:1904-17
242. Glockner G, Eichinger L, Szafranski K, et al. Sequence and analysis of chromosome 2 of Dictyostelium discoideum. Nature 2002;418:79-85
243. Yagi R, Ishimaru S, Yano H, et al. A novel muscle LIM-only protein is generated from the paxillin gene locus in Drosophila. EMBO Rep 2001;2:814-20
244. Wheeler GN.Hynes RO. The cloning, genomic organization and expression of the focal contact protein paxillin in Drosophila. Gene 2001;262:291-9
245. Crawford BD, Henry CA, Clason TA, et al. Activity and distribution of paxillin, focal adhesion kinase, and cadherin indicate cooperative roles during zebrafish morphogenesis. Mol Biol Cell 2003;14:3065-81
246. Ogawa M, Hiraoka Y, Taniguchi K, et al. mRNA sequence of the Xenopus laevis paxillin gene and its expression. Biochim Biophys Acta 2001;1519:235-40
247. Mazaki Y, Uchida H, Hino O, et al. Paxillin isoforms in mouse. Lack of the gamma isoform and developmentally specific beta isoform expression. J Biol Chem 1998;273:22435-41
248. Tumbarello DA, Brown MC, Hetey SE, et al. Regulation of paxillin family members during epithelial-mesenchymal transformation: a putative role for paxillin delta. J Cell Sci 2005;118:4849-63
249. Brown MC, Curtis MS.Turner CE. Paxillin LD motifs may define a new family of protein recognition domains. Nat Struct Biol 1998;5:677-8

250. Turner CE. Paxillin is a major phosphotyrosine-containing protein during embryonic development. J Cell Biol 1991;115:201-7
251. Hagel M, George EL, Kim A, et al. The adaptor protein paxillin is essential for normal development in the mouse and is a critical transducer of fibronectin signaling. Mol Cell Biol 2002;22:901-15
252. Mazaki Y, Hashimoto S.Sabe H. Monocyte cells and cancer cells express novel paxillin isoforms with different binding properties to focal adhesion proteins. J Biol Chem 1997;272:7437-44
253. Fujita H, Kamiguchi K, Cho D, et al. Interaction of Hic-5, A senescence-related protein, with focal adhesion kinase. J Biol Chem 1998;273:26516-21
254. Brown MC, Perrotta JA.Turner CE. Identification of LIM3 as the principal determinant of paxillin focal adhesion localization and characterization of a novel motif on paxillin directing vinculin and focal adhesion kinase binding. J Cell Biol 1996;135:1109-23
255. Herreros L, Rodriguez-Fernandez JL, Brown MC, et al. Paxillin localizes to the lymphocyte microtubule organizing center and associates with the microtubule cytoskeleton. J Biol Chem 2000;275:26436-40
256. Nishiya N, Iwabuchi Y, Shibanuma M, et al. Hic-5, a paxillin homologue, binds to the protein-tyrosine phosphatase PEST (PTP-PEST) through its LIM 3 domain. J Biol Chem 1999;274:9847-53
257. Cote JF, Turner CE.Tremblay ML. Intact LIM 3 and LIM 4 domains of paxillin are required for the association to a novel polyproline region (Pro 2) of protein-tyrosine phosphatase-PEST. J Biol Chem 1999;274:20550-60
258. Shibanuma M, Mashimo J, Kuroki T, et al. Characterization of the TGF beta 1-inducible hic-5 gene that encodes a putative novel zinc finger protein and its possible involvement in cellular senescence. J Biol Chem 1994;269:26767-74
259. Fujimoto N, Yeh S, Kang HY, et al. Cloning and characterization of androgen receptor coactivator, ARA55, in human prostate. J Biol Chem 1999;274:8316-21
260. Nishiya N, Sabe H, Nose K, et al. The LIM domains of hic-5 protein recognize specific DNA fragments in a zinc-dependent manner in vitro. Nucleic Acids Res 1998;26:4267-73
261. Barrett TJ.Spelsberg TC. Steroid receptors at the nexus of transcriptional regulation. J Cell Biochem Suppl 1998;30-31:185-93
262. Miyamoto Y, Yamauchi J, Chan JR, et al. Cdk5 regulates differentiation of oligodendrocyte precursor cells through the direct phosphorylation of paxillin. J Cell Sci 2007;120:4355-66
263. Hyman BT.Trojanowski JQ. Consensus recommendations for the postmortem diagnosis of Alzheimer disease from the National Institute on Aging and the Reagan Institute Working Group on diagnostic criteria for the neuropathological assessment of Alzheimer disease. J Neuropathol Exp Neurol 1997;56:1095-7
264. Morris JC, Heyman A, Mohs RC, et al. The Consortium to Establish a Registry for Alzheimer's Disease (CERAD). Part I. Clinical and neuropsychological assessment of Alzheimer's disease. Neurology 1989;39:1159-65
265. Caltagarone J, Rhodes J, Honer WG, et al. Localization of a novel septin protein, hCDCrel-1, in neurons of human brain. Neuroreport 1998;9:2907-12
266. Kress GJ, Dineley KE.Reynolds IJ. The relationship between intracellular free iron and cell injury in cultured neurons, astrocytes, and oligodendrocytes. J Neurosci 2002;22:5848-55

267. Ben-Yehoyada M, Ben-Dor I.Shaul Y. c-Abl tyrosine kinase selectively regulates p73 nuclear matrix association. J Biol Chem 2003;278:34475-82
268. Holland T. The comparative power of the discriminant methods used in toxicological pathology. Toxicol Pathol 2005;33:490-4
269. Nakamura K, Yano H, Uchida H, et al. Tyrosine phosphorylation of paxillin alpha is involved in temporospatial regulation of paxillin-containing focal adhesion formation and F-actin organization in motile cells. J Biol Chem 2000;275:27155-64
270. Carneiro AM, Ingram SL, Beaulieu JM, et al. The multiple LIM domain-containing adaptor protein Hic-5 synaptically colocalizes and interacts with the dopamine transporter. J Neurosci 2002;22:7045-54
271. Young BA, Taooka Y, Liu S, et al. The cytoplasmic domain of the integrin alpha9 subunit requires the adaptor protein paxillin to inhibit cell spreading but promotes cell migration in a paxillin-independent manner. Mol Biol Cell 2001;12:3214-25
272. Heitzer MD.DeFranco DB. Hic-5/ARA55, a LIM domain-containing nuclear receptor coactivator expressed in prostate stromal cells. Cancer Res 2006;66:7326-33
273. Wilkinson BL.Landreth GE. The microglial NADPH oxidase complex as a source of oxidative stress in Alzheimer's disease. J Neuroinflammation 2006;3:30
274. Amador-Ortiz C, Lin WL, Ahmed Z, et al. TDP-43 immunoreactivity in hippocampal sclerosis and Alzheimer's disease. Ann Neurol 2007;61:435-45
275. Santi MR.Golden JA. Periventricular heterotopia may result from radial glial fiber disruption. J Neuropathol Exp Neurol 2001;60:856-62
276. Kumar U.Patel SC. Immunohistochemical localization of dopamine receptor subtypes (D1R-D5R) in Alzheimer's disease brain. Brain Res 2007;1131:187-96
277. Kalman M.Szabo A. Immunohistochemical investigation of actin-anchoring proteins vinculin, talin and paxillin in rat brain following lesion: a moderate reaction, confined to the astroglia of brain tracts. Exp Brain Res 2001;139:426-34
278. Johanson C, McMillan P, Tavares R, et al. Homeostatic capabilities of the choroid plexus epithelium in Alzheimer's disease. Cerebrospinal Fluid Res 2004;1:3
279. Serot JM, Bene MC, Foliguet B, et al. Altered choroid plexus basement membrane and epithelium in late-onset Alzheimer's disease: an ultrastructural study. Ann N Y Acad Sci 1997;826:507-9
280. Serot JM, Bene MC, Foliguet B, et al. Morphological alterations of the choroid plexus in late-onset Alzheimer's disease. Acta Neuropathol (Berl) 2000;99:105-8
281. Silverberg G, Mayo M, Saul T, et al. Elevated cerebrospinal fluid pressure in patients with Alzheimer's disease. Cerebrospinal Fluid Res 2006;3:7
282. Silverberg GD, Heit G, Huhn S, et al. The cerebrospinal fluid production rate is reduced in dementia of the Alzheimer's type. Neurology 2001;57:1763-6
283. Crossgrove JS, Li GJ.Zheng W. The choroid plexus removes beta-amyloid from brain cerebrospinal fluid. Exp Biol Med (Maywood) 2005;230:771-6
284. Padmanabhan J, Clayton D.Shelanski ML. Dibutyryl cyclic AMP-induced process formation in astrocytes is associated with a decrease in tyrosine phosphorylation of focal adhesion kinase and paxillin. J Neurobiol 1999;39:407-22